AN EVALUATION OF MEMBRANE MATERIALS FOR THE TREATMENT OF HIGHLY CONCENTRATED SUSPENDED SALT SOLUTIONS IN REVERSE OSMOSIS AND NANOFILTRATION PROCESSES FOR DESALINATION

A Thesis

by

TRENTON WHITING HUGHES

Submitted to the Office of Graduate Studies of
Texas A&M University
in partial fulfillment of the requirements for the degree of

MASTER OF SCIENCE

December 2006

Major Subject: Civil Engineering

AN EVALUATION OF MEMBRANE MATERIALS FOR THE TREATMENT OF HIGHLY CONCENTRATED SUSPENDED SALT SOLUTIONS IN REVERSE OSMOSIS AND NANOFILTRATION PROCESSES FOR DESALINATION

A Thesis

by

TRENTON WHITING HUGHES

Submitted to the Office of Graduate Studies of
Texas A&M University
in partial fulfillment of the requirements for the degree of

MASTER OF SCIENCE

Approved by:

Co-Chairs of Committee,	Timothy Kramer
	Bill Batchelor
Committee Members,	Roy Hann
	Charles Glover
Head of Department,	David Rosowsky

December 2006

Major Subject: Civil Engineering

ABSTRACT

An Evaluation of Membrane Materials for the Treatment of Highly Concentrated Suspended Salt Solutions in Reverse Osmosis and Nanofiltration Processes for Desalination. (December 2006)

Trenton Whiting Hughes, B.S., Auburn University

Co-Chairs of Advisory Committee: Dr. Timothy Kramer
Dr. Bill Batchelor

This thesis presents a study to enhance and improve a zero liquid discharge (ZLD) reverse osmosis process that uses seed crystals to promote crystallization of the dissolved salts in the residual brine while it is being treated by identifying those membrane materials that are most suitable for the process.

In the study, a one plate SEPA Cell module by GE Osmonics was used to determine which membranes were most susceptible to fouling and/or membrane hydrolysis. A cellulose acetate (CA), polyamide (PA) low MWCO, and PA high MWCO membrane were tested under reverse osmosis conditions. The CA and thin film (TF) membranes were also tested for nanofiltration.

The cell was operated under conditions that were determined to be optimum for each membrane by the manufacturer, GE Osmonics. A high pressure, low flow, positive displacement diaphragm pump circulated the saturated calcium sulfate solution with 2 % suspended solids through the cell while the reject and permeate were recycled back to the feed, thereby preserving a saturated solution to promote crystal growth and simulate the seeded reverse osmosis process. The temperature was maintained constant by adding

an ice pack to the feed vessel when necessary. The transmembrane pressure differential was maintained constant by adjusting a back pressure valve on the concentrate outlet.

The results illustrate that if potable drinking water is the intended use, then the nanofiltration cellulose acetate membrane should be used. If irrigation is the desired use, then the nanofiltration thin film membrane should be used. Overall, the reverse osmosis cellulose acetate membrane was observed to outperform all membranes when all performance parameters were normalized. However, this membrane was observed to be prone to degradation in a seeded slurry and therefore its lifetime should be analyzed further. The polyamide membrane initially had a high water transport coefficient, but fouling led to its rapid decline which was attributed to the membrane's rough and protrusive surface. A lifetime test on the thin film and cellulose acetate revealed that when operated at their maximum pressure specified by GE Osmonics for a duration of 8 hours that no decrease in rejection occurred.

DEDICATION

First and foremost, I dedicate this work to Jesus Christ who makes all things possible if you believe and trust in him. Next I dedicate this to my parents, Tal and Susan Hughes, for providing me with a foundation to know a savior and for their incessant support/love. Finally I dedicate this work to my siblings, Travis and Shannon Hughes, for their great love and sibling camaraderie.

ACKNOWLEDGMENTS

There are five individuals that I would like to thank for their guidance, help, and support. To my advisors, Dr. Tim Kramer and Dr. Bill Batchelor, I would like to thank you for all the insight, assistance, and patience you have provided me in the completion of this work. Not only have you shown me what it means to be a tenacious researcher, you have also set a wonderful example of what it means to be a professional in all aspects of life. I would also like to remember Mr. Carl Vavra for his willingness to let me use his equipment thereby making this thesis possible. Finally, I appreciate the willingness, time, and support from my two committee members, Dr. Charles Glover and Dr. Roy Hann.

TABLE OF CONTENTS

Page

Page

Page

LIST OF FIGURES

FIGURE Page

FIGURE Page

FIGURE Page

FIGURE Page

LIST OF TABLES

TABLE Page

1. INTRODUCTION

1.1 Background

The demand for fresh water and population accretion are directly related. Our water resources will remain constant as the world's population, which is now approximately six billion people, is expected to double within the 50-90 years. Currently, over 400 million people live in regions where there are severe freshwater shortages. This number is projected to climb to 2.8 billion people by 2025 (RosTek Associates et al. 2003).

As a result, the limited supply of freshwater will become scarce. The intensifying scarcity of harvestable water is a characteristic fact of modern water resources planning and management. The international crisis with respect to water supply hinges on the economic inconvenience of producing water from transformative industrial processes. Water is essential to human life and the health of cities, with no substitute. Unfortunately, the scarcity of water is inevitably depicted by the U. S. Geological Survey, which estimates that 0.3% of water resources are usable by humans. The other 99.7% is transformable by some process into clean potable water. The transformation can be pumping, melting, condensing, desalting, or any other process that moves, stores, liquefies, or purifies the resource into the potable commodity.

Desalination of saline water to produce clean water is both a "high-cost invention" and an "alternative source". However, it is the most economical option for producing pure freshwater if saline water is in the vicinity of a freshwater-deprived

---

The style and format of this thesis follows that of *Journal of Environmental Engineering.*

community. Desalting is not news because of its technological innovation but because of the increasing number of communities worldwide that have reached the backstop price of harvested water that makes desalting viable. In fact, desalination of seawater to produce freshwater has been used for hundreds of years. Nearly half a millennium before Christ, sailors evaporated seawater on sponges to produce freshwater. Not only are resources becoming scarcer, but infrastructure costs and health and environmental regulations are increasing simultaneously, thereby driving the costs of providing municipal water supplies toward the backstop price (AMTA 2001). Particularly in Texas, Karama and Wurbs (1995) note the problem by saying "Water in the three main stream reservoirs (in TX) is unsuitable for municipal use without costly desalinization processes. The quality of the river improves significantly in the lower basin with dilution from good quality tributaries. Population and economic growth combined with depleting groundwater reserves are resulting in ever-increasing demands on the surface water resources of Texas and the Brazos River Basin."

If the application of this expensive method (desalting) to produce a water supply is an indication of the availability of alternatives, water has indeed become scarce. Today, desalination is no longer limited to converting solely seawater into freshwater. Advanced technology has now expanded the application of desalination to other sources, commonly known as the "impaired" sources which include, but are not limited to, brackish groundwater, brackish surface water, wastewater effluent, and industrial water (AMTA 2001).

Important limitations still face the desalting industry, including the cost of plant construction, reliability and costs of operation, and environmental impact. A moderately-sized plant can take 4 or 5 years to build due to the design complexities of accommodating feedwater, electrical power access, and distribution of products and disposal of wastes. In some cases, construction issues have become much more severe, as in Tampa Bay, Florida, where a large $110 million plant initiated in 1997 is only producing at 10% capacity after the successive bankruptcy of several contractors and commercial partners over financing and operational troubles. The current estimated wholesale price of water from the facility is $2.49/1000gal. The largest seawater reverse osmosis plant under construction at present is the Ashkelon plant in Israel. It is projected to cost $212 million for three times the capacity of the Tampa Bay project. Economies of scale are evident in this industry, to the extent that most cities cannot afford a state-of-the-art facility.

Furthermore, most desalting plants operate between 30-65% of their capacity due to concentrated salts being so corrosive that system parts have to be replaced every 2-4 years. Unfortunately, this frequent maintenance makes it difficult for plants to operate efficiently due to their inactivity.

The biggest single problem for desalting plant operators is the concentrated brine byproduct. This concentrated saline solution is an environmental hazard. It is either dumped into a body of surface water, injected into a well, or evaporated in ponds. Injection is the simplest solution, but it tends to contaminate adjacent water supplies. Federal law in the U. S. permits injection only as a last resort. Dumping is similarly

complicated in jurisdictions with mature environmental restrictions. Dilution with the desalted water product obviously reduces net yield of the process. In Tampa Bay, brine is diluted with cooling water and released into the sea, drawing political resistance from at least one local environmental group. Evaporation ponds tend to be large and are under the influence of the weather. The new approach is to reduce disposal costs by minimizing the volume of reject brine or striving to achieve a zero-liquid discharge (ZLD) (Kurihara 2003).

Currently, the most cost effective method for desalination is forcing the saline water through a membrane, also known as reverse osmosis. This process was discovered in the early 1970's, but was inhibited by technical and cost limitations at that particular time. Unfortunately, as with all other desalination techniques, a drawback to this process is the large quantity of residual saline brines that are produced (Gutman 1987). Therefore, it is most desirable to attain a reject that is totally in its solid state, which is known as "zero-liquid discharge" (ZLD). Another major limiting factor for membrane technology in the treatment of water and wastewater is the fouling of the membrane surface. In a membrane filtration process, the term "fouling" is used to describe a particulate material's adhesion to the external surface or internal surface within the membrane's pore structure. Adhesion of particles results in a reduction in the flux across the membrane. There are many factors that cause fouling including operational parameters of the system, solute properties, and membrane properties. However, the main limitation with conventional reverse osmosis is the potential of dissolved

compounds precipitating to form solid phases when their solubility is exceeded, which will cause scaling and immediate fouling (Hess et al. 1988)

As the popularity of membrane technology increases, research efforts have begun to focus on methods for the reduction of fouling in these treatment processes. The use of various forms of feedwater pretreatment have proven to provide benefits to the membrane filtration process in the reduction of fouling. Some of these pretreatment options include: clarification of the feedwater, lime softening, coagulation-flocculation, the addition of a metal oxide or metal hydroxide to the feedwater, the addition of powdered activated carbon, and chemical cleaning of the membrane surface (Maartens et al. 2000). However, according to Hess et al. (1988), "The costs of operating and maintaining RO plants with associated pretreatment systems have limited its acceptance and use in the electric utility industry."

1.2 Importance and Significance of the Project

A promising alternative treatment called seeded reverse osmosis (SRO) is an approach that combines precipitative removal of scale-forming compounds with the desalination process itself. In an SRO operation, seed crystals are added to the saturated solution being desalinated, so that the precipitation of minerals occurs on the surface of the seed rather than on the surface of the membranes. This fouling prevention technology is important because the major limitation in achieving zero-liquid discharge (ZLD) is membrane fouling due to precipitation of solid phases that become oversaturated during concentration in the reverse osmosis (RO) system. This system was first used for sea water desalination. A seeded reverse osmosis (SRO) system

requires the solute to be slightly above its saturation concentration, thereby promoting precipitation upon addition of the seed crystal. Full scale operations can achieve this by using multiple stages where the reject brine flows to multiple successive modules until it becomes near saturation levels, where if a seed is added the solute will precipitate on it, instead of the membrane (Juby et al. 2000). Hess et al. (1988) summarizes the advantages of the SRO process, stating, "Therefore, wastewaters, with dissolved species approaching their solubility limits, can be processed without pretreatment. In addition, a better quality permeate may be achievable with SRO systems…"

In addition to fouling, membrane hydrolysis is also a concern when using membrane technology due to decreasing amounts of solute rejection. Membrane hydrolysis has occurred when there is a large increase of the solute concentrations in the permeate, thereby indicating destruction of the membrane material. The causes are not well understood to date, but the degree of hydrolysis varies membrane by membrane. SRO membranes are prone to destruction due to the high level of suspended solids that they are exposed to (Juby et al. 2000).

A typical culprit of scaling is the salt, calcium sulfate ($CaSO_4$). Surface waters in the southwestern region of the United States, especially the Brazos River Valley region in Texas, are highly contaminated with calcium sulfate along with the mining wastewaters in Africa. Its scaling characteristics have induced many costly problems to the desalination processes of these waters (RosTek Associates 2003).

Unfortunately, most waters that are contaminated with calcium sulfate are so highly concentrated that conventional RO systems cannot withstand the calcium sulfate

scaling. In fact, the saturation of the feedstream must be less than 20% if typical conventional RO systems are to be used. However, SRO systems require that the feed be at or exceed saturation levels, thereby making SRO prevalent for calcium sulfate removal if the concentration of calcium sulfate is greater than 20%.

Operating costs in reverse osmosis systems are highly contingent upon the membranes life. Therefore, careful evaluation of the various membranes used in SRO should be conducted (Juby et al. 2000). In fact, a multistage system was operated with different RO membranes for treatment of cooling water and major differences were observed in the performance of the membranes. This investigation led to the conclusion that the SRO process is technically viable, but that the correct selection in membrane material is critical to the operating cost. Therefore, identification of membranes that will withstand fouling/abrasions and operate for long periods of time is a key factor in developing this economically efficient process (SRO) which aids in achieving ZLD (Hess et al. 1988).

1.3 Scope of Work and Structure of This Thesis

Four decades ago President John F. Kennedy said, "If we could produce fresh water from salt water at a low cost, that would indeed be a great service to humanity, and would dwarf any other scientific accomplishment." The developing seeded reverse osmosis process has potential to meeting former President Kennedy’s proposition. The SRO process has been shown to be a technically viable technology by preventing scaling on the membrane surface. However, the literature has also indicated that the choice of membrane is critical to the success of the SRO process. Some membranes are more

vulnerable to high levels of fouling and are less effective at resisting abrasion by the suspended solids. Therefore these membranes have reduced service lives, resulting in higher operational costs. As a result, one goal of this research was to evaluate the efficacy of commonly used membrane material in a seeded reverse osmosis application. In particular, a cellulose acetate, thin film, and polyamide membrane were evaluated in an SRO process. A membrane that is more suitable for desalination in SRO will indeed lower operating cost significantly, as opposed to using one that is less efficient. Furthermore, a more suitable membrane will also increase the possibility of achieving the ultimate goal of ZLD. The membranes that performed well were run through the SRO simulation process again at their specified maximum pressures for a duration of 8 hours to determine their lifetime and/or whether or not membrane degradation was occurring.

A second goal of this research was to determine if nanofiltration technology could yield the same or better product water quality as reverse osmosis technology for removal of calcium sulfate in a seeded environment (2 % or 20 g/L of suspended calcium sulfate). Operating cost reductions would incur from being able to use nanofiltration technology instead of reverse osmosis technology.

In the study, a one plate SEPA cell module by Osmonics was used to determine which membranes were most susceptible to fouling and/or membrane hydrolysis. A cellulose acetate (CA), polyamide (PA) and thin film (TF) membrane were all tested under reverse osmosis conditions. The CA and TF membranes were also tested for nanofiltration.

In the succeeding sections, a review of all literature relevant to this study is given, along with the methodology for conducting the simulations. The sections that succeed the methodology will give a technical review of the results. After the technical analysis, conclusions and future research recommendations will be conferred.

2. LITERATURE REVIEW

There is a considerable body of literature that exists on the subject of desalination. However, only a limited number of studies have been conducted related to the seeded reverse osmosis process. In particular, there has been no evaluation of the types of membranes that can be used for SRO applications.

2.1 Membranes and Reverse Osmosis

Osmosis is the natural process of water diffusing from a solution with lower concentration of solute to a solution with higher concentration of solute in order to equilibrate the solute concentration. Reverse osmosis is the contrary; water is forced under pressure from a solution with higher concentration to one with a lower concentration. Figure 2-1 shows the osmosis and reverse osmosis processes.

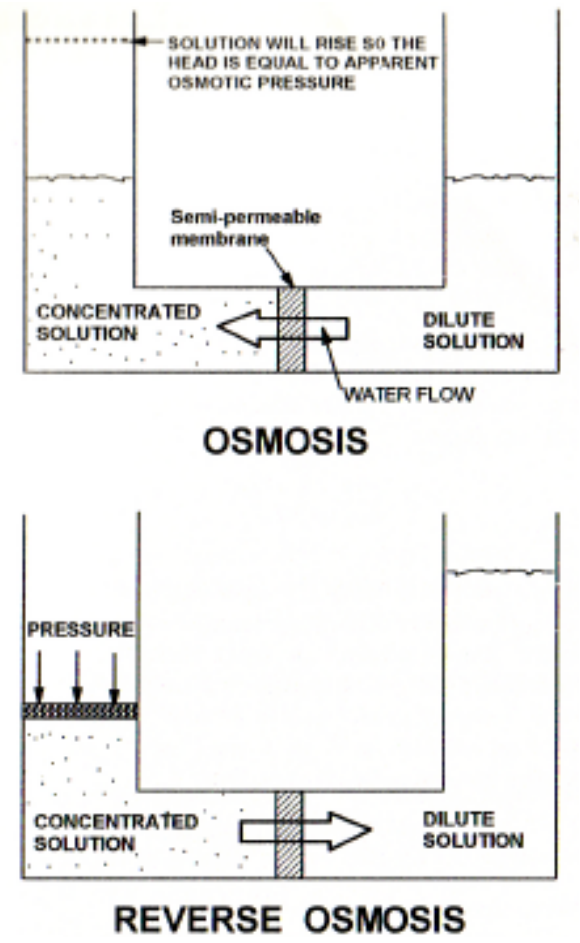

FIG. 2-1. Osmosis and reverse osmosis diagrams (Cheryan 1998)

Reverse osmosis is the filtration mechanism used in desalination plants, where water is forced from a high concentration salt to a lower concentration salt.

Filtration refers to the separation of heterogeneous solid particles from liquid or gaseous streams using a porous media. Typically, membranes are used as the media which selectively permits the passage of certain components and denies the access to others. RO membranes are made of long chain organic molecules or polymers which

have an affinity for water. This hydrophilic characteristic allows water to pass while preventing the passage of dissolved solids. In any reverse osmosis system, there will be the concentrate (also known as “retentate” or “reject”), which is that part of the fluid stream that is captured by the membrane and the permeate (also known as the product), which is that part of the fluid stream that passes through the membrane (Cheryan 1998).

2.1.1 Classification of Membrane Separation Processes

Usage of membranes for separation purposes can cover a wide array of particle sizes and fluid applications based on the utilization technique of the membrane. The application of hydraulic pressure to speed up the filtering process helps to distinguish the common pressure-driven processes (microfiltration, ultrafiltration, nanofiltration, and reverse osmosis). For these processes, the pore size of the membrane is the controlling factor in determining those components which are retained, and those that permeate.

Membranes are classified according to their pore size and/or the molecular weight cut-off (MWCO). Microfiltration describes those processes which use pore sizes ranging from 0.1-0.5 microns. For pore sizes ranging from 0.001-0.02 microns, the term ultrafiltration is used, while the term nanofiltration refers to those processes which use pore sizes ranging from 0.0005-0.006 microns. Reverse osmosis is the process which retains the smallest of all particles, having pore sizes ranging from 0.0002-0.003 microns, thereby blocking all components, only allowing the solvent (water) to pass (Cheryan 1998). This can be observed in Figure 2-2 below.

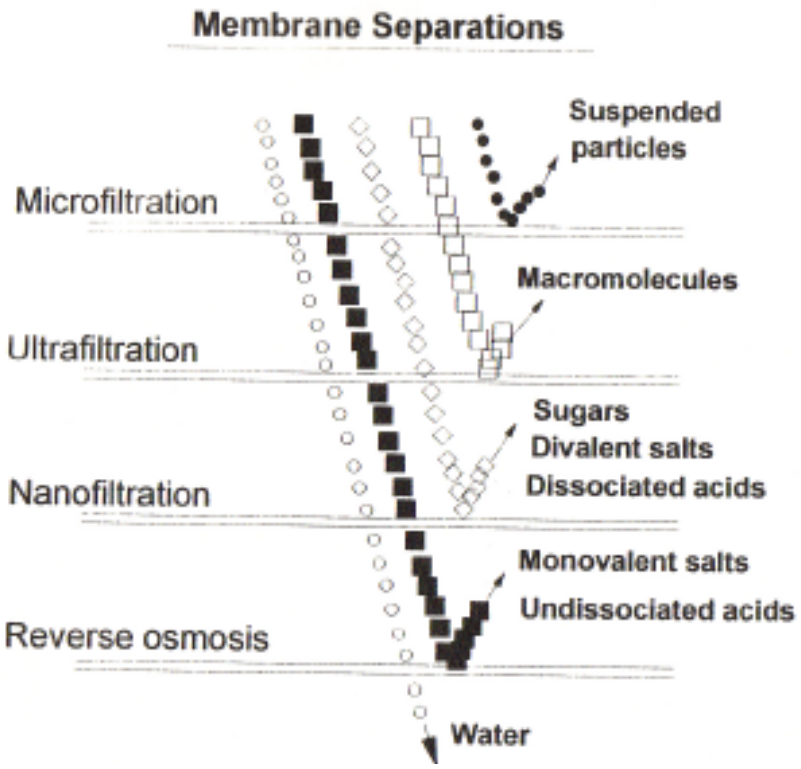

FIG. 2-2. An illustration of what permeates and is retained by the various membrane technologies (Cheryan 1998)

2.1.2 Composition of Membranes

With desalination becoming a necessity to meet society's needs, and reverse osmosis becoming the most efficient means to achieving that need, there has been intense investigation on enhancing the process. Currently, the limiting factor in any reverse osmosis system is the lifetime of the membrane. As a result, there are over 130 materials that are used to manufacture RO membranes. The most common synthetic

membranes that are used today comprise materials such as polyamide (PA), polysulfone (PS), cellulose acetate (CA), and the thin film membrane (TF).

2.1.2.1 Cellulose Acetate

The cellulose acetate membrane is the most commonly used membrane in reverse osmosis systems. The membrane is made from cellulose found in wood pulp and cotton linters, which then is reacted with acetic acid, anhyrdride, and sulfuric acid. Polymerization of the cellulose in the membrane is the key factor in fabricating an optimum membrane.

There are advantages to cellulose acetate membranes. One is that it can be manufactured to a wide range of pore sizes, which aids in molecular selectivity. Furthermore, CA membranes are relatively inexpensive and easy to manufacture. Cellulose acetate's most prominent advantage is that the membrane minimizes fouling by rejecting particular matter due to its hydrophilic characteristics.

There are also a few well pronounced drawbacks to CA membranes. First, the conditions of the water to be treated must be taken into account. Optimum operating temperatures are found to be less than 30° C and a pH range from 3 to 8. Furthermore, the chemical constituents in the water to be treated must be suitable for the membrane. For example, chlorine is known to deteriorate the CA membrane due to its oxidizing characteristics. CA membranes are also very biodegradable, leaving them susceptible to microbial decomposition.

2.1.2.2 Polysulfone Membranes

The polysulfone membrane is a widely applicable membrane for reverse osmosis processes. The diphenylene sulfone repeating units in the molecule structure make the membrane strong, creep resistant, and strong. Polysulfone membranes have proven to be very useful for reverse osmosis processes due to their favorable material properties. Characteristics such as a wide pH tolerance (1<pH<13) and temperature tolerance (max of 125 degrees Celsius), resistance to chlorine, manufacturing ease, and the availability of a variety of pore sizes attribute to the membrane material being one of the most common used in RO processes. On the contrary, a disadvantage of using this membrane is its susceptibility to membrane fouling due to the hydrophobic nature of the polysulfone membrane surface interacting with several solutes and organic compounds (Cheryan 1998).

2.1.2.3 Polyamide Membranes

The nomenclature for polyamide (PA) membranes comes from the amide bond in its molecular structure. The structural difference aids in compensating for the cellulose acetate membrane's limitations, such as the PA's ability to operate at a wide pH range (Cheryan 1998). Similar to CA, the membrane's ability to withstand high pressure makes them suitable for reverse osmosis applications (Gutman 1987). A disadvantage of PA membranes is their vulnerability to chlorine degradation and biofouling tendencies (Cheryan 1998).

2.1.2.4 Thin Film Membranes

Thin film membranes are semi-permeable membranes that are used in reverse osmosis. The thin film membrane is essentially a molecular sieve constructed of multiple layers of polyamide material with polysulfone as a porous support layer. More specifically, the thin film polyamide membrane comprises (1) a top ultra-thin (0.1 micron) skin polyamide layer, (2) a middle polysulfone porous support (0.2 micron thickness) and (3) bottom non-woven fabric for reverse osmosis (0.35 micron thickness).

A limitation of the thin film membrane is that when operating under pressure, the membrane thin film composites suffer from compaction effects. As the pressure increases, the polymers become squeezed together resulting in a lower porosity, thereby limiting the efficiency of the system designed to use them.

Some advantages of the thin film membrane include excellent thermal stability, pH stability, microbiological resistance, and salt rejection (Devmurari et al. 2006).

2.1.3 Membrane Geometrical Configurations

Membranes can be arranged in four different configurations: tubular, hollow fiber (HF), spiral wound, and plate type for various water treatment applications.

2.1.3.1 Tubular Membranes

The tubular membrane was one of the first industrial sized membranes designed. Tubular membranes are cast on the inside of a plastic tube with diameters ranging from 12.5 to 25 millimeters and lengths ranging from .6 to 6.4 meters. The diameter of the tube is determined by a compromise between the cost of making membranes and support tubes with minimal diameters and optimum size for minimum energy requirements.

This configuration permits the treatment of slurries with large particles due to its large channel diameters, thereby making it suitable for SRO applications. Conversely, the tubular membrane has the lowest surface area to volume ratio of all the configurations. They are also expensive to start up and to maintain (capital cost) (Cheryan 1998). Figure 2-3 depicts the membrane configuration.

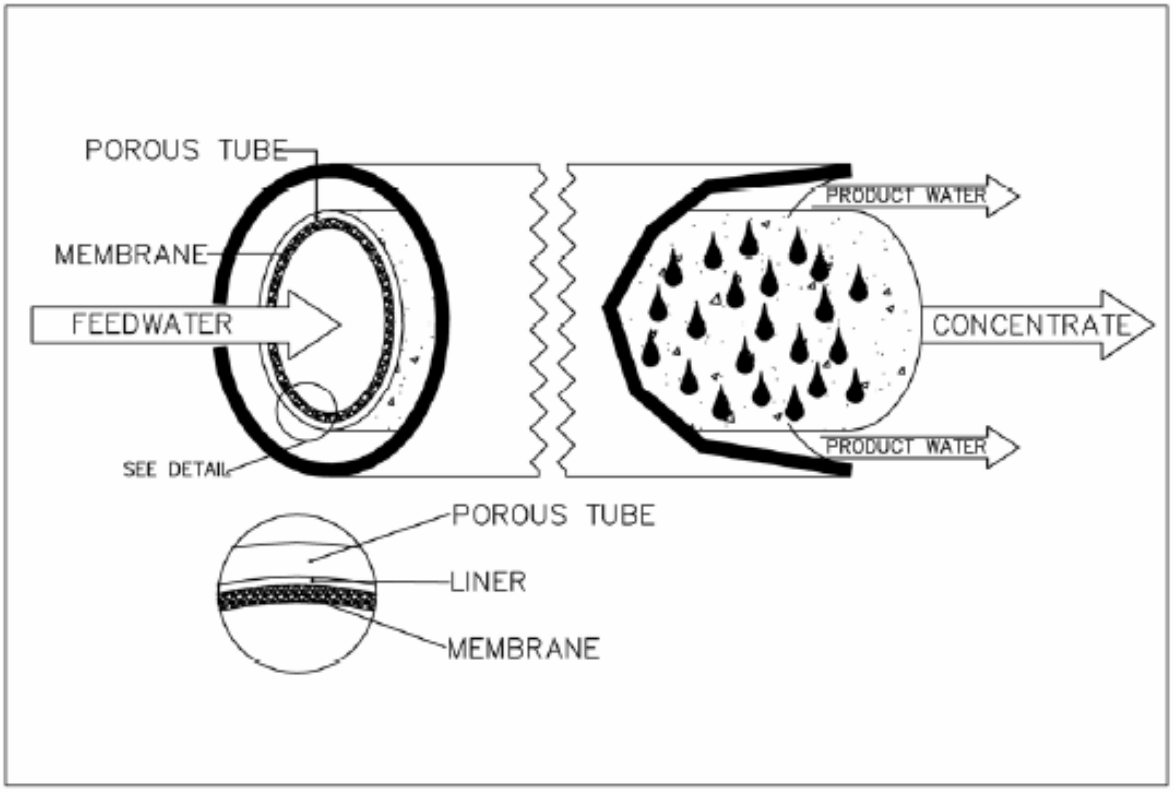

FIG. 2-3. Tubular membrane configuration (RosTek Associates 2003)

2.1.3.2 Hollow Fiber Membranes

Similar to the tubular membrane the hollow fiber membrane is in the form of a tube, but they are in the form of two concentric self-supporting cylinders unlike the tubular membrane. The membrane is attached to the inner cylinder and the feed is

pumped through the inner core of the tube and then disseminates outward through the support structure into a collection system. Figure 2-4 depicts the membrane configuration.

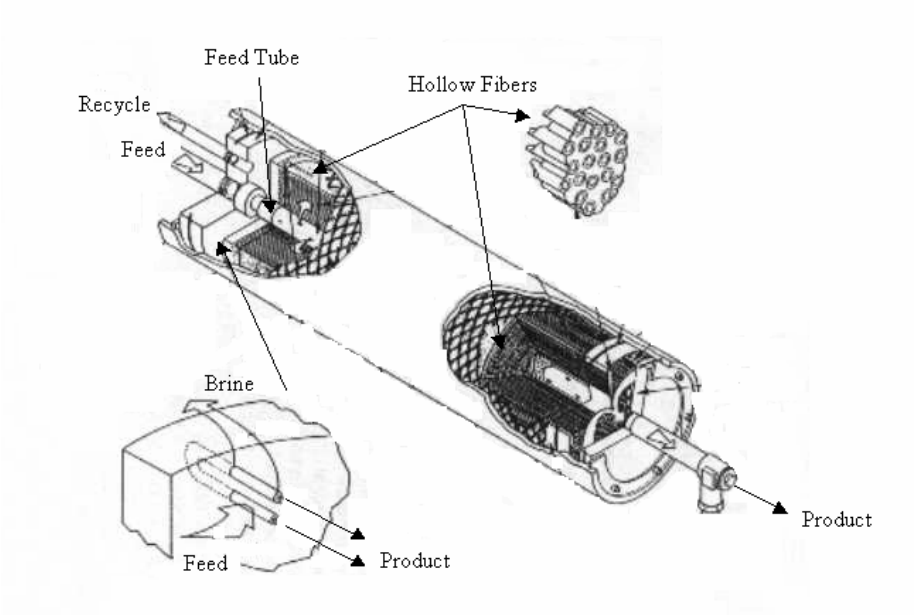

FIG. 2-4. Hollow fiber membrane configuration (Cheryan 1998)

This configuration is used for water treatment due to its advantageous characteristics such as possessing the highest surface area to volume ratio and being easy to backwash due to its self supporting nature. Another advantage is that it can be used in a crossflow filtration mode which is very efficient (Cheryan 1998; Gutman 1987).

2.1.3.3 Spiral Wound Membranes

The spiral wound configuration consists of flat sheets that are placed together with their active sides facing away from each other. It is one of the most compact and inexpensive configurations available. Each pair of sheets is separated by a mesh-like

material and then glued together on three sides. The remaining side is then fixed in place around a perforated center tube. Another spacer is placed on one side of the envelope which creates space for a channel and is therefore called the "feed channel spacer." The assembly is then rolled around the center tube into a spiral configuration. The feed is pumped lengthwise along the unit, while the treated permeate is forced through the membrane sheets into a channel and flows in the direction of the perforated center collection tube. Figure 2-5 illustrates the design and configuration.

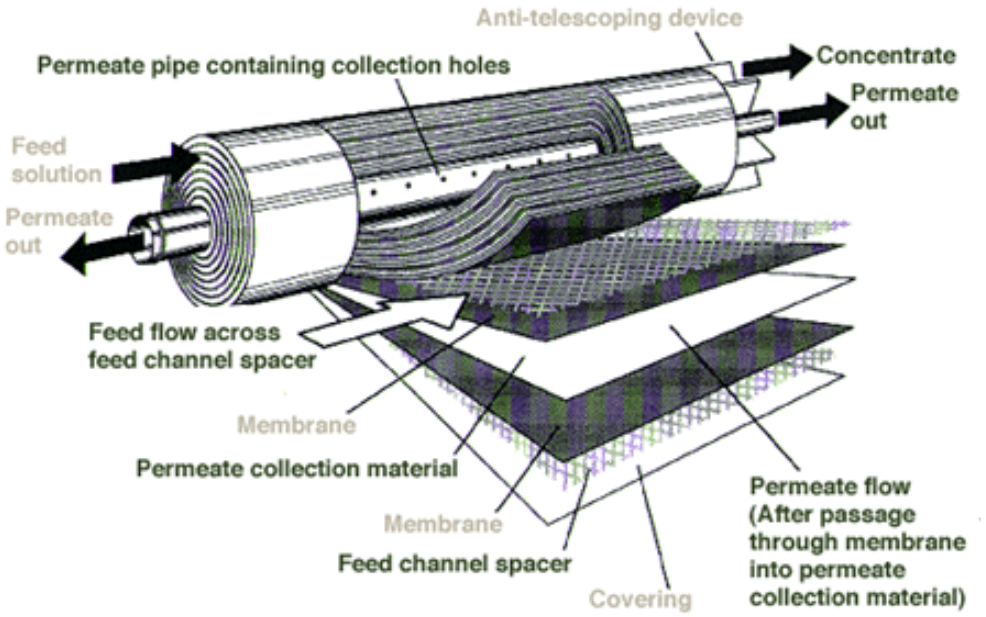

FIG. 2-5. Spiral wound membrane configuration (Pankratz and Tonner 2003)

One limiting factor of the spiral wound configuration is the high pressure drop in the feed channel that results from the friction drag exerted by the spacer. Another disadvantage is the formation of dead spots behind the mesh spacers in the flow path.

Conversely, an advantage is the high surface area to volume ratio, averaging from 200-300 ft^2/ft^3 (Cheryan 1998).

2.1.3.4 Plate Type Membranes

The plate membrane configuration consists of a membrane which is placed in between two plates. In between the plate and one surface of the membrane is a net like material known as a scrim which provides a channel for the permeate to flow. The plates are sealed together, while allowing a method for the removal of the reject (Cheryan 1998). Figure 2-6 illustrates this configuration.

2.1.4 Membrane Filtration Mechanisms

The method in which a membrane filtration system operates differs greatly due to the various applications and configurations. The dead end operation is the simplest design configuration while most applications favor the cross-flow (tangential flow) operation.

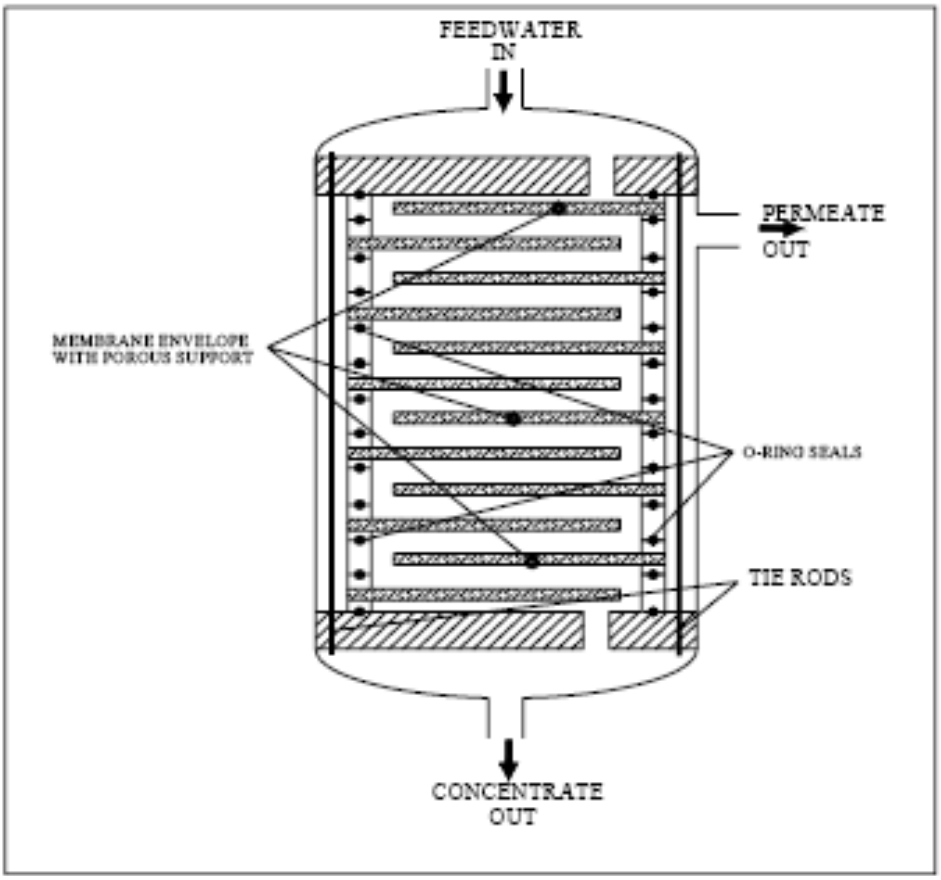

FIG. 2-6. Plate-type membrane configuration (RosTek Associates 2003)

2.1.4.1 Cross-flow Operation

Most of the membrane processes are operated in a cross-flow mode to reduce concentration polarization and fouling. In the cross-flow operation, the feed flows parallel (tangential) to the membrane surface. The feed is separated into a permeate stream and a retentate stream by the applied transmembrane pressure which forces some of the inflow through the membrane (Mulder 1996). Along the membrane (with space) the mean tangential velocities of the inflow decreases due to the loss of permeate

through the membrane (Wiesner and Chellam 1992). The portion of the inflow that is not forced through the membrane is then recycled back to the start of the treatment. The operation is shown in Figure 2-7.

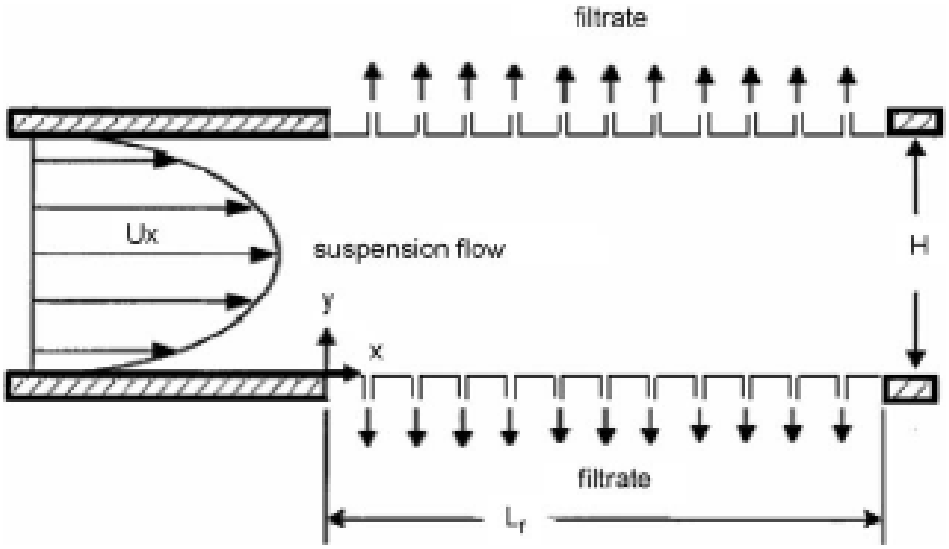

FIG. 2-7. Crossflow operation (Kim and Zydney 2006)

Cross-flow operation is advantageous in that it limits fouling by limiting the accumulation of solids on the membrane surface. The solids are suspended by the tangential velocity of the feedstream which results in less accumulation, thereby permitting more permeate through the membrane. As a result, there is a higher average flux using this operation as opposed to the dead end operation (Cheryan 1998).

2.1.4.2 Dead-end Operation

Dead-end operation is the opposite of cross-flow operation, in that the flow is perpendicular to the membrane surface. As a result of the inflow being normal to the

membrane, the rejected material accumulates as a cake layer on the membrane surface, thus causing a rapid permeate flux decline (Gutman 1987). Using this method of operation, the cake will grow with time and consequently the flux will decrease with time. Dead-end operation is illustrated in Figure 2-8.

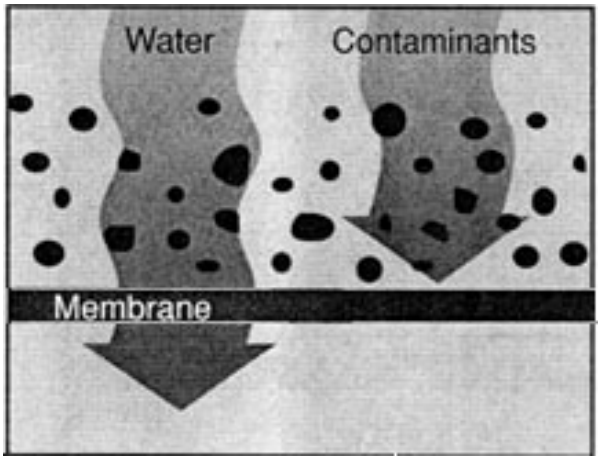

FIG. 2-8. Dead-end filtration (Cheryan 1998)

2.1.5 Membrane Fouling

Fouling can be best described by Gutman (1987) as “the accumulation of material at the surface and in the internal porous structure of the membrane”. In any filtration system, fouling can be seen as a loss in flux with time of operation caused by a reduction in the permeability of the membrane (Cheryan 1998; Gutman 1987).

Membrane fouling can be described in two ways, reversible and irreversible. Reversible fouling is attributed to materials that have formed on the membrane surface that can be removed by chemical or physical methods. Reversing the direction of flow

through the membrane, commonly known as backwashing is a common physical method of cleaning membranes (Gutman 1987). This hydrodynamic scouring (backwashing) restores a part of the initial flux that is lost due to fouling. Applying cleaning agents such as acids, bases, surfactants or chelating agents can also clean membranes.

Irreversible fouling is the permanent loss of flux through the membrane overtime that can be viewed as the portion of the initial flux that cannot be restored by hydrodynamic or chemical means (Lahoussine-Turcaud et. al. 1990). Irreversible fouling takes place when there is a rapid decline in flux in the initial period of filtration followed by a more gradual decline over an extended period of time. The accumulation of solute components on the membrane surface and inside the pores of the membrane causes permanent flux loss and irreversible fouling (Cheryan 1998).

Membrane fouling is caused by many factors. There are three facets of operation that can control fouling in membrane filtration. These are membrane material properties, solute properties, and the operating parameters of the system (Cheryan 1998).

2.1.5.1 Membrane Properties Affecting Fouling

A major factor that affects membrane fouling is whether or not the membrane is hydrophilic or hydrophobic. A hydrophobic material tends to sorb to those materials which are hydrophobic and to repel water. Sorption is most detrimental because it causes the most rapid cases of fouling. As a result, when aqueous feed streams are to be filtered, the ideal membrane is one that is hydrophilic due to its attraction for water and rejection of solute particles (Cheryan 1998). In fact, the hydrophilic membrane has been confirmed to show less loss in flux than hydrophobic membranes (Laine et al. 1989).

However, a major disadvantage of the hydrophilic membrane is that it is thermally unstable and is susceptible to chemical degradation. Therefore, most membranes used are hydrophobic, which are most susceptible to fouling (Maartens et al. 2000).

In addition, fouling of the membrane is also affected by the charge on the membrane surface. To a greater degree, irreversible fouling is caused by Van der Waals forces and electrostatic attractions (Gutman 1987). Many membranes are negatively charged thereby rejecting negatively charged solute particles by repelling them. On the other hand, if the particles are positively charged then the attractive force between the particle and the membrane will increase membrane fouling and the rate of flux loss (Cheryan 1998).

Furthermore, the surface roughness of the membrane is another factor that affects fouling. Some membranes are rough and comprise many protrusions which make them vulnerable to collecting particles on the surface, while membranes such as the cellulose acetate membrane are smooth and uniform and therefore leave little room for particle collection. As a result, smooth membranes are not very susceptible to membrane fouling.

Finally, membrane pore size plays a key role in determining the amount of fouling. Previous research indicates that membranes with large pore sizes have higher initial fluxes than those with small pore sizes. However, membranes with large pores will exhibit a greater overall flux decline over longer time periods. Large pores permit the smaller particles to lodge themselves deep into the membrane without necessarily passing through the membrane. Over an extended period of time, the pressure will have

to increase to maintain the flow rate, thus lodging the particles even deeper into the membrane. However, when using a membrane with pores much smaller than the particles being filtered, the particles will be retained at the surface where they can be removed by shear forces produced by the flow; thus preventing fouling (Cheryan 1998).

2.1.5.2 Solute Properties Affecting Fouling

The pH of the feedstream plays an active role in fouling the membrane. It determines the solubility of the components in the aqueous system. Furthermore, the pH affects the effectiveness of the membrane itself as described in section 3.1.2.

The type of solute compound in the feedstream also affects fouling. Membrane fouling is significantly increased by proteins, oils, and humic substances. Proteins are a culprit of fouling due to the charge density within the protein molecule, along with the varying degree of hydrophobicity, and its interaction with other molecules in the feedstreams.

Oils present a problem in that if the membrane is hydrophobic it will attract the hydrophobic oil, thereby coating the membrane and resulting in a rapid flux decline (Cheryan 1998).

In addition to oils and proteins, humic substances are weak acidic electrolytes that are hydrophobic at acidic pH values and as a result tend to deposit on hydrophobic membranes at low pHs. This also causes a major flux decline (Jucker and Clark 1994).

2.1.5.3 Operational Parameters Affecting Fouling

Transmembrane pressure and crossflow velocity are the two most important operational parameters that affect fouling. As transmembrane pressure increases the

permeate flux increases. Ultimately, the accumulation of solute will reach a limiting concentration on the surface of the membrane thereby causing the flux to become independent of the pressure. At this point the flux is controlled by the mass transport adjacent to the membrane and any increase in pressure will only increase the flux until the equilibrium is re-established between the rate of solute transport to and from the membrane. As a result, increasing the pressure may result in a lower flux due to compression of the cake layer, making it more impermeable.

Increasing the crossflow velocity in tangential modes of flows typically reduces fouling. High crossflow velocities increase the shear rate which aids in removing deposited material and reduces the hydraulic resistance of the fouling layer. However, if a high crossflow velocity is coupled with a high transmembrane pressure, larger particles in the feedstream will be lifted away from the membrane's surface, while the smaller particles stratify on the membrane surface. This results in fouling due to the particles tendency to lodge in the pores of the membrane.

Temperature is also an operational parameter of importance, but not very well understood. In theory, the flux should increase with increasing temperatures due to a decrease in viscosity and an increase in diffusivity. This phenomena is described by the Hagen-Poiseuille model. However, as described in section 1.2, temperatures can degrade and expand the pores of certain membranes thus reducing the effectiveness of the membrane (Cheryan 1998).

2.2 Pretreatment Methods

While the increase in reverse osmosis filtration is proliferating, methods for improving the efficiency of RO systems are also receiving more attention. One of the methods to achieve higher operational efficiency is pretreatment of the feed. Research on the removal of disinfection by-product precursors (DBP's), pesticides, heavy metals, natural organic matter (NOM), pesticides, and taste and odor components indicate that reverse osmosis cannot achieve significant removal of these compounds due to the high molecular weight cut-off ranges of the membrane in relation to those contaminants, which will cause fouling, thereby decreasing efficiency (Jacangelo et al. 1995).

Furthermore, fouling is a major operational concern in any RO process. Although it is not possible to completely eliminate fouling, pretreating the raw water can reduce the amount of fouling agents that would be exposed to the membrane. As a result, the implementation of pretreatment steps has been investigated. Two means of pretreatment are pre-coagulation and chemical addition.

2.2.1 Pre-coagulation

One method of pretreatment is coagulation of raw water. Lahoussine-Turcaud et al. (1990) found that if the coagulants ferric chloride and polyaluminum are used, then the amount of reversible fouling is greatly reduced. However, the rate of irreversible fouling was unaffected by coagulation which indicates that the small particles that were not removed by coagulation are the primary cause of irreversible fouling. The decrease in the rate of reversible fouling is attributed to the complexation of humic material with

relatively high molecular weight by products of metal hydrolysis. As a result it can be inferred that the humic material substance is what is resolubilized by chemical backwashing because after the raw water was pretreated using coagulation, the use of chemical addition proved to be ineffective in restoring the membranes performance characteristics (Lahoussine-Turcaud et al. 1990). Furthermore, it was observed that when using a aluminum chloride as a coagulant a reduction in fouling took place due to conditioning the filter cake, thereby making it easier to remove with the shear forces of the cross flow (Laine et al. 1990).

2.2.2 Chemical Pretreatment

Maartens et al. (1998) demonstrated that natural organic matter could easily be removed by filtration. However, its removal led to a rapid decline in the flux, which was caused by fouling. As a result, Maartens et al. (2000) investigated the chemical pretreatment of the membrane itself with the nonionic surfactants, Triton X-100 and Pluronic F108. In this study, the hydrophobic membranes were coated with hydrophilic surfactants. The results of the study were not good and led to little or no reduction in the amount of fouling (Maartens et al. 2000).

2.3 Methods of Salt Removal from Drinking Water

Generally speaking, desalination is accomplished in two different manners: thermal evaporation, and filtration.

2.3.1 Filtration

Filtration technology comprises reverse osmosis, nanofiltration, electrodialysis and electrodialysis reversal.

2.3.1.1 Reverse Osmosis

The first municipal reverse osmosis (RO) system was located in Coalinga, California. Today RO systems provide more than 50% of the world's desalination capacity and are the fastest growing technique for desalination. RO is used for all applications such as desalination of seawater, brackish water, and water reclamation projects. In fact, RO systems are even found under the sinks in residential households to purify water for drinking purposes.

Osmosis is the natural process of water diffusing through a semipermeable membrane to dilute a more concentrated solution. Water will continue to diffuse through the membrane until the concentration gradient between the two solutions is equal to zero. Reverse osmosis is the process of reversing osmosis, i.e. forcing a liquid to go somewhere that is thermodynamically unfavorable by utilizing pressure. This applied pressure must be greater than the osmotic pressure, which is proportional to the concentration of solute. Therefore, higher concentrations require higher pressure to "reverse" osmosis. Reverse osmosis relies on the water molecules ability to diffuse through the membrane more readily than the solute, thereby making it a pseudo-filtration process (Pankratz and Tonner 2003).

Generally, the operating pressure of a reverse osmosis operation is on the order of 500-1500 psi. The pore sizes of reverse osmosis membranes range from 0.0002-0.003

microns (Cheryan 1998). Reverse osmosis utilizes various types of membranes for different types of applications. For water quality and removal of pathogens, microfiltration and ultrafiltration is used. Nanofiltration is used to remove radionuclides, color, harness, and chemicals (RosTek Associates et al. 2003).

2.3.1.1.1 Seeded Reverse Osmosis

Currently, an enhanced form of reverse osmosis is being investigated, known as seeded reverse osmosis (SRO). During SRO, the feedwater is brought to saturation concentration with respect the solute of interest to remove. Once saturation concentration has been achieved, a seed crystal is added to the feed, thereby promoting precipitation of aqueous calcium sulfate onto the crystal instead of the membrane surface. Previous research has indicated that seeded reverse osmosis was a viable option for the treatment of mine service water in South Africa. Presence of high levels of calcium sulfate was considered as the characteristic of these mine waters that made the application of the conventional pretreatment systems costly and the recovery of the permeate less than waters not contaminated with calcium sulfate. The gold mine service waters also contained membrane foulants which made it difficult for reverse osmosis membranes to treat the water. A SRO process was incorporated into a pilot plant having a flow of 5 m^3/day for the treatment of the mine service water. Seeded reverse osmosis was observed to be capable of achieving a high recovery rate for scaling type of water (Harries 1985). Figure 2-9 shows the process of seeding the feed water with calcium sulfate crystals.

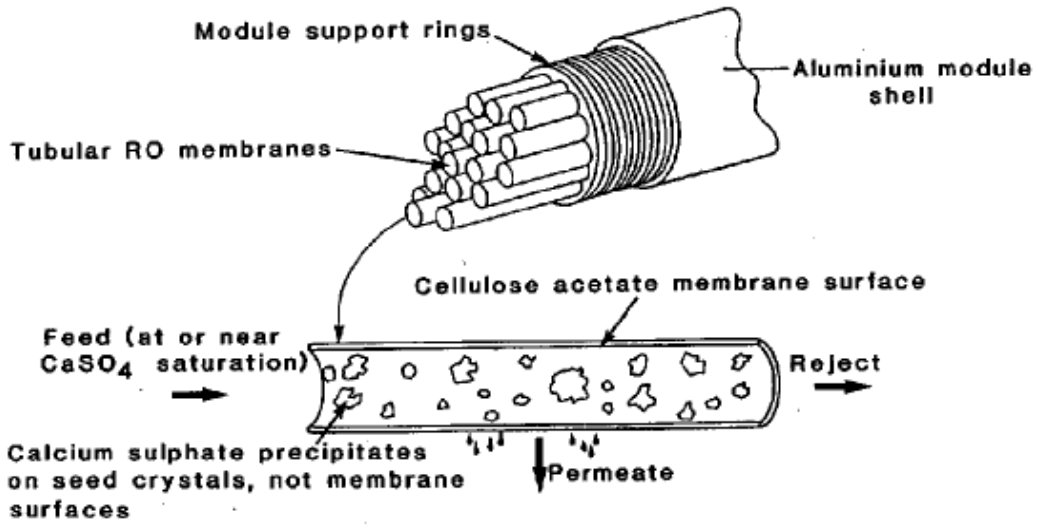

FIG. 2-9. Inside of a membrane in a SRO process (Harries 1985)

In the seeding process, calcium sulfate crystals were mixed with the feed water of a tubular reverse osmosis system. The aqueous calcium sulfate precipitated on the crystals rather than precipitating on the membrane surfaces, thus reducing the scale formation. The seed crystals were recycled from the brine into the feed water. The tubular membrane system was used for the enhanced form of reverse osmosis since the feed water to the reverse osmosis system had the solids percentage in the range of 3 to 10 percent, which would not be tolerated by the spiral or hollow fiber membrane modules (Harries 1985).

Figure 2-10 represents a schematic flow diagram of the seeded reverse osmosis pilot plant. The feed water was passed through a 50 micron cartridge filter and was sent to the seed recycle tank. From the recirculation tank, the feed liquid was put under a pressure of 145 psi and then passed through reverse osmosis module. The permeate was continuously removed from the reverse osmosis module and the remaining solution

became more concentrated. The salts in the concentrated solution then started precipitating on the crystals when their solubility's started reaching the limits of supersaturation. After passing the feed through the reverse osmosis module the reject brine was sent to the hydrocyclone. The hydrocyclone concentrated the solid seed material and recycled back to the recirculation sump.

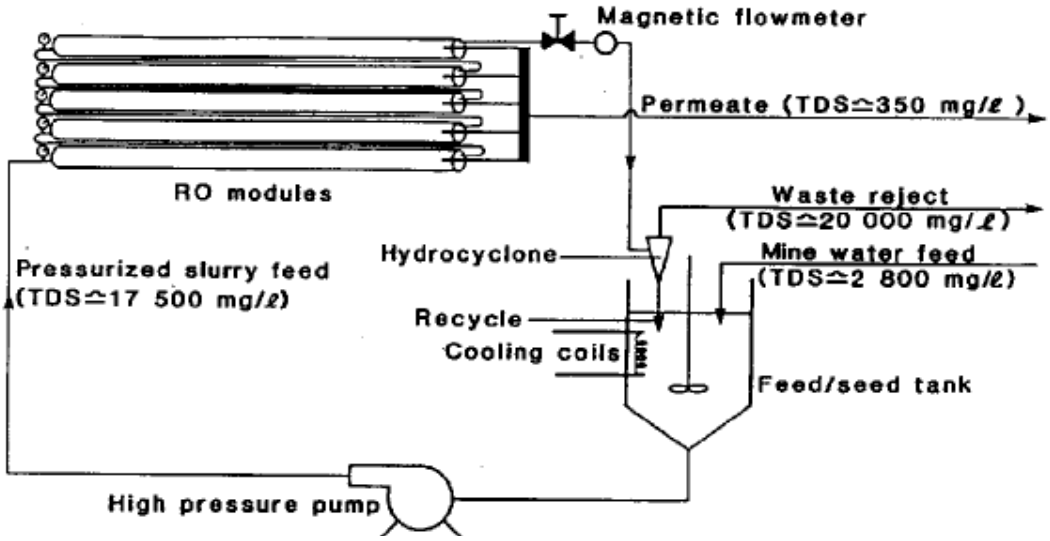

FIG. 2-10. Schematic flow diagram of the SRO pilot plant (Harries 1985)

The analysis of the SRO pilot plant for a period of 5000 hours indicated that the plant operated at 92 to 96 percent of recovery of the feed water without pretreatment. The results also indicated scaling of calcium sulfate did not play a key role in membrane fouling. However, a significant amount of membrane wear and hydrolysis was observed on the membrane which resulted in a decrease in salt rejection (Harries 1985).

Juby et al. (1996), Pulles et al. (1992), and Hess et al. (1988) also found this process to be technically viable with a high quality potable water product recovery above

95%, but with significant declines in flux. Later, Juby and Schutte (2000), observed a significant decline in flux and membrane hydrolysis. The membrane hydrolysis appeared to be a result of the exposure to the seed crystals. Furthermore, the team confirmed that research should be designated for the testing of membranes in SRO applications by stating, "Membrane materials other than CA may be more suitable and should be investigated."

2.3.1.2 Nanofiltration

Similar to reverse osmosis, nanofiltration is also a pressure driven process. However, the pressure required to drive the process is much smaller than that of reverse osmosis and is on the order of 150-450 psi. The pore sizes of nanofiltration membranes range from 0.0005 - 0.006 microns. Nanofiltration uses charged membranes with pores that are just larger than RO membranes, but not big enough to permit the permeation of organic compounds such as sugars. Furthermore, the nanofiltration membranes can separate dissociated forms of a compound from the undissociated form. For example, acetic acid can pass at low pHs, but the acetate ion which is formed at higher pH values is rejected. In summary, nanofiltration blocks larger molecules, divalent salts, dissociated acids, while passing monovalent ions, undissociated acids, and water. The main difference between nanofiltration and reverse osmosis is that nanofiltration does not retain monovalent ions and can operate at much lower pressures (Cheryan 1998).

2.3.1.3 Electrodialysis / Electrodialysis Reversal

Electrodialysis and electrodialysis reversal are electrochemical processes that have membranes which are selective for anions and cations. The feedwater is passed

through a double bounded membrane (one on each side of the feed water), one allowing the anions to pass and the other allowing the cations to pass, thus creating three streams: one with pure water, and the other two being ionic water or concentrate (RosTek Associates et al. 2003). Figure 2-11 gives a depiction of electrodialysis.

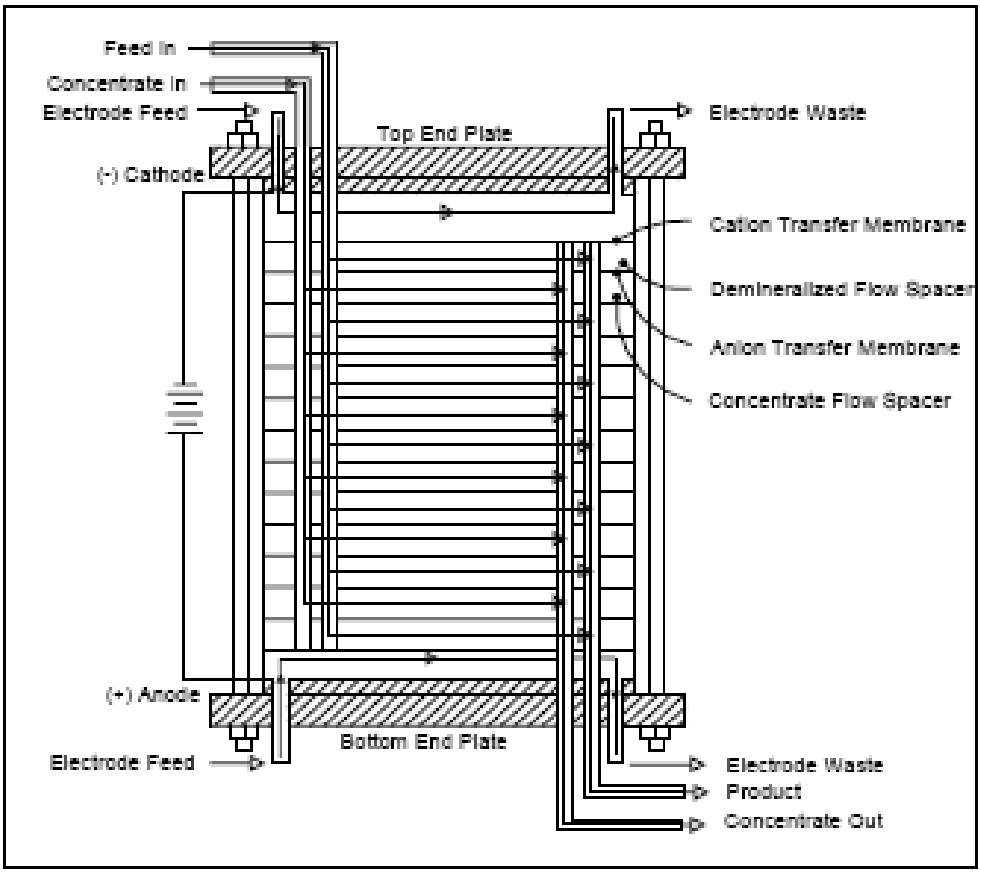

FIG. 2-11. Electrodialysis process (RosTek Associates 2003)

2.3.2 Thermal Evaporation

Thermal evaporation is simply the physical process of removing water from a salt solution, capturing the freshwater in a gaseous form, and retaining the salt in the solid or aqueous phases. Thermal technologies include multiple effect distillation, multiple stage flash distillation, and vapor compression.

2.3.2.1 Multiple Effect Distillation

Multiple effect distillation involves a network of horizontal heating coils which are arranged in chambers that each have successively lower pressure. The feed water is passed through each chamber vertically and a portion of the feed water vaporizes and the concentrate drops to the next chamber. This process continues until there is no water left to vaporize. The vapors are then condensed and the product water is removed. Often times, multiple effect distillers are arranged vertically and the feedwater actually passes through a tube that is immersed in a steam bath and therefore the heated seawater vaporizes leaving the reject brine behind (Cipollina et al. 2005). Figure 2-12 illustrates this process.

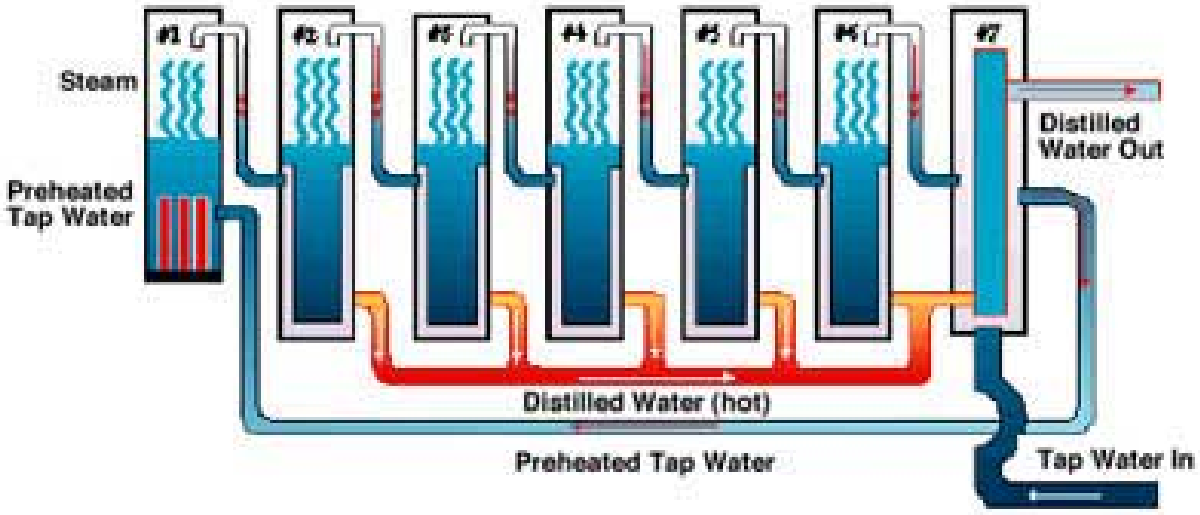

FIG. 2-12. Multiple effect distillation process (Pankratz and Tonner 2003)

2.3.2.2 Multiple Stage Flash Distillation

Multiple stage flash distillation is a simple process. The intake (seawater) is heated under a constant high pressure so that the sea water does not boil. The heated sea water is then instantaneously moved to a low pressure environment where the freshwater quickly turns into its gaseous state which is then moved to a condenser and can be collected. The brine concentrate is removed and collected (Al-Roumi et al. 1999). Figure 2-13 depicts multiple stage flash distillation.

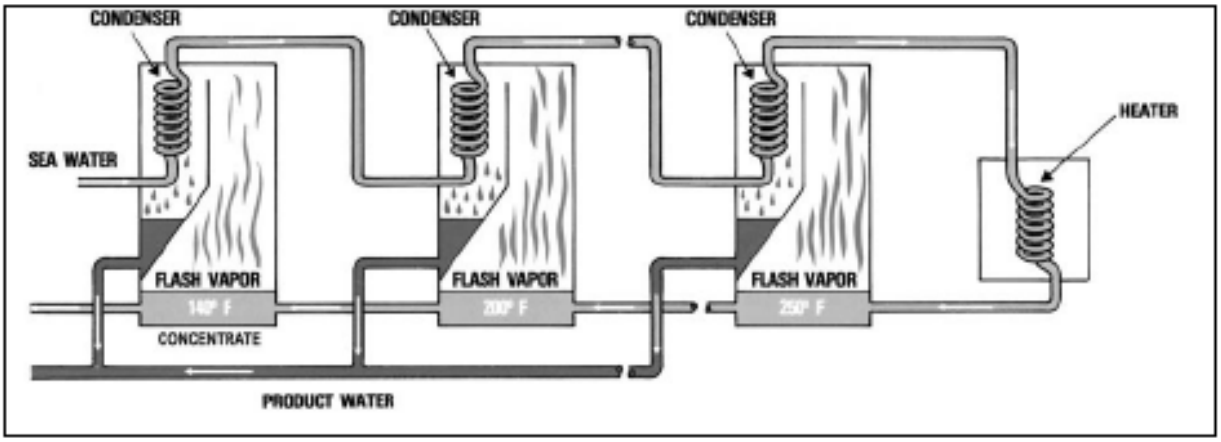

FIG. 2-13. Multiple stage flash distillation (RosTek Associates 2003)

2.3.2.3 Vapor Compression

Vapor compression is probably the most efficient of the thermal processes because it uses the product as an energy source for the process. Again, the saltwater is sprayed over a manifold of heated horizontal tubes which causes the salt water to vaporize while the brine reject collects at the bottom of the unit. The vapor is then heated further and compressed creating a extremely hot gas. The gas is then forced in the manifold of horizontal tubes and acts as the heat source. As the vapor transfers its heat to the incoming saltwater it cools and condenses to form freshwater (Bahar et al. 2004). Figure 2-14 depicts vapor compression.

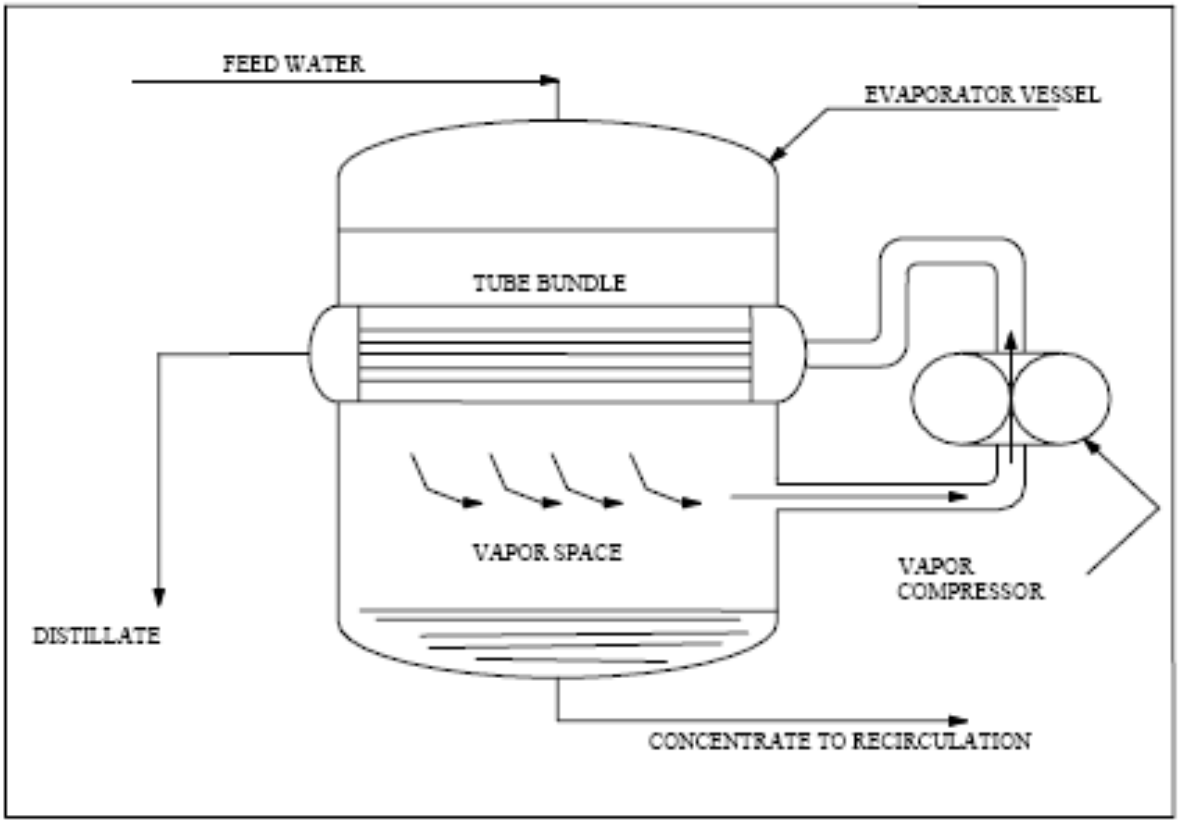

.

FIG. 2-14. Vapor compression process (RosTek Associates 2003)

2.4 Calcium Sulfate

Calcium sulfate is a natural occurring salt that is formed during the formation of rock. Much of the southwestern United States' surface water is contaminated with calcium sulfate, and can therefore be described as brackish water. For example, the Brazos River basin's surface waters are contaminated with high levels of calcium sulfate due to the geological formations that contain it and that underlie portions of the upper watersheds in the Brazos, Pecos, Colorado, Canadian, Red, and Arkansas Rivers. The primary source of salt contamination comes from groundwater emissions in the upper

basin comprising the Salt Fork Brazos River watershed, and portions of the Double Mountain Fork Brazos River and North Croton Creek watersheds (Karama and Wurbs 1995).

Calcium sulfate is a white solid which is also referred to as gypsum. It has a molar mass and density of 136.142 g/mol, 2.96 g/cm^3 with chemical formula of $CaSO_4$. In water, calcium sulfate will readily dissociate, until the product of the activities of calcium and sulfate equal $10^{-4.85}$. If the product is higher than $10^{-4.85}$ the reaction would be reversed producing solid calcium sulfate. The concentrations of calcium and sulfate in a solution formed by dissolving calcium sulfate until equilibrium would be approximately 3.8 mM.

The laboratory form of calcium sulfate is produced by desiccating gypsum into its anhydrous form and is known as anhydrite, or commercially as Drierite. This calcium sulfate form has a solubility of 17.6 mM in water at 20 degrees Celsius.

Calcium sulfate has a reverse solubility curve, meaning that the solubility decreases with an increase in temperature. Therefore, higher temperatures lead to a greater rate of precipitation and greater potential for scale formation. (Benjamin 2002). For this research, the activity coefficient assumed to be one for simplicity and therefore the terminology, “activity” and “molar concentration” will be used interchangeably. Also, the anhydrous form of calcium sulfate will be used to simulate the SRO process, which means that the maximum concentration of calcium sulfate should not exceed 2.4 g/L if the temperature is maintained at 20 degrees Celsius.

2.4.1 Precipitation/Crystallization/Nucleation

Generally, precipitation occurs if the solute has exceeded its saturation concentration levels and crystals exist on which to precipitate. During precipitation, the aqueous solute turns into its solid phase. However, precipitation cannot occur readily without a surface to deposit on, and therefore causes fouling to occur on the membrane surface during filtration operations.

Unlike crystal growth, nucleation does not need a surface, because it is the process of forming a solid particle. Nucleation and crystal growth occur if and only if the solute is supersaturated, but nucleation typically requires much higher levels of supersaturation to occur at a reasonable rate. During nucleation, a nucleus is formed and then further precipitation onto that nucleus occurs by crystallization.

Crystallization is the process of solid growth from the aqueous solute. In fact, this is the phenomena that SRO exploits. The goal of seeded reverse osmosis is to prevent membrane fouling while achieving the same levels of treatment of a conventional reverse osmosis system. As described in the section 2.1.1.1, the very reason why seeded reverse osmosis works to prevent fouling is that the seed (or crystal) acts as a surface of precipitation, instead of the membrane surface. The key is to maintain the solution at or above saturation concentration of the solute to be removed. The crystals work as precipitation sites for the saturated calcium sulfate. The quantity of the crystals to be maintained is such that the total surface area of the crystals promotes a rate of precipitation that is high enough to keep the degree of saturation ($[Ca^{+2}][SO_4^{-2}] / K_{sp}$) low enough to avoid nucleation on the membrane surface. As the crystals reach a

certain size, they break up into smaller particles due to the shear forces of the flow. Ultimately, they will settle out of solution, resulting in the solids removal from solution (Benjamin 2002).

3. METHODS, MATERIALS AND PROCEDURES

3.1 Apparatus Setup

The membranes were exposed to a saturated solution of calcium sulfate in a SEPA CF II cell manufactured by GE Osmonics. The cell has an effective membrane area of 140 cm^2 with a hold-up volume of 70 mL. The cell can withstand a pressure of 1000 psig, and therefore is suitable for reverse osmosis applications. This lab scale crossflow membrane filtration unit provides fast and accurate performance data with small lab scale features such as expense, time, and membrane surface area. Its design simulates the flow dynamics of full scale operation. It is the most suitable technology for membrane testing. The actual SEPA CF II cell by GE Osmonics used for this SRO simulations is seen below in Figure 3-1.

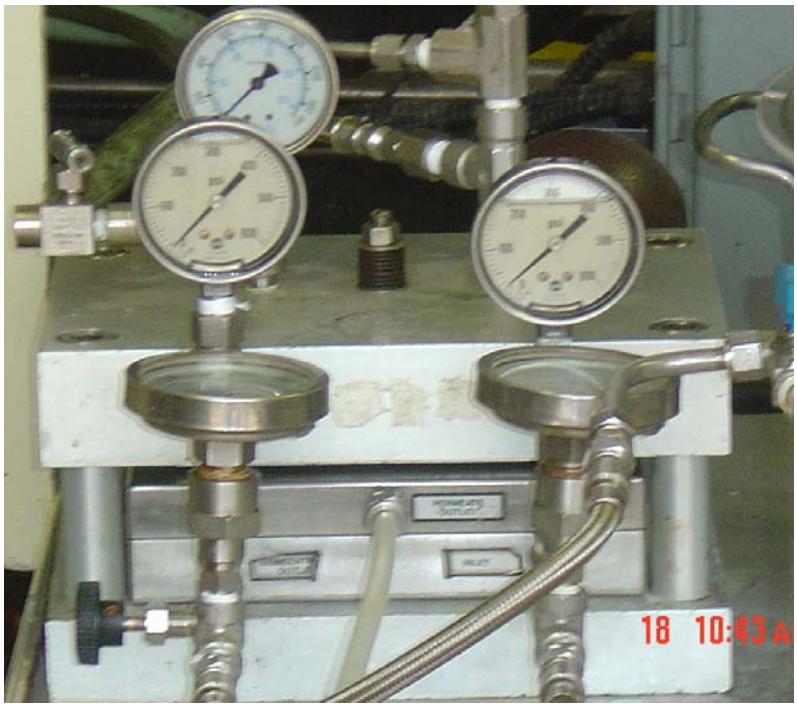

FIG. 3-1. The SEPA CF II Cell by GE Osmonics used for seeded reverse osmosis simulations

Contrary to what typical full scale operations would use, only one RO plate membrane module was used in these experiments, because the objective of the research was to investigate membrane characteristics and not other characteristics of a RO/NF system. The reject was recycled back into the feedtank, thus maintaining oversaturated conditions of calcium sulfate in the tank. The permeate was also recycled to ensure that all membranes were exposed to the same concentration of suspended solids, regardless of the permeate flux of each membrane. The feed tank maintained a seeded calcium sulfate solution with crystals that are smaller than 75 microns, or that pass the #200 sieve shaker. The concentration of suspended solids was 20 g/L or 2 % to simulate typical

SRO applications. The plate membranes received the same feed and operate under that particular membrane's optimum conditions in a constant pressure declining flux mode. The pressure was applied using a compressed air tank next to the apparatus. Constant pressure was maintained by adjusting a pressure relief valve located at the concentrate outlet pressure gauge. A diagram and flow diagram of the whole apparatus is shown below in Figure 3-2 and Figure 3-3.

The feed was pumped through the system using a Hydra-Cell, high pressure, low flow, model number D10-04 pump which was purchased from Texas Pump & Equipment Co. The pump is shown below in Figure 3-4. In order to prevent pulsation, pressure was added to the pump outlet to dampen the pressure fluctuation between the suction and driving forces. This pressure was maintained by opening and closing a valve located on the tube going from the air tank to the dampener.

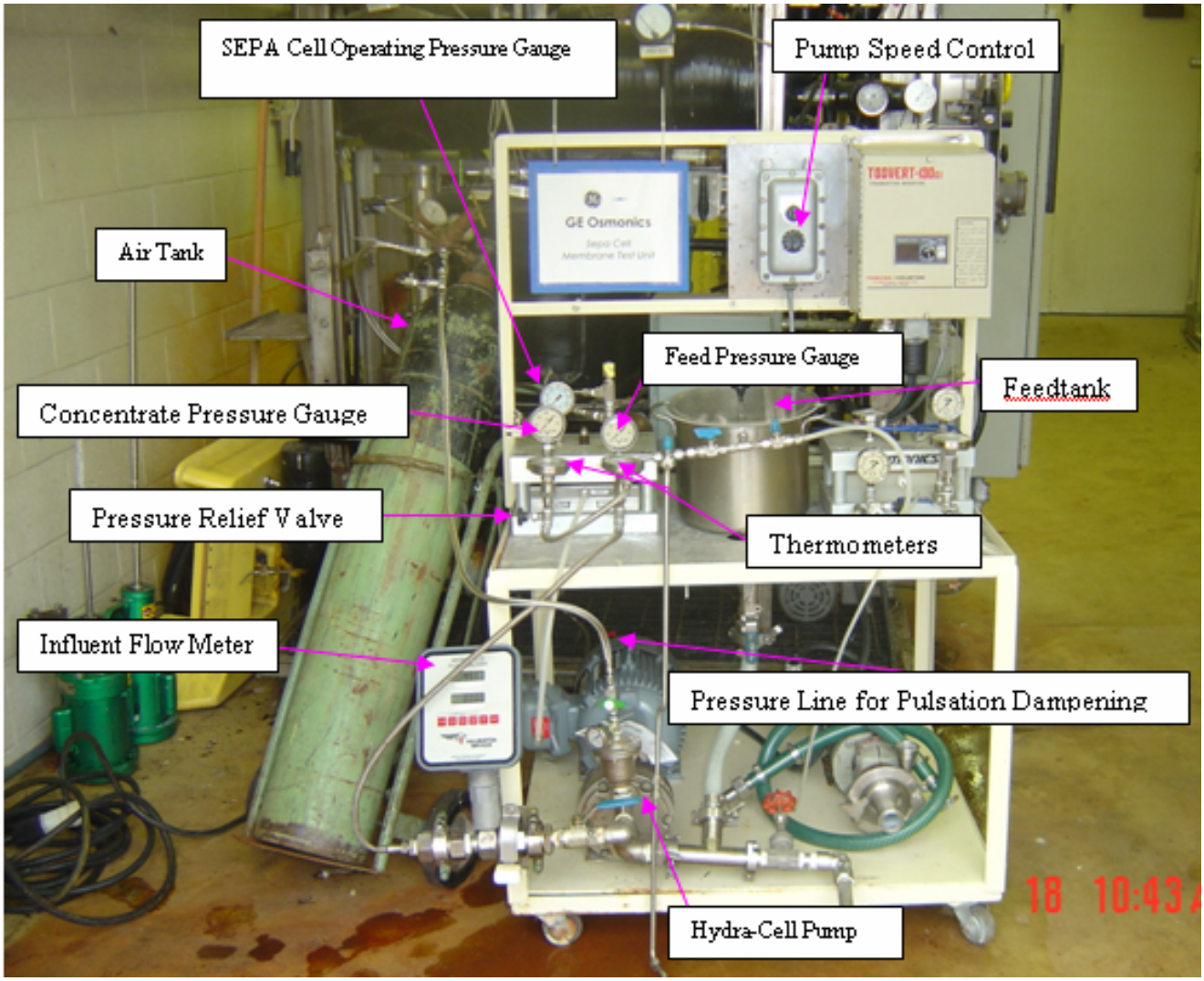

FIG. 3-2. The apparatus setup with all components

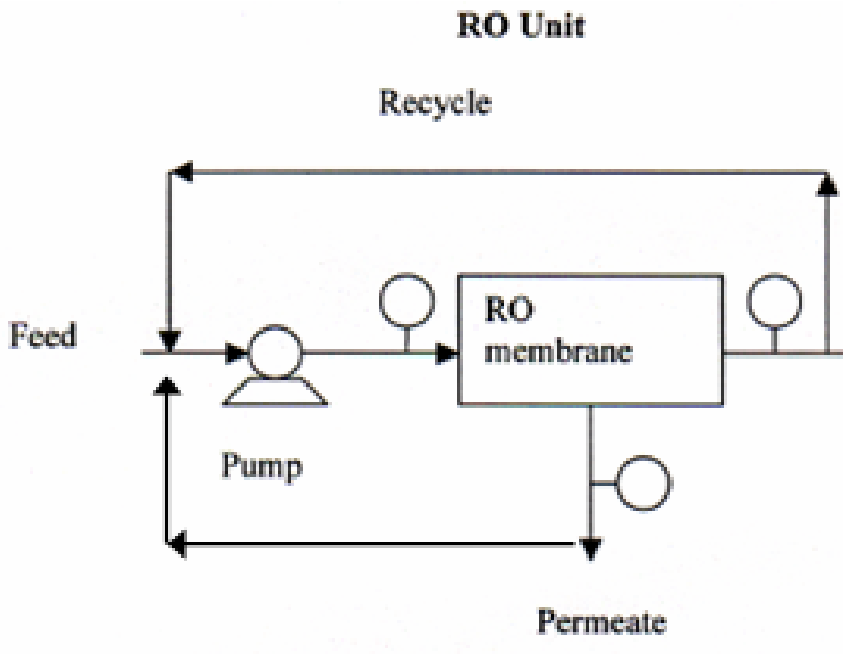

FIG. 3-3. Apparatus flow diagram

FIG. 3-4. Hydra-Cell, Model # D10-04 pump used for SRO simulation

3.2 Aqueous Calcium Sulfate Solution

A saturated solution of calcium sulfate was prepared and exposed to the membranes. At room temperatures, this corresponds to a calcium sulfate concentration of approximately 2.4 g/L. However, the solutions was prepared by dissolving the calcium sulfate into solution as it was being cooled, thereby increasing the solubility to ensure saturated conditions at room temperature, which is the temperature that the experiments were conducted. The addition of calcium sulfate was stopped upon observation of solid phase calcium sulfate settling at the bottom of the mixing vessel. At this point, the solution was saturated and decanted into the feedtank vessel. After the

feed tank was filled with the saturated calcium sulfate solution, a predetermined amount of calcium sulfate was added to the tank to obtain a concentration of 20 g/L (2 %).

3.3 Operational Paramaters / Technique

Each membrane was tested twice in an experiment for 4 hours under optimal operating pressures, pH values, and inflow volumetric flow rate for that particular membrane. Operating at conditions that meet a particular membranes specification reduced the amount of variability in making conclusions about which membrane is most suitable for seeded reverse osmosis processes. Generally, in order to control an experiment that is used to make comparisons among two or more things, similar operating conditions are desired. However, membranes have different optimum operating conditions and therefore in order to draw conclusions based on their performance it is necessary to operate the system at that particular membranes optimum operating conditions.

The calcium sulfate solution was first pumped through the plate membrane at a pump speed that initially correlates to a flowrate of 1 gallon per minute (gpm) which is close to the optimum flow, as specified by the manufacturer (GE Osmonics). Table 3-1 shows the optimum pressures and flowrates for the different membrane materials. The pump speed was gradually increased until the optimum inflow rate was reached. This ensured limited agitation and adequate circulation of feed.

Once the desired flow rate was achieved, the back pressure relief valve on the concentrate outlet was closed until the optimum pressure was reached as specified by GE Osmonics. The pump speed and back pressure valve had to be tweaked until both the

flow and pressure were at their optimum values. This was an iterative process because the flow and pressure were directly related to eachother. The optimum pressure was found based on pure water's flux at different operating pressures. The inlet and outlet pressure gauges of the membrane were monitored during the duration of the simulation and the back pressure valve located on the concentrate outlet was adjusted to maintain constant pressure.

The permeate flow rate, influent flow rate, and concentrations were monitored every 15 minutes for the first hour and then every 30 minutes for the remainder of the test. Membranes that performed well, were run in the SRO simulation process for a period of 8 hours at their maximum specified pressure to determine their lifetime. The maximum pressure corresponded to 600 psi for the cellulose acetate membrane and 500 psi for the thin film membrane.

TABLE 3-1. Optimum operating pressures and flow rates for different membrane

OPTIMUM OPERATING PRESSURES AND FLOW RATES FOR DIFFERENT MEMBRANE MATERIAL			
Membrane	Process	Optimum Pressure (psig)	Optimum Flow Rate (L/min)
Cellulose Acetate	Reverse Osmosis	420	3
Polyamide (low MWCO)	Reverse Osmosis	225	3
Polyamide (high MWCO)	Reverse Osmosis	115	3
Cellulose Acetate	Nanofiltration	220	3
Thin Film	Nanofiltration	100	3

3.4 Data Retrieval

The following data was monitored simultaneously throughout the course of each simulation at specified intervals.

3.4.1 Influent Flow

The influent flow was measured and monitored using a Halliburton Service Flow Analyzer, Model MC-II and is shown in below in Figure 3-5.

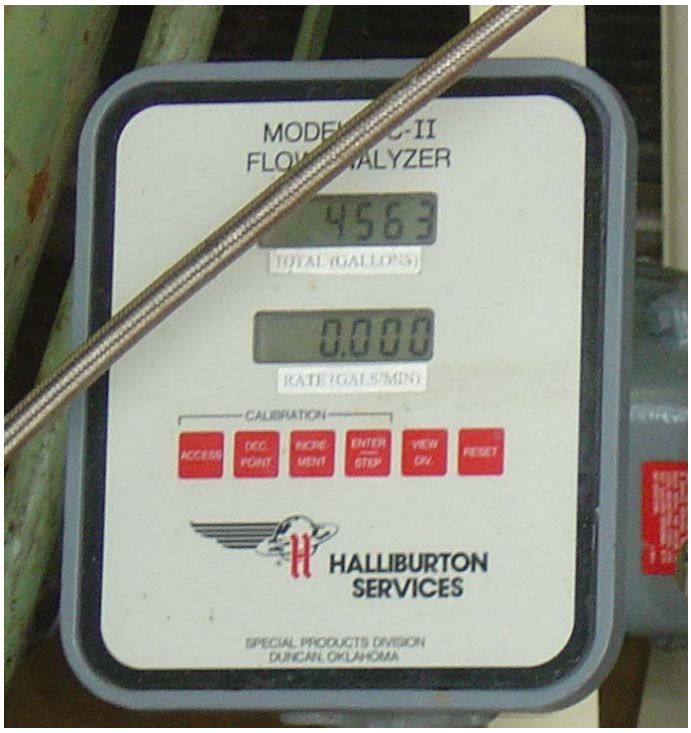

FIG. 3-5. Halliburton service flow analyzer – Model MC-II

3.4.2 Calcium Sulfate Concentration

The concentration was measured and monitored using a Corning conductivity meter, Model 441, and is shown below in Figure 3-6. Conductivity is not an absolute measurement of concentration, but it is a relative comparison that can be used against a standard to give an approximate concentration. It therefore provides an approximate measure of the amount of salt in the water when there is a mixture of ions. However, the conductivity is very accurate for describing the amount of ions in solution when there is only one pair of ions (Ca^{+2} and SO_4^{-2}). The conductivity increases with higher

concentrations of dissolved salts. Pure water is a poor conductor, while seawater has a high conductivity (RosTek Associates 2003).

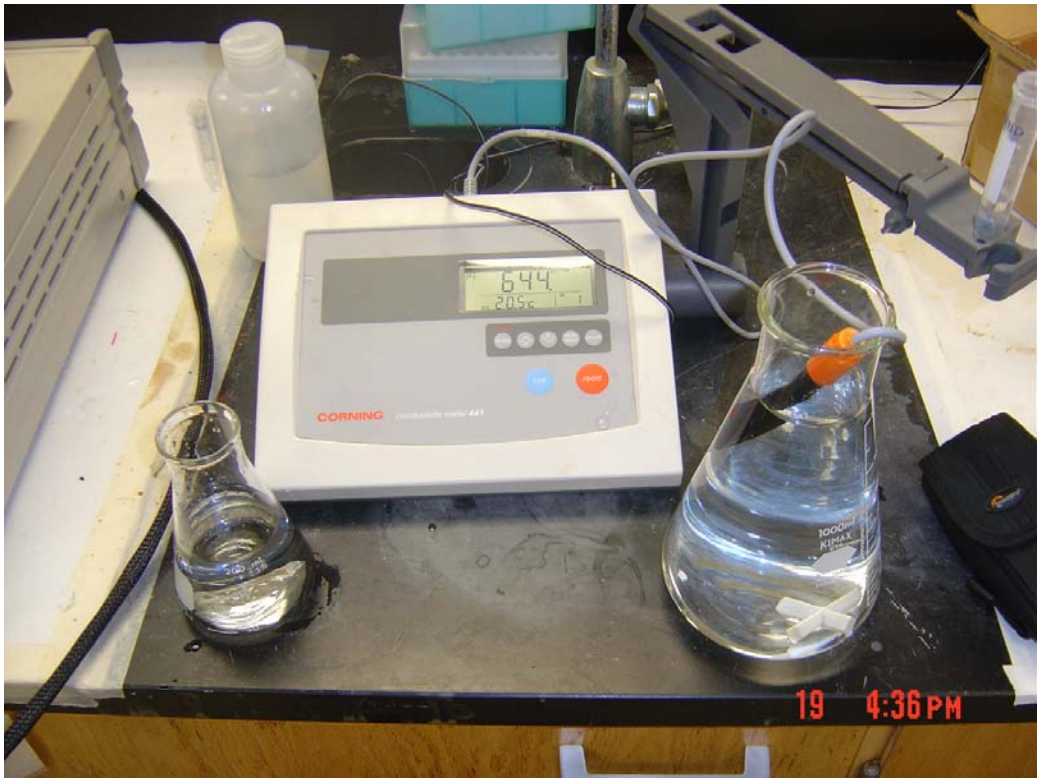

FIG. 3-6. Conductivity meter – Model 441

The conductivity was calibrated to correspond to calcium sulfate concentrations. As a result, conductivities were measured during the experiment and concentrations were determined from the calibration regression. The calibration curve ranging from those concentrations that are below the saturation concentration along with its regression are shown below in Figure 3-7.

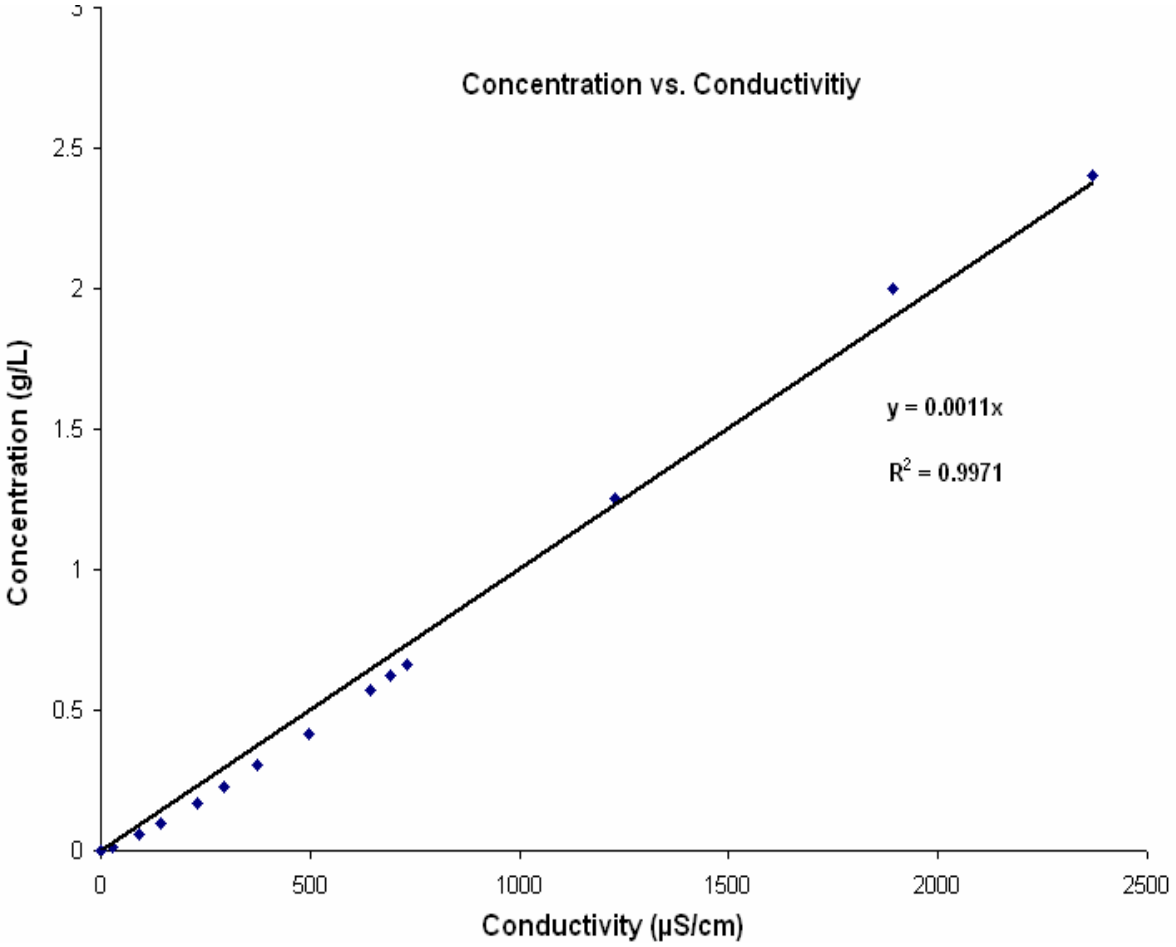

FIG. 3-7. Calcium sulfate concentration vs. conductivity

The plot does not include those concentrations higher than 2.7 g/L (this concentration is around the saturation concentration that concurs with literatures saturation concentration for commercial calcium sulfate) due to inaccuracies in using a conductivity meter for concentrations that exceed solubility concentrations. During the simulations, samples of the feed and product were taken in order to determine the calcium sulfate concentration in each.

3.4.3 Permeate Flow

The permeate flow was measured using a graduated cylinder and stopwatch. The time was monitored for a predetermined volume of permeate to be achieved.

3.4.4 Membrane Integrity

An autopsy of the membrane's integrity was observed using optical microscopy with an Olympus microscope, Model 52-PT and is seen below in Figure 3-8. After undergoing optical microscopy, the samples were taken to the microscopy and imaging center located near the Trigon on Texas A&M's campus to under go environmental scanning electron microscopy. The environmental scanning electron microscope, Electroscan ESEM E-3 is seen below in Figure 3-9.

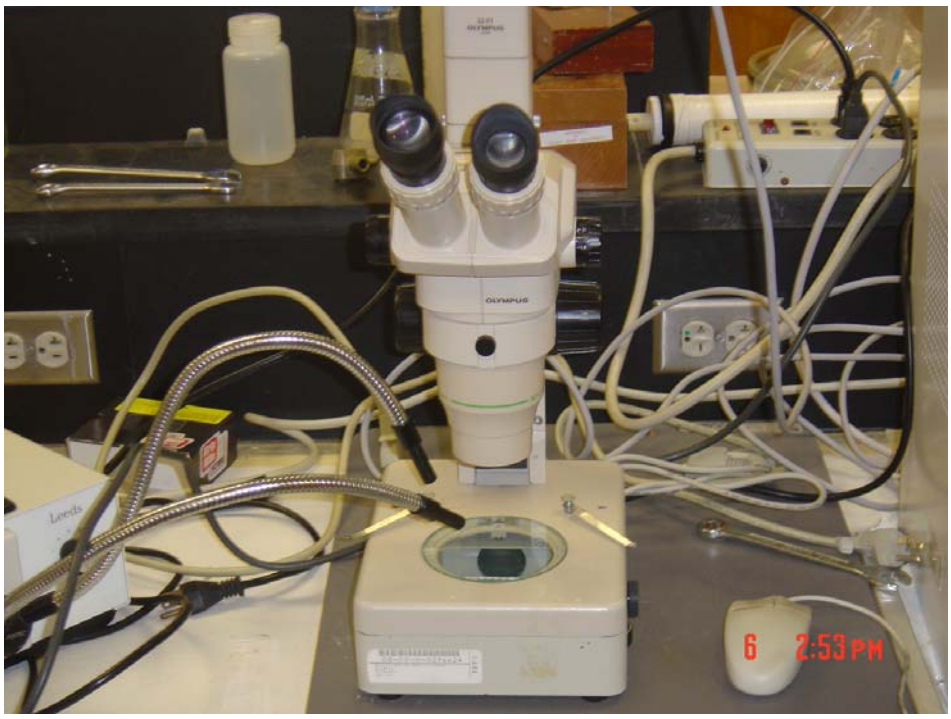

FIG. 3-8. Optical microscope used for observing membrane wears

FIG. 3-9. ESEM microscope used for observing membrane wear/fouling

3.5 Analysis

The ideal membrane would be one that performed with maximum water flux, salt rejection, and lifetime, while using minimum transmembrane pressure to operate the process. The efficacy of the membranes was evaluated based on recovery, effectiveness, membrane integrity, fouling, water mass transfer, and solute mass transfer.

3.5.1 Recovery

Recovery is the percentage of the feed that is treated and is defined as the permeate flow divided by the feed flow and multiplied by 100. Striving to achieve ZLD (i.e., maximizing the recovery) will increase efficiency of the system by utilizing more of the feed, thereby reducing the volume of the reject. Generally, the recovery will

decrease with time due to fouling, and therefore a model of recovery vs. time was developed for all membranes and the coefficients were compared. The equation for recovery is shown in Equation (3-1).

Equation 3-1: Water Recovery Equation

$$R = \frac{Q_p}{Q_F}(100\%) \qquad (3\text{-}1)$$

R = percentage of feed that is turned to water (%)

Q_p = product flow rate ($\frac{m^3}{s}$)

Q_F = feed flow rate ($\frac{m^3}{s}$)

3.5.2 Effectiveness

In determining whether or not membrane hydrolysis is occurring, the concentrations of Ca^{+2} and SO_4^{-2} in the permeate were monitored with time for all membranes. If there are relatively high concentrations of both these ions, then the conclusion that part of the membrane's integrity has been destroyed is valid. The concentration of calcium sulfate was measured using a calibrated conductivity meter. For each run, the effectiveness was determined and comparisons were drawn based on significant differences in the models. Effectiveness was computed by subtracting the permeate calcium sulfate concentration from the influent calcium sulfate concentration and dividing the difference by the influent concentration. This was plotted with time and the coefficients were determined and then compared for all membranes.

3.5.3 Membrane Integrity

At the end of each operational run, the membranes were removed from the SEPA cell and examined by optical microscopy (OM) and scanning electron microscopy (SEM). These observations aided in drawing conclusions on the effects of particle scour on the integrity of the membrane. This is important in the seeded reverse osmosis processes because the membrane's integrity is prone to destruction due to the high solids concentrations coming into contact with the membrane surface (Chen et al. 2000). The integrity was compared for all membranes.

3.5.4 Fouling

In the operation of a membrane filtration system, fouling marks itself as a loss in flux with time of operation by a reduction in the permeability of the membrane (Cheryan 1998; Gutman 1987). Fouling can therefore be measured indirectly using the net driving force or the flux.

3.5.4.1 Flux

The flux was measured indirectly using the percentage recovery. It is defined as the permeate flow divided by the membrane surface area. The flux is used in the calculation of water mass transfer, which is used in the analysis.

3.5.4.2 Net Driving Force

The net driving force was used in the water mass transfer coefficient equation which was used to characterize the amount of fouling that was occurring within a membrane. It is a measure of the energy required to produce water. Fouling increases the net driving force required to maintain a constant flux (in this experiment the flux was

not held constant). The net driving force was calculated by taking the average of the feed and concentrate pressures and subtracting the permeate pressure and change in osmotic pressure as seen in Equation (3-2) below:

Equation 3-2**:** Transmembrane Pressure Computation

$$P_{tm} = \frac{P_i + P_o}{2} - P_p - \Delta\pi \qquad (3\text{-}2)$$

where,

P_{tm} = transmembrane pressure

P_i = pressure at the inlet of the membrane module

P_o = pressure at the outlet of the membrane module

P_p = filtrate pressure

$\Delta\pi$ = change in osmotic pressure across membrane

The outlet and inlet pressures were monitored using pressure gauges by GE Osmonics located on the concentrate stream. The transmembrane pressure was maintained constant by adjusting a pressure relief valve on the concentrate outlet. The osmotic pressure was monitored at 15 minute time intervals and 30 minute time intervals by using the concentration of solute in the feed and the concentration of solute in the permeate. The difference in osmotic pressure was found by subtracting permeate osmotic pressure from the feed osmotic pressure. Due to the flux being very small, the influent salt concentration was about equal to the retentate salt concentration and therefore, the average osmotic pressure in and out of the feed side was not necessary to use as the feed osmotic pressure. The osmotic pressure was found using the osmosis equation as seen below in Equation (3-3).

Equation 3-3**:** Osmotic Pressure Equation

$$\pi = iMRT \qquad (3\text{-}3)$$

where,

π = osmotic pressure

i = van 't Hoff factor

M = molarity

R = gas constant

T = temperature

3.5.5 Water Mass Transfer

Water mass transfer (K_w) plays a key role in predicting long term membrane permeate production. It is calculated by dividing the flux of water by the net driving force. It is defined by Equation (3-4).

Equation 3-4: Water Flux Equation

$$Q_w = K_w(P_{tm}) \qquad (3\text{-}4)$$

Where,

P_{tm} = transmembrane pressure differential (psi)

K_w = water mass transfer coefficient $(\frac{m^3}{m^2*s*psi})$

Q_w = water flux through membrane $(\frac{m^3}{m^2*s})$

The water mass transfer coefficient will decrease with time if operating at constant conditions. The coefficient is useful because it incorporates the production rate of water and the net energy required to produce it.

3.5.6 Solute Mass Transfer

The solute flux was calculated by multiplying the permeate volumetric flow rate times the concentration of calcium sulfate in the permeate. The relationship between the solute flux and the concentration difference across the membrane is shown in Equation (3-5).

Equation 3-5**:** Solute Flux Equation

$$Q_s = K_s(\Delta C) \qquad (3\text{-}5)$$

Where,

Q_s = mass flow of salt through membrane (mg/s)

K_s = membrane salt permeability coefficient (L/s)

ΔC = salt concentration difference across the membrane (mg/L)

The product of the permeate volumetric flow and calcium sulfate concentration was divided by the differences in concentration between the two sides of the membrane. The solute mass transfer coefficient was plotted versus time and the coefficients was determined and compared for each membrane. The solute flux was not normalized by dividing by the area of the membrane due to each membrane having the same effective area. However, if the goal of this research was to characterize the membrane for full scale operation, then the solute flux would have been normalized by dividing the solute flux by the effective membrane area. Also note that in order to be consistent with

literature, the letter “Q” is used to denote a mass flow which is typically seen elsewhere to denote volumetric flows.

4. RESULTS AND DATA DISCUSSION

4.1 Reverse Osmosis – Cellulose Acetate Membrane

4.1.1 K_w, Salt Rejection, and Membrane Wear

The water mass transfer coefficient and salt rejection are plotted against time in Figure 4-1 and Figure 4-2, respectively. Figure 4-3 and Figure 4-4 shows microscopic views of the membrane after the experiment was conducted.

The experimental results in Figure 4-1 indicate that there was no fouling for the RO-CA membrane. The water transport coefficient remained steady at approximately 0.0002 mL/(cm^2*psi*min) under the constant pressure applied throughout the duration of the test. Limited fouling indicates that this membrane is well suited for the treatment of calcium sulfate ions. This result corroborates the previous research done by Harries (1985) where there was little or no fouling observed. However, other literature states the contrary, i.e., that cellulose acetate membranes are highly susceptible to membrane fouling due to its asymmetric structure, where compaction occurs when the thin dense layer of the membrane becomes thicker after merging with the porous substructure (Cheryan 1998).

The salt rejection shown in Figure 4-2 ranged from approximately 99.4% to 99.7% and remained steady throughout the four hours of operation. This result concurs with Hess et al. (1988) who reported rejections to be in the same range. The plot appears to be deceiving because the range of rejection is so small that it magnifies a small change in rejection. The plot that uses a large range of rejection and therefore decreases

the visual magnified difference can be seen in section 5.1.2. The slight gradual increase in rejection might be attributed to the membrane not being completely intact with the O-ring during the first 15 minutes of the experiment. It could also be attributed to the heavy pressure and its tendency to compact the membrane layers and thereby decreasing the pore spaces. It is not likely for the increase to be attributed to suspended particles/ion impregnation of pore spaces to CA's smooth surface, without many protrusions.

The membrane autopsy shown in Figure 4-3 and Figure 4-4 of the cellulose acetate membrane shows some spots that appear to be abraded and this observation also concurs with the literature. Cheryan (1998) reported that CA membranes are not resistant to degradation. The abrasions can be attributed to the solid salts cross flow shearing affects on the membrane.

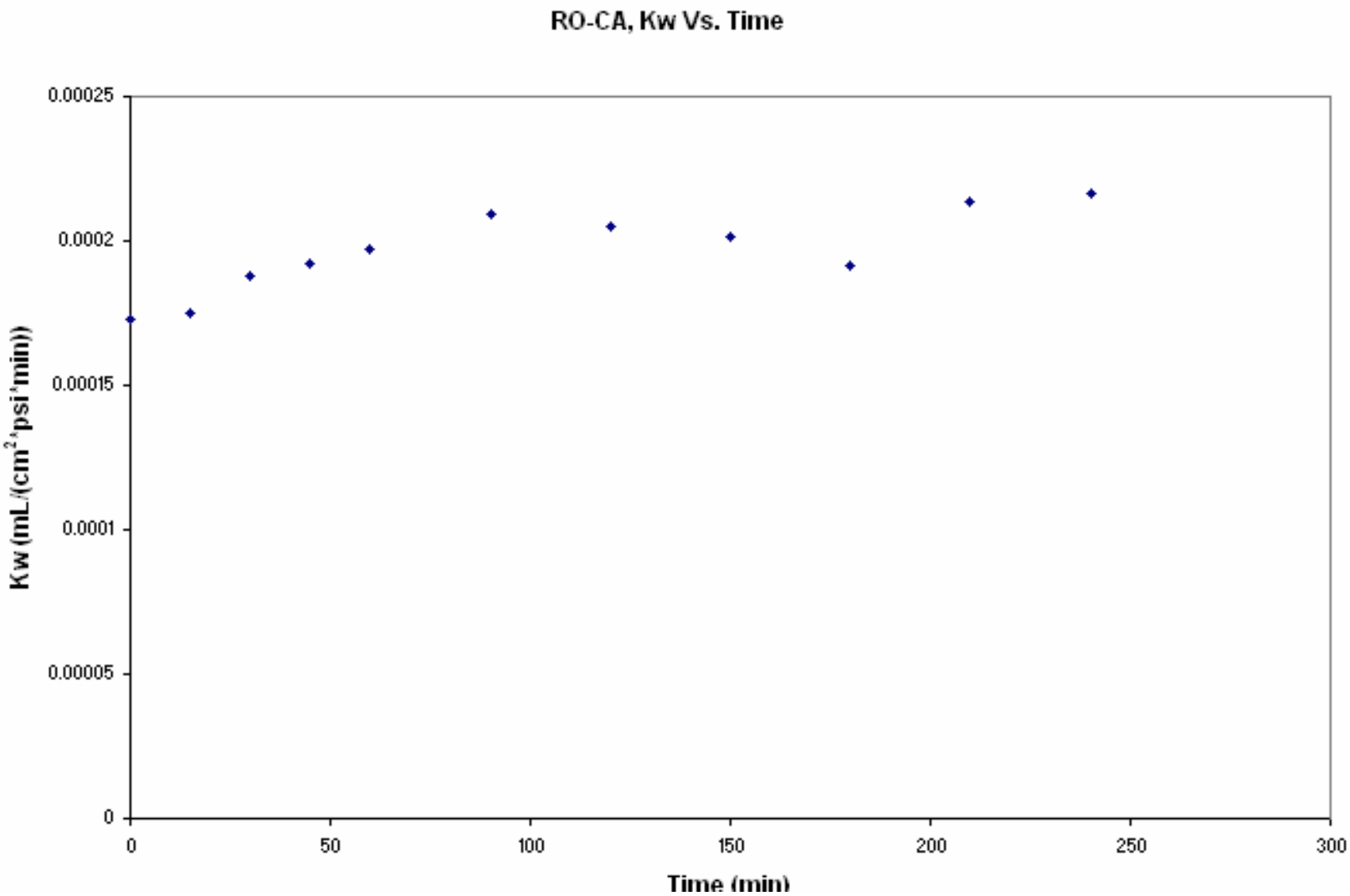

FIG. 4-1. RO-CA, K_w Vs. Time

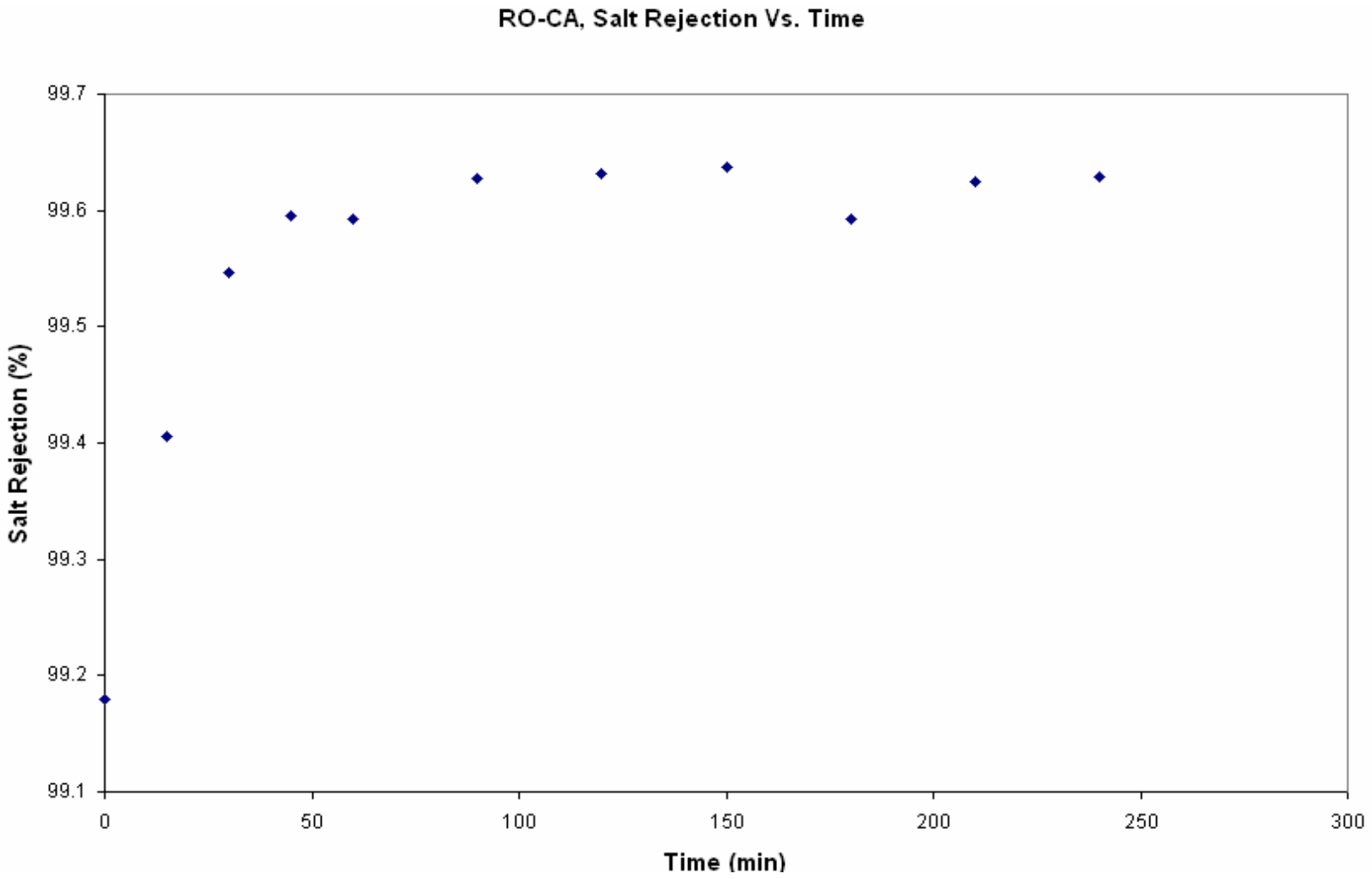

FIG. 4-2. RO-CA, Salt Rejection Vs. Time

FIG. 4-3. RO-CA, membrane wear viewed using optical microscopy

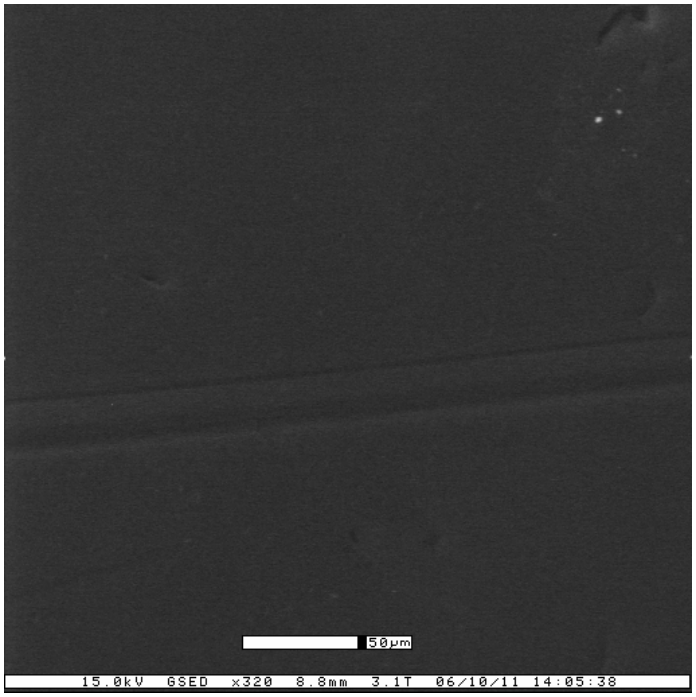

Virgin Membrane

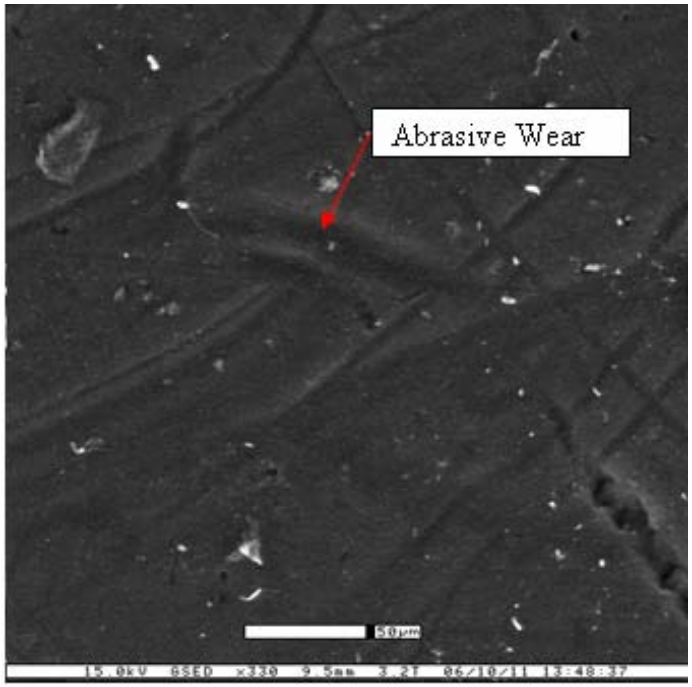

Membrane after Simulation

FIG. 4-4. RO-CA, membrane wear viewed using scanning electron microscopy

4.2 Reverse Osmosis – Polyamide Membrane (High MWCO)

4.2.1 K_w, Salt Rejection, and Membrane Wear

The water mass transfer coefficient and salt rejection are plotted against time in Figure 4-5 and Figure 4-6, respectively. Figure 4-7 and Figure 4-8 shows microscopic views of the membrane after the membrane had undergone the experiment.

The experimental results shown in Figure 4-5 depict fouling. The water transport coefficient decreases with time while a constant transmembrane pressure was continuously applied. It decreases from approximately 0.00075 to 0.00025 mL/(cm^2*psi*min). This is about a 67 % decrease over a four hour period. The decrease was most probably imputed to the scaling that is observed (viewed as white speckles) in Figure 4-7. The water transport coefficient decline could also be attributed to the large calcium and sulfate ions clogging up the inner pore spaces of the membrane, but this is not probable due to the rejection decrease. According to literature, the fouling is attributed to the polyamide's rough surface, thereby providing many locations for suspended matter to lodge into the protrusive surface (Cheryan et al. 1998). Typically, if accumulation of ions within the membrane were the culprit, an increase in rejection would occur, but in this case, the rejection decreased. One possible explanation for the simultaneous water transport coefficient and rejection decline is that as the flux of pure water decreased, the mass transport of ions through the membrane remained constant, thereby increasing the concentration of ions in the permeate.

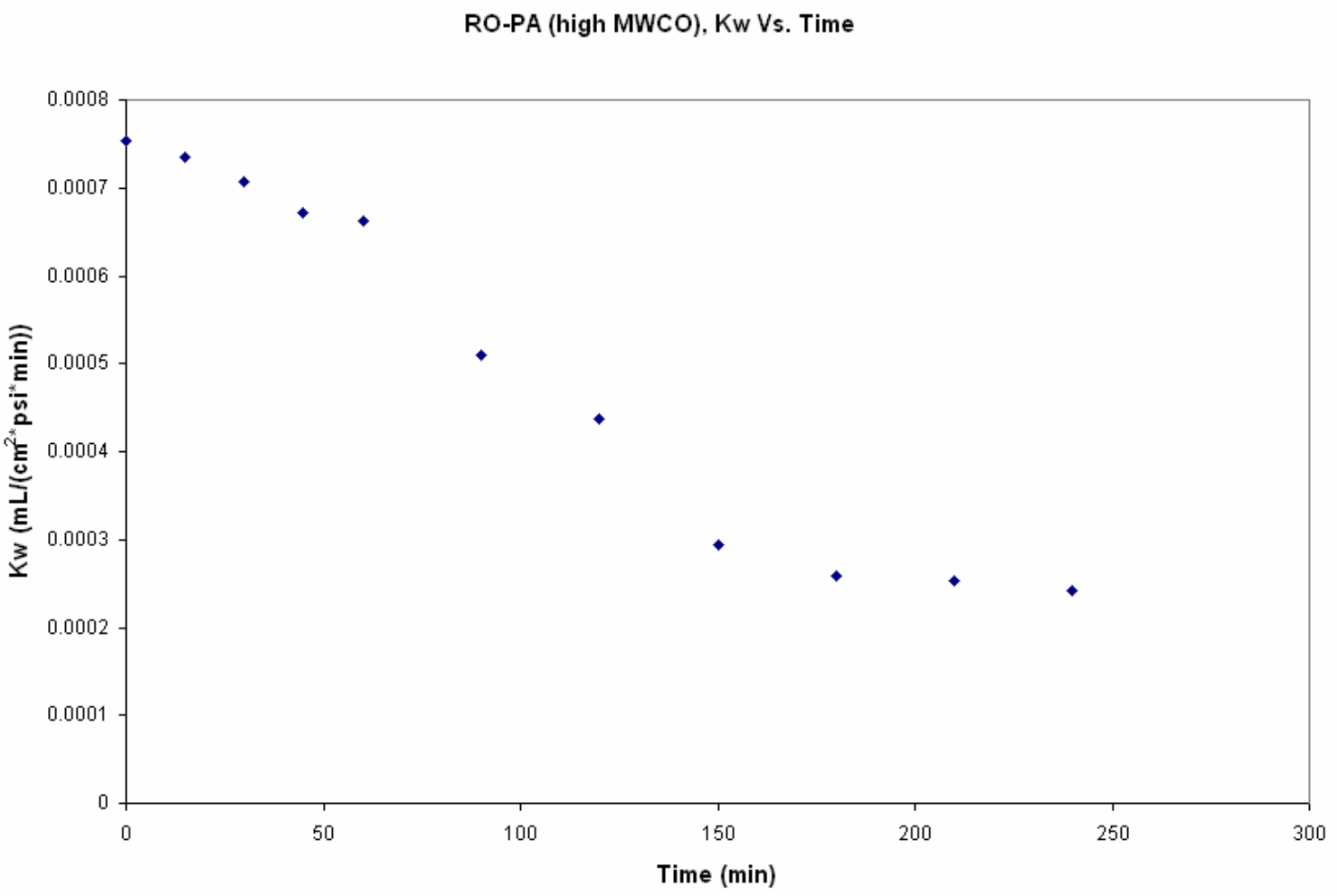

FIG. 4-5. RO-PA (high MWCO), Kw Vs. Time

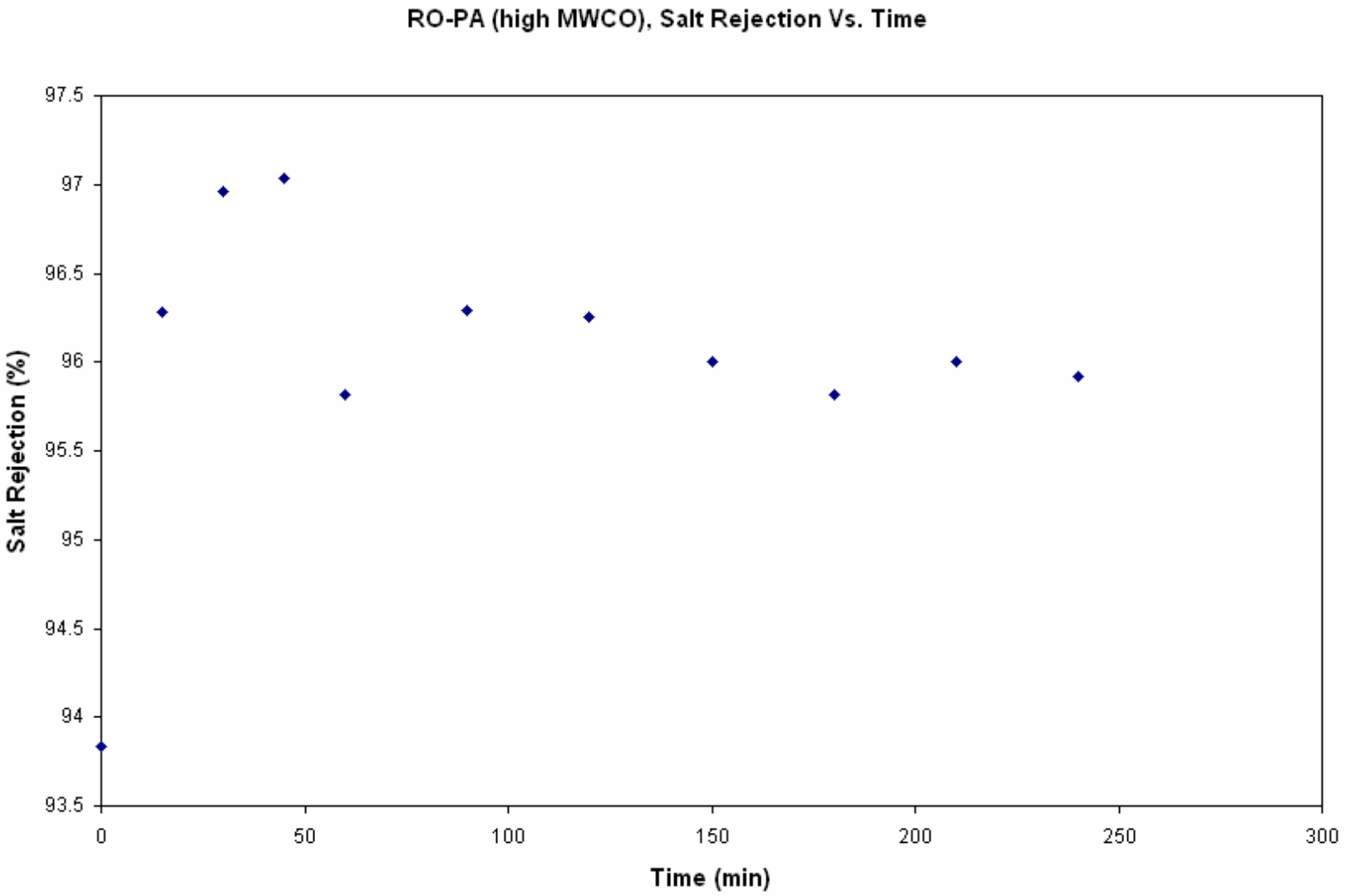

FIG. 4-6. RO-PA (high MWCO), Salt Rejection Vs. Time

71

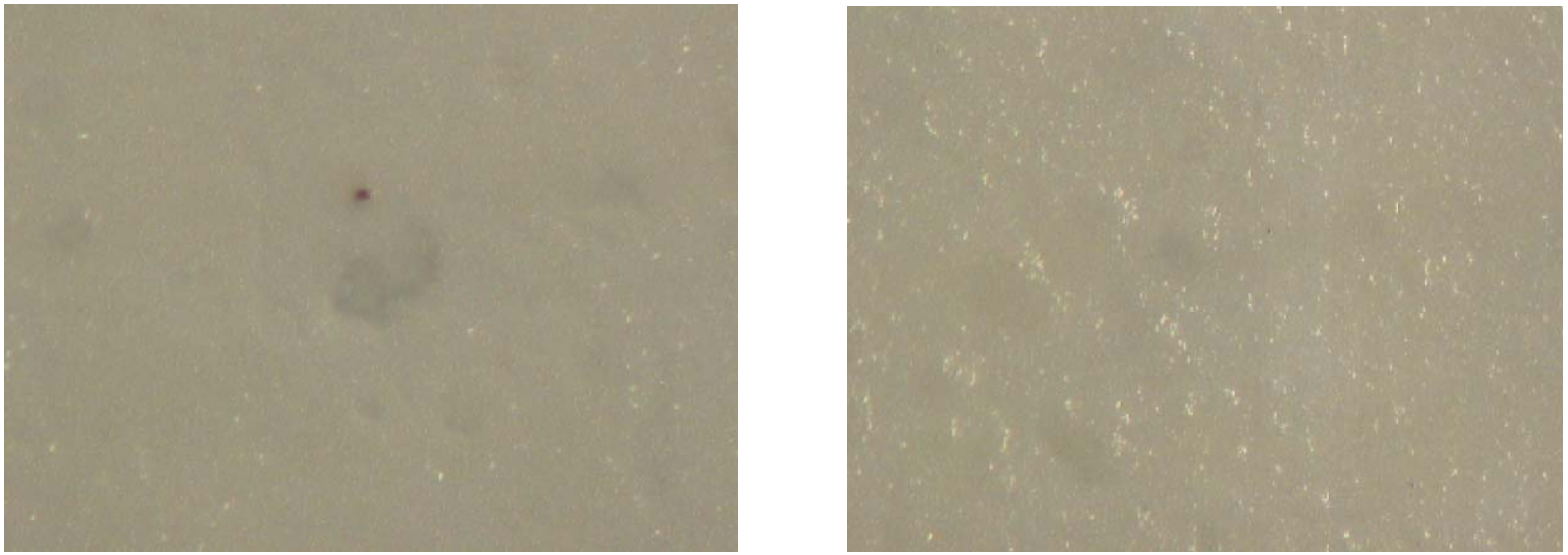

FIG. 4-7. RO-PA (high MWCO), membrane wear viewed using optical microscopy

72

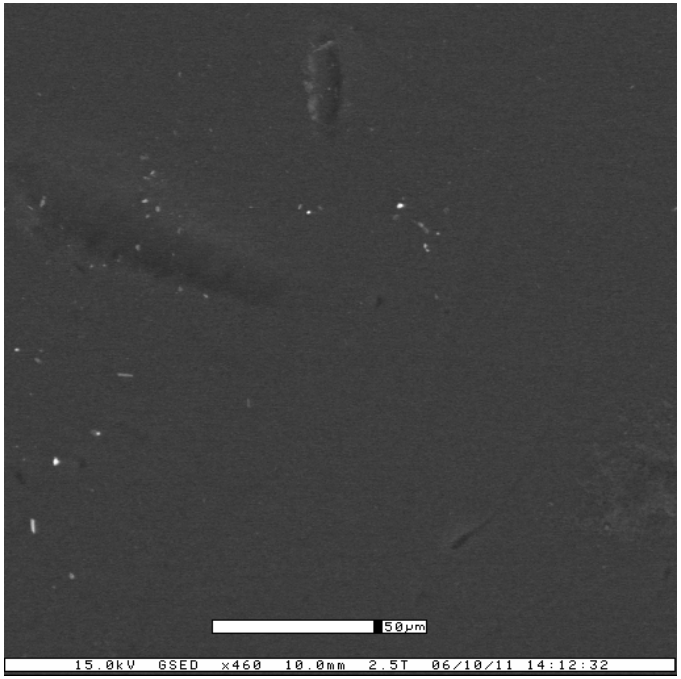

Virgin Membrane

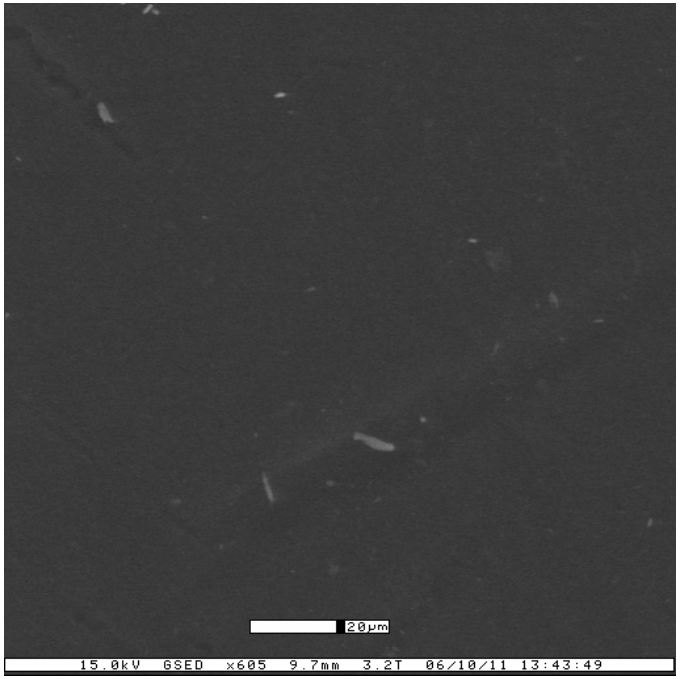

Membrane after Simulation

FIG. 4-8. RO-PA (High MWCO), membrane wear viewed using scanning electron microscopy

73

Rejection percentages ranged from approximately 95.8 to 97 %. The slight decrease in rejection is difficult to explain due to the decline in water transport coefficient happening simultaneously. Typically, decreases in rejection result from membrane wear, thereby increasing the flux but permitting more ions to pass. The decrease in rejection could be attributed to steady flow of ions through the membrane with decreasing water flux, thereby increasing the salt concentration in the permeate. The initial increase in rejection also be attributed to the heavy pressure and its tendency to compact the membrane layers and thereby decreases the pore spaces.

After undergoing a membrane autopsy, there were few abrasions observed which concurs with literature (Cheryan 1998), but there were scaling deposits on the membrane.

4.3 Reverse Osmosis – Polyamide Membrane (Low MWCO)

4.3.1 K_w, Salt Rejection, and Membrane Wear

The water mass transfer coefficient and salt rejection are plotted against time in Figure 4-9 and Figure 4-10, respectively. Figure 4-11 and Figure 4-12 shows microscopic views of the membrane after the experiment.

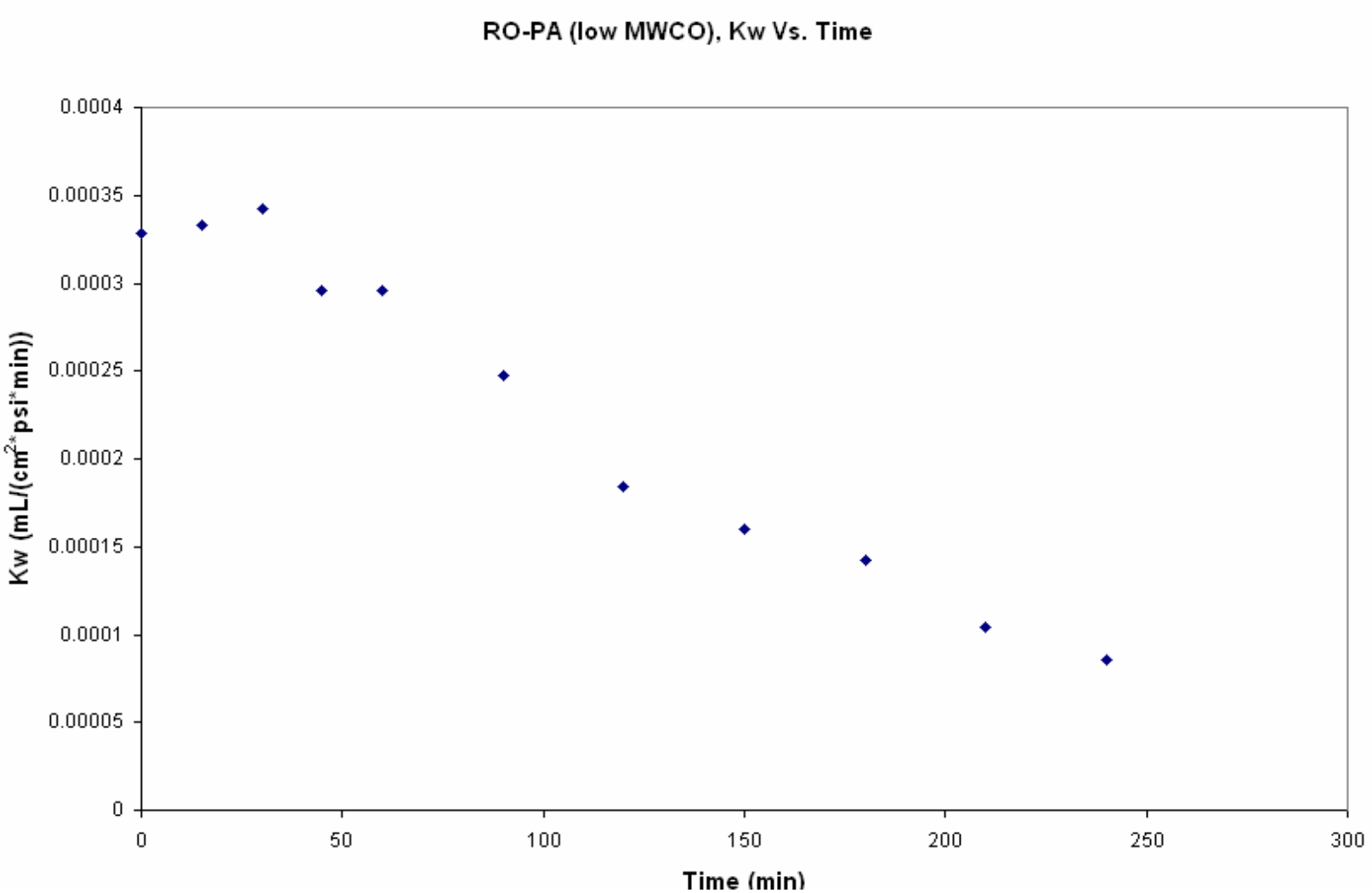

FIG. 4-9. RO-PA (low MWCO), Kw Vs. Time

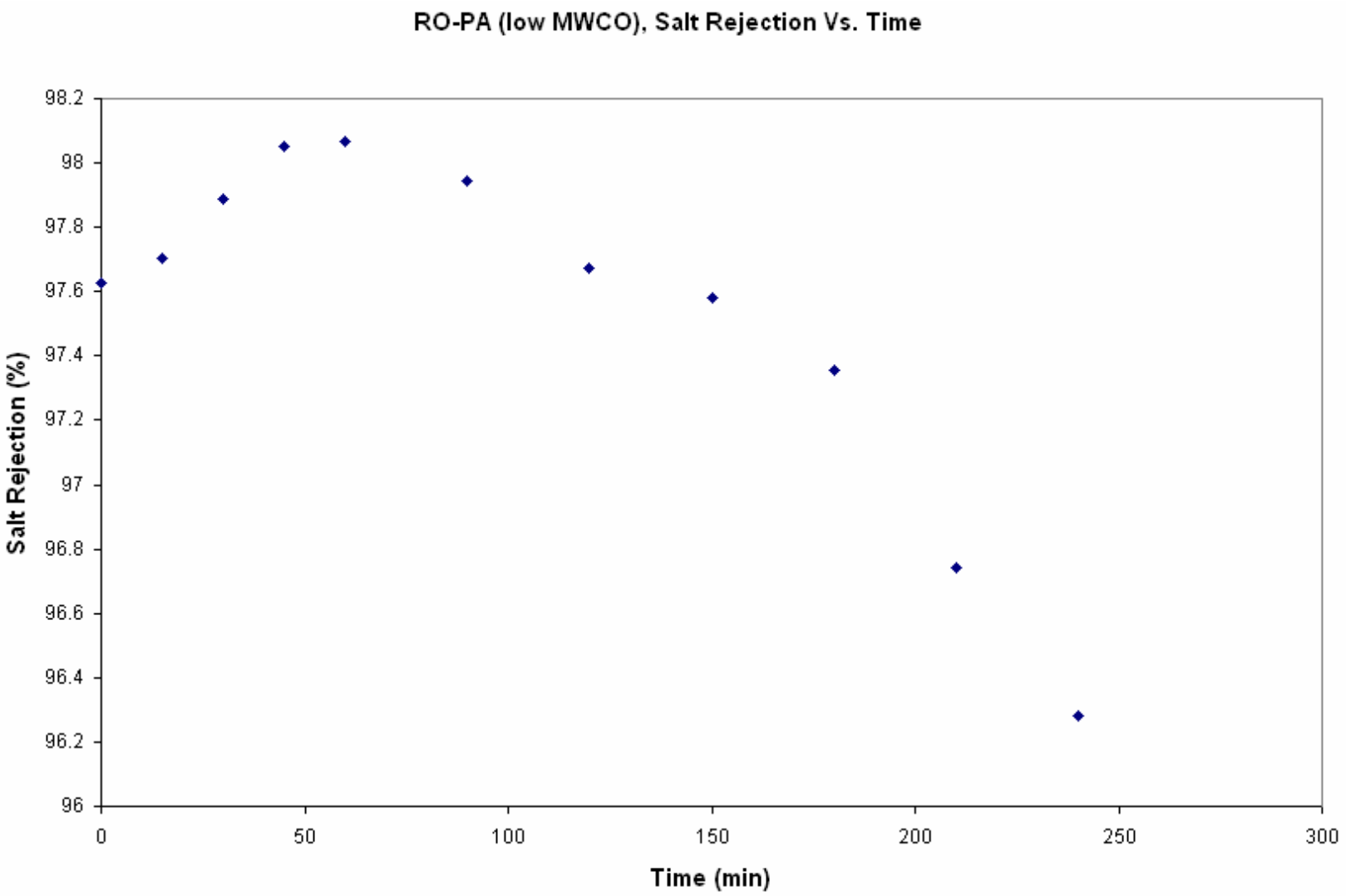

FIG. 4-10. RO-PA (low MWCO), Salt Rejection Vs. Time

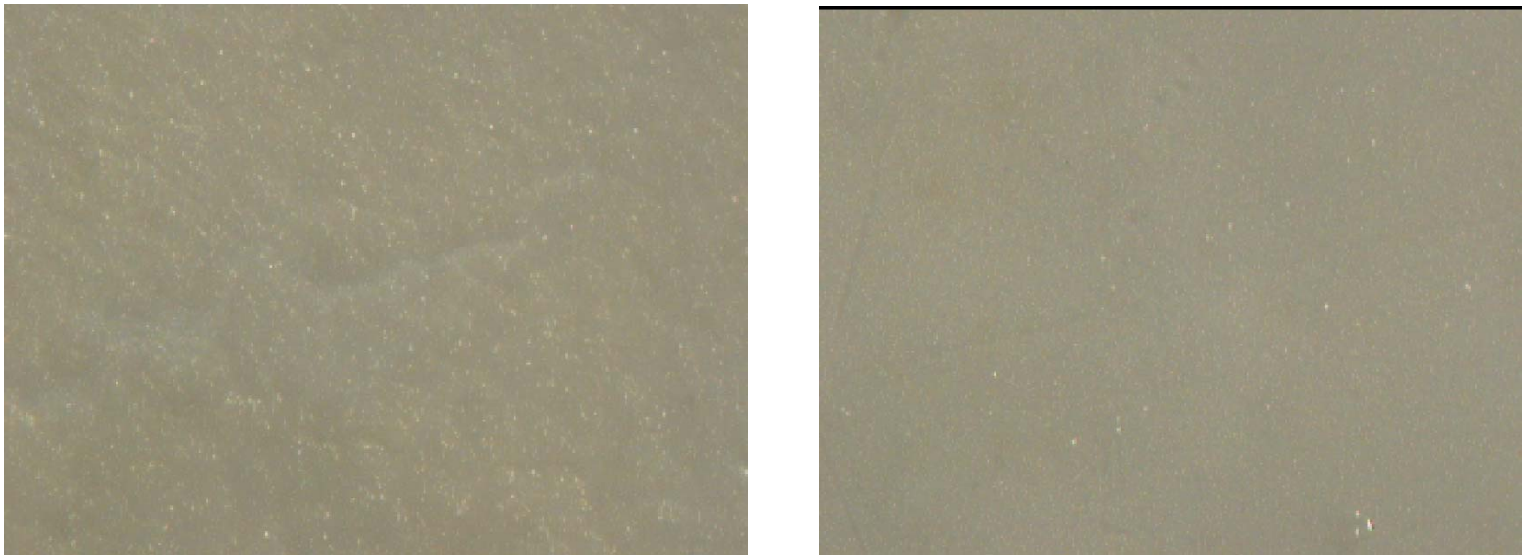

FIG. 4-11. RO-PA (low MWCO), membrane wear viewed using optical microscopy

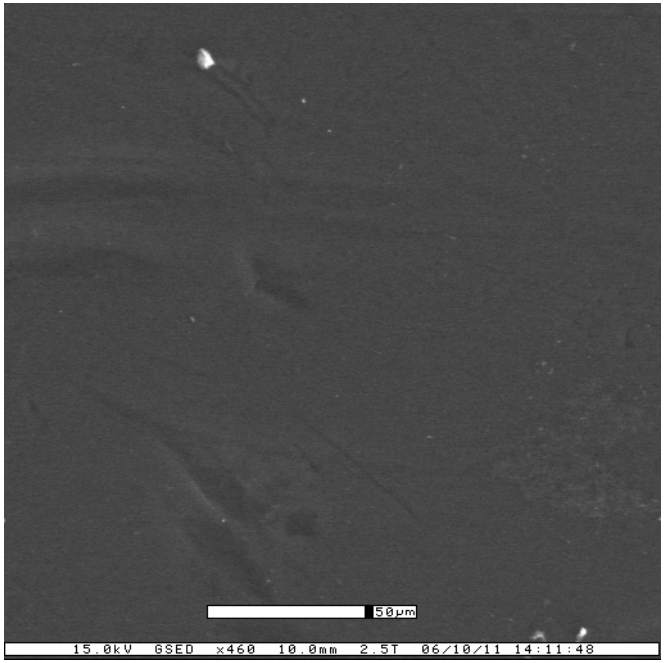

Virgin Membrane

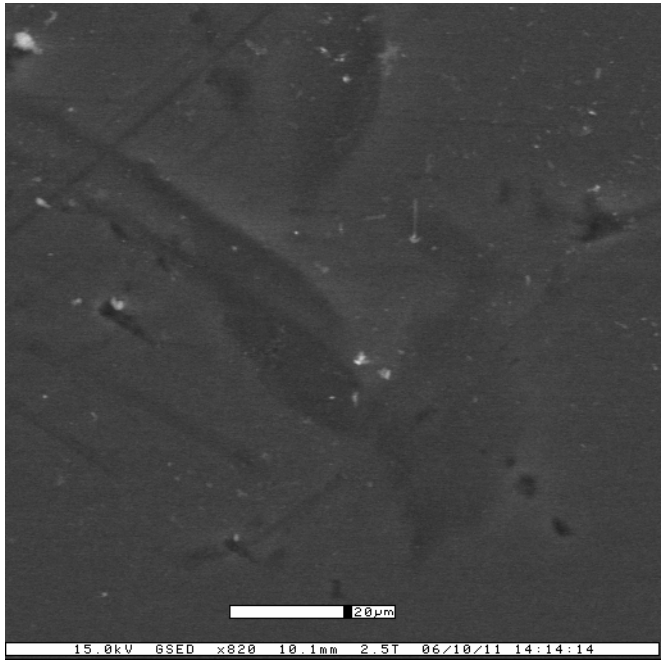

Membrane after Simulation

FIG. 4-12. RO-PA (low MWCO), membrane wear viewed using scanning electron microscopy

This low MWCO polyamide membrane exhibited fouling as depicted in Figure 4-9. The water transport coefficient ranged from about 0.00035 to 0.0001 mL/(cm^2*psi*min) which is approximately a 71 % decrease. According to literature, this fouling is attributed to the polyamide's rough surface, thereby providing many locations for suspended matter to lodge into the protrusive surface (Cheryan et al. 1998).

The increased rejection that was observed in the first hour of operation was most likely due to the impregnation of ions/suspended particles within the membrane . It could also be attributed to the heavy pressure and its tendency to compact the membrane layers and thereby decreases the pore spaces. After an hour, the rejection decreased due to unknown reasons. One possible reason is that the temperature might have decreased during the experiment, even though attempts were made to keep it constant. A decrease in temperature would make calcium sulfate more soluble and the concentrations of calcium sulfate would be higher in solution. Therefore, the concentration gradient from one side of the membrane to the other would increase which would ultimately promote a higher driving force for the transport of ions across the membrane. Another possible reason is the one used to describe the decreased rejection in the high MWCO PA membrane, i.e., that there was a steady flow of ions through the membrane with decreasing water flux, thereby increasing salt concentration in the permeate.

The autopsies shown in Figure 4-11 and Figure 4-12 reveal calcium sulfate scale on the surface of the membrane with minimal abrasive wear which corroborates the flux decline that was observed.

4.4 Nanofiltration – Thin Film Membrane

4.4.1 K_w, Salt Rejection, and Membrane Wear

The water mass transfer coefficient and salt rejection are plotted against time in Figure 4-13 and Figure 4-14, respectively. Figure 4-15 and Figure 4-16 shows microscopic views of the membrane after the experiment.

During the four hour trial, the water transport coefficient remained steady at 0.0006 mL/(cm^2*psi*min). There was a slight decrease from 0.00065 to 0.0006 mL/(cm^2*psi*min) during the last 100 minutes but not enough to illustrate a significant amount of fouling.

The salt rejection increased steadily from approximately 86 to 91% during the first hour as seen in Figure 4-14. This was most probably due to initial impregnation of ions/suspended particles within the membrane, thereby acting as barriers to other ions by obstructing their passage. It could also be attributed to the heavy pressure and its tendency to compact the membrane layers and thereby decreases the pore spaces. After 90 minutes, the rejection drops down to 88 % and then increases at a steady rate around 88.5 %. Interestingly, at 90 minutes the water transport coefficient has a slight increase which could be attributed to membrane wear due to the decrease in rejection occurring simultaneously.

The membrane autopsies shown in Figure 4-15 and Figure 4-16 indicate very little abrasions or scaling thereby corroborating the steady water transport coefficient with no decline data.

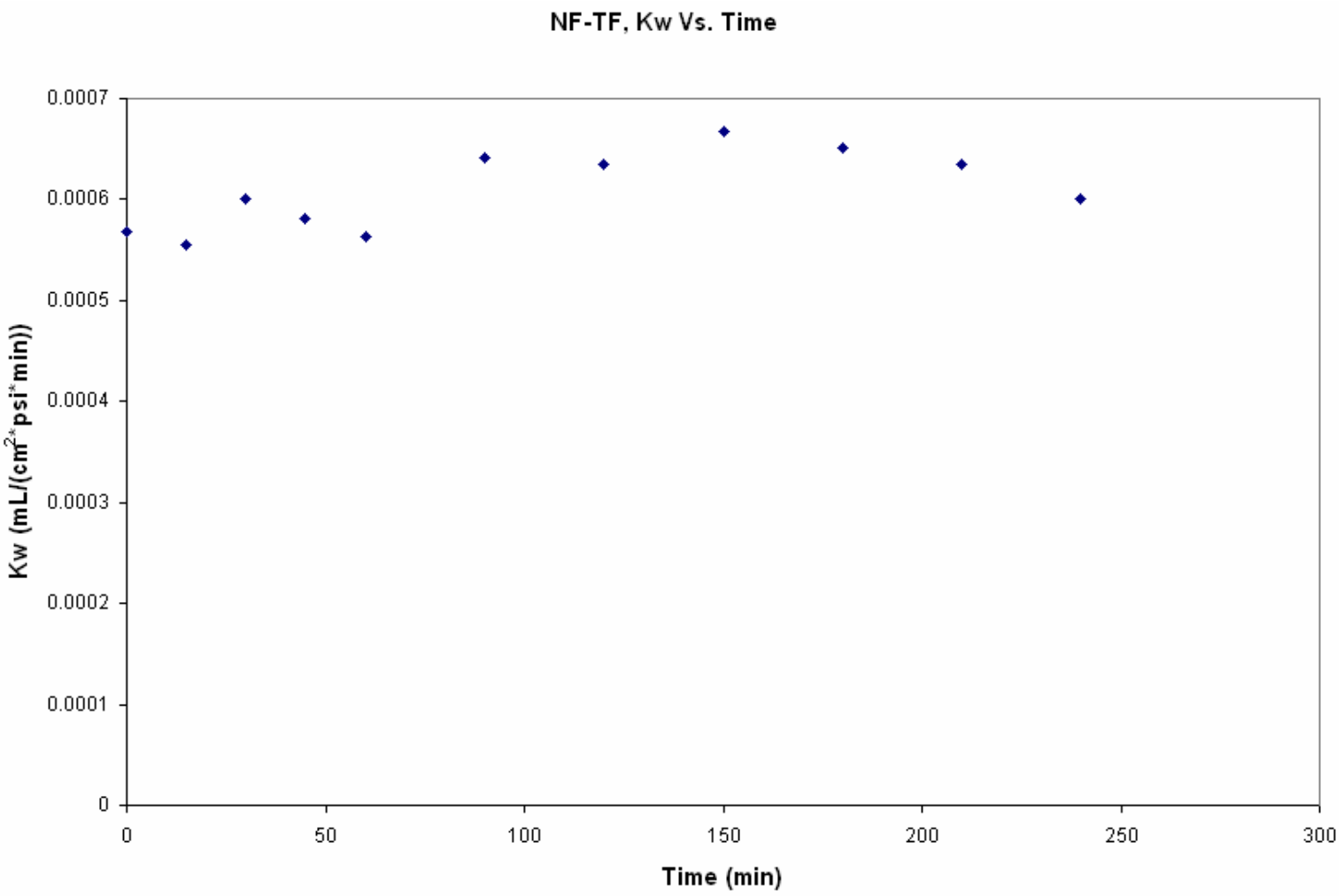

FIG. 4-13. NF-TF, K_w Vs. Time

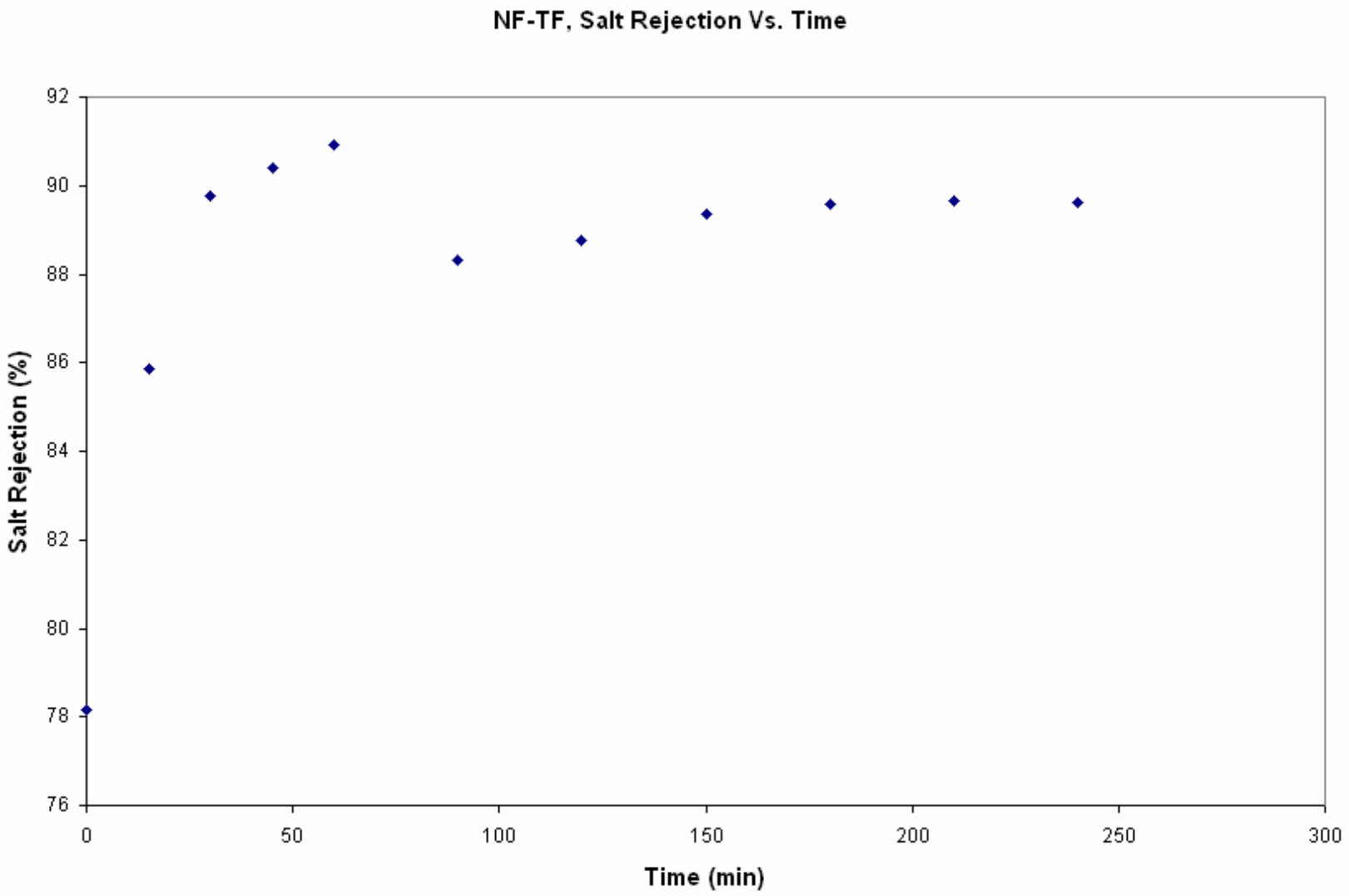

FIG. 4-14. NF-TF, Salt Rejection Vs. Time

FIG. 4-15. NF-TF, membrane wear viewed using optical microscopy

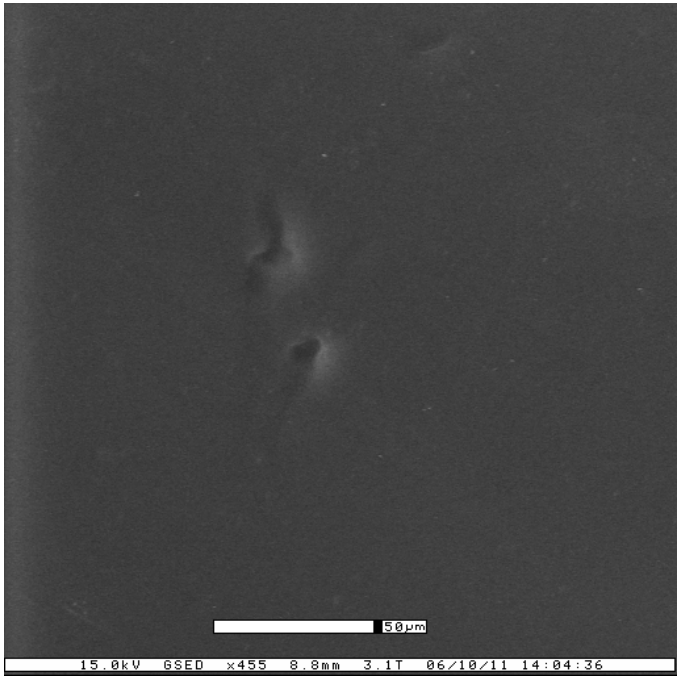

Virgin Membrane

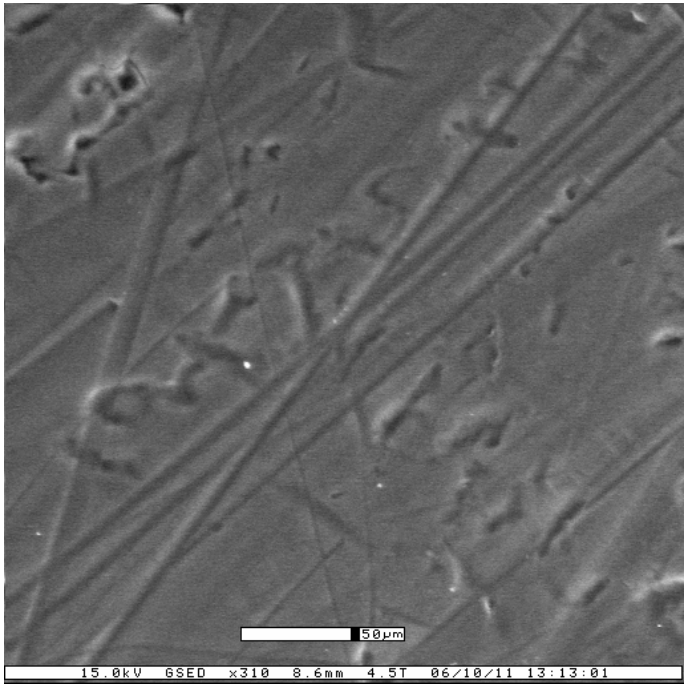

Membrane after Simulation

FIG. 4-16. NF-TF, membrane wear viewed using scanning electron microscopy

4.5 Nanofiltration – Cellulose Acetate Membrane

4.5.1 K_w, Salt Rejection, and Membrane Wear

The water mass transfer coefficient and salt rejection are plotted against time in Figure 4-17 and Figure 4-18, respectively. Figure 4-19 and Figure 4-20 shows microscopic views of the membrane after the experiment.

As shown from the experimental results in Figure 4-17, the water transport coefficient remains fairly stable at 0.00038 mL/(cm^2*psi*min) during the first 100 minutes. During the next 150 minutes, the flux steadily drops to 0.00028 mL/(cm^2*psi*min), which is approximately a 27 % decrease . The decrease in the coefficient was most probably attributed to compaction and fouling of the membrane surface.

The rejection ranges from approximately 93.4 to 97.7 % as depicted in Figure 4-18. The increase was most likely due to ion/suspended particle impregnation within the membrane over time, resulting in more resistance to ion passage through the membrane. It could also be attributed to the heavy pressure and its tendency to compact the membrane layers and thereby decreasing the pore spaces.

The membrane autopsy shows some minor abrasions and wear, thus corroborating the evidence shown during the reverse osmosis application with the cellulose acetate membranes. Furthermore, Cheryan et al. (1998) describe these membranes as easily degradable.

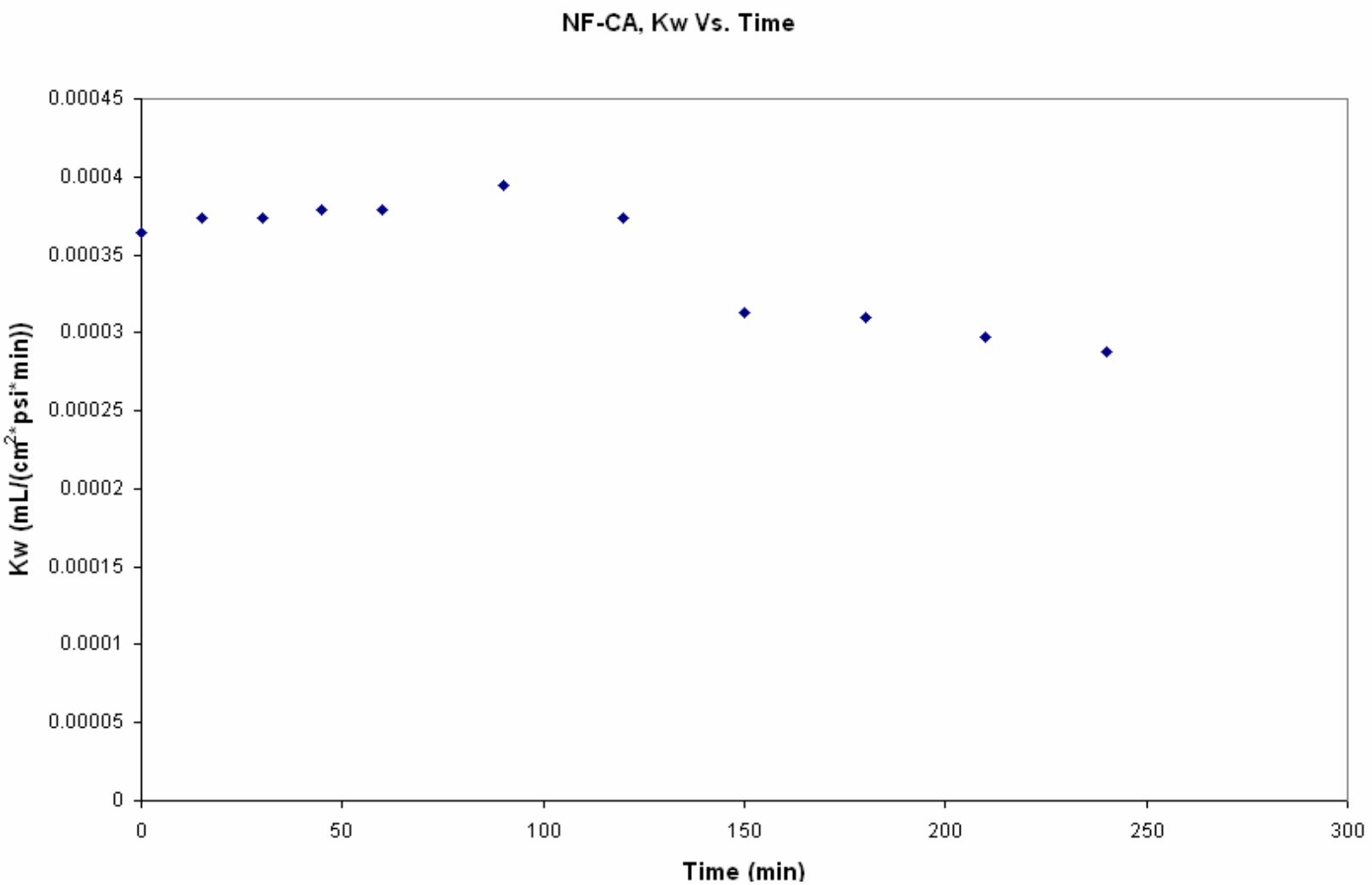

FIG. 4-17. NF-CA, Kw Vs. Time

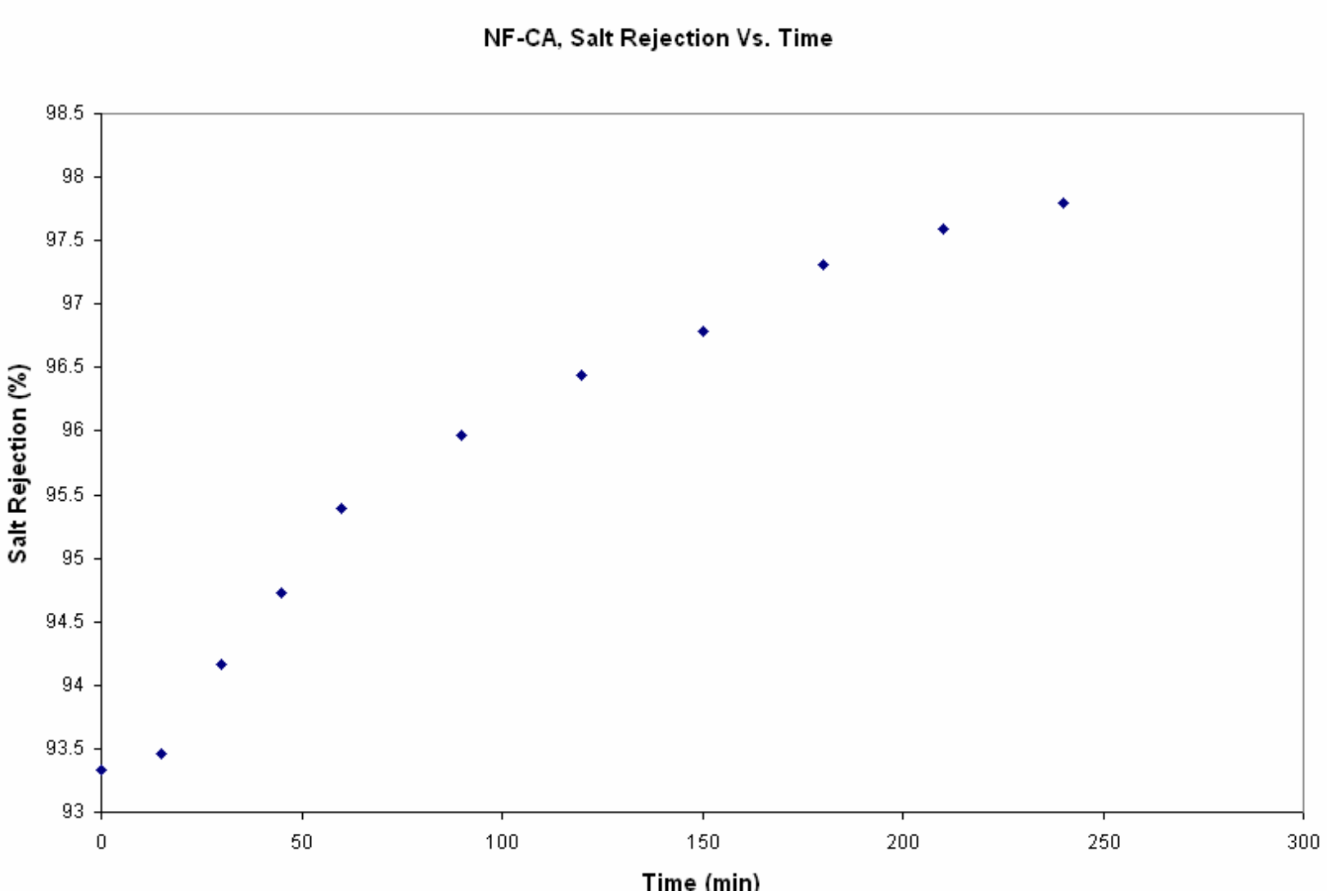

FIG. 4-18. NF-CA, Salt Rejection Vs. Time

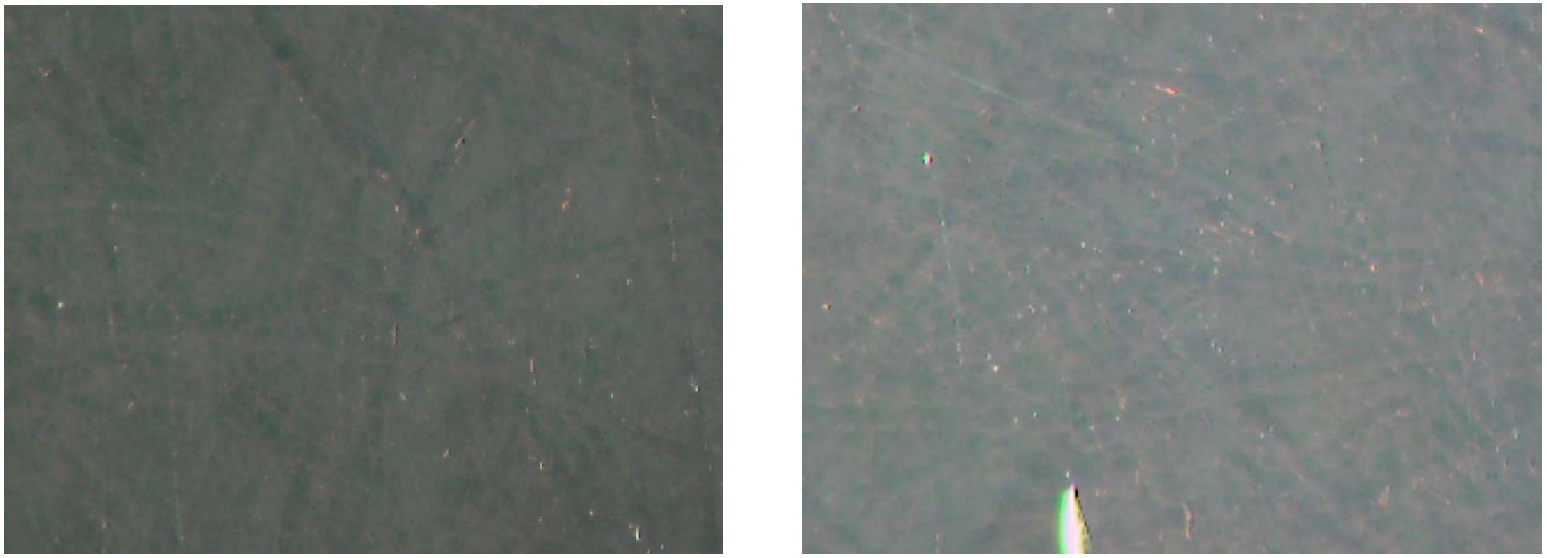

FIG. 4-19. NF-CA, membrane wear viewed using optical microscopy

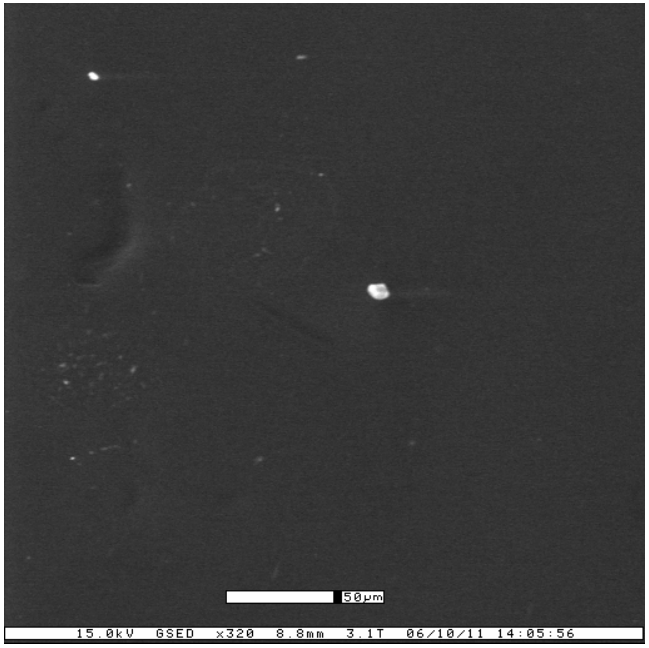

Virgin Membrane

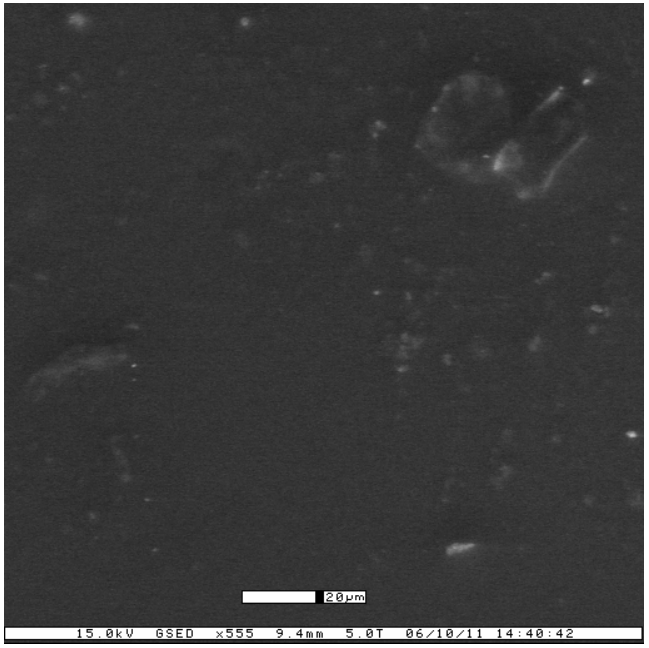

Membrane after Simulation

FIG. 4-20. NF-CA, membrane wear viewed using scanning electron microscopy

5. COMPARISONS, SUMMARY, AND CONCLUSIONS

5.1 Comparison of Membrane Performance

5.1.1 Water Mass Transfer Coefficient, K_w

The following figure shows the experimental results for the water mass transfer coefficient for each membrane.

Figure 5-1 shows that the cellulose acetate membranes and the thin film membrane performed with limited fouling and therefore good reliability. Although the highest water mass transfer coefficient was observed when using the polyamide, high MWCO membrane, it also had the highest fouling rate. The initial water mass transfer coefficient was approximately 0.00075 mL/(cm^2*psi*min) and then dropped to 0.00025 mL/(cm^2*psi*min) over a four hour period. Similar to the polyamide, high MWCO membrane, the polyamide, low MWCO membrane also exhibited fouling. The high MWCO membranes tended to foul at a higher rate due to their large pore spaces providing many spaces for ions and other particles (if any) to lodge and accumulate within the membrane. Concurring with Cheryan et al. (1998) these membranes had a relatively high initial coefficient, but exhibited a greater total coefficient decline. This is imputed to their rough surfaces becoming clogged with ions and suspended solids (if the crossflow velocity was not high enough to shear them into the retentate flow).

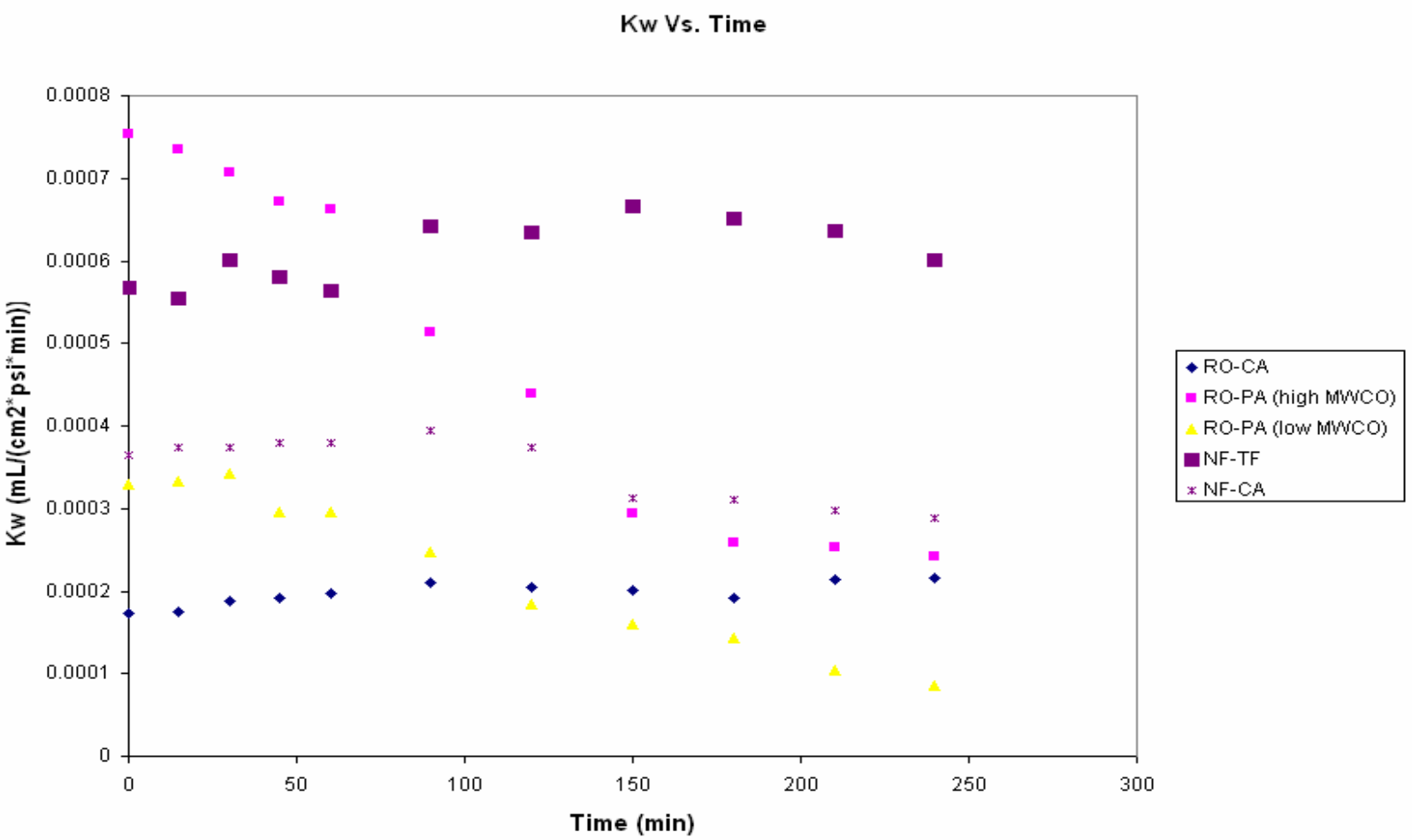

FIG. 5-1. Kw Vs. Time

Among all the membranes, the thin film membrane exhibited the highest constant coefficient at approximately 0.0006 mL/(cm^2*psi*min), while the cellulose acetate membranes also appears to be promising, operating at a constant coefficient of approximately 0.0002 mL/(cm^2*psi*min) for the reverse osmosis – cellulose acetate membrane and 0.00035 mL/(cm^2*psi*min) for the nanofiltration – cellulose acetate membrane. These results can be viewed below in Table 5-1.

TABLE 5-1. Water transport coefficient for membranes that did not foul

Water Transport Coefficient with little to no Fouling mL/(cm^2*psi*min)	
Membrane	**Coefficient**
Nanofiltration - TF	0.0006
Nanofiltration - CA	0.00035
Reverse Osmosis - CA	0.0002

5.1.2 Salt Rejection

Figure 5.2 shows the experimental results of the salt rejection percentages for each membrane.

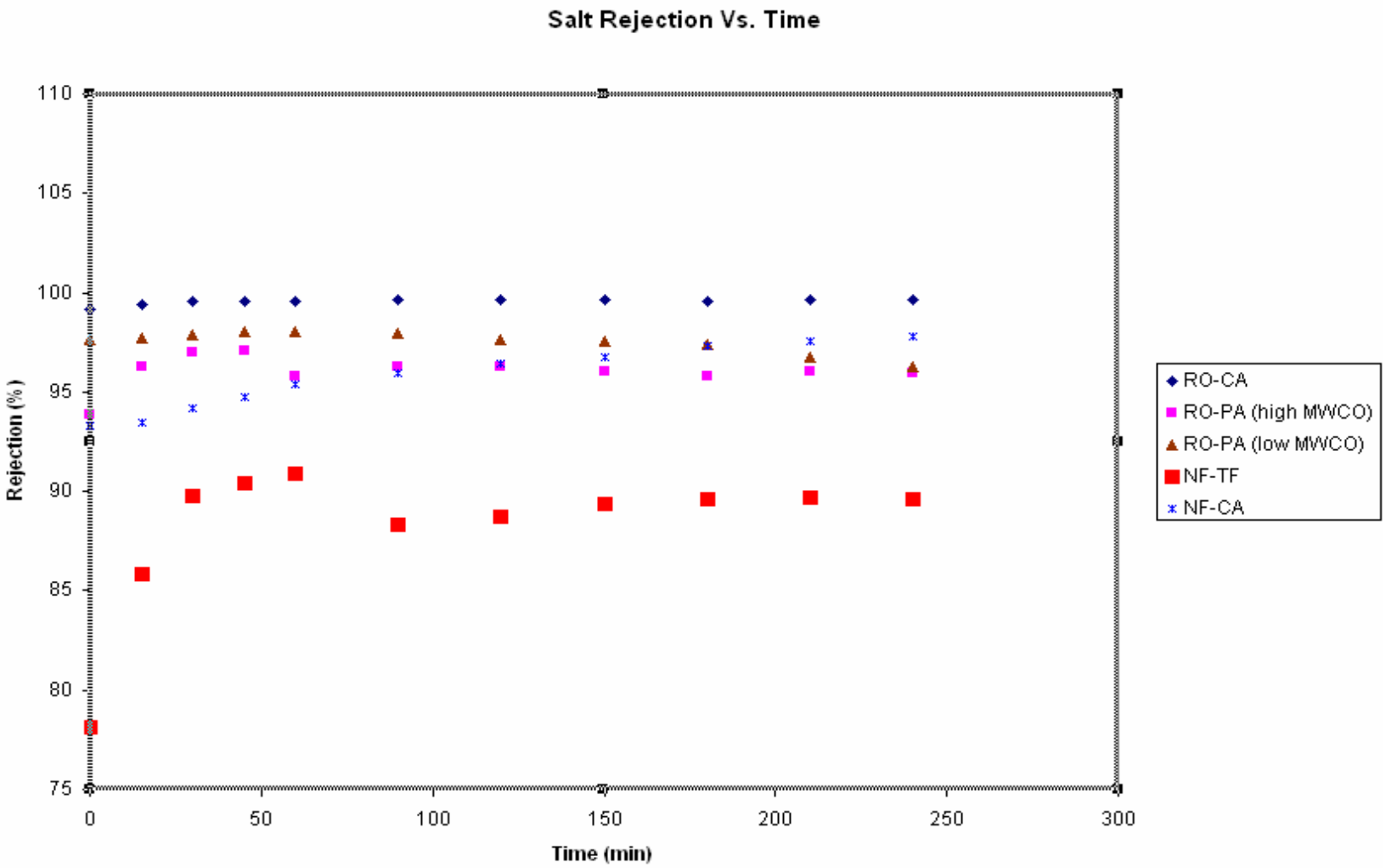

FIG. 5-2. Salt Rejection Vs. Time

Among all the membranes, the cellulose acetate exhibited the highest salt rejection when used in a reverse osmosis process averaging approximately 99.6 %. The next highest rejection was observed when using the low MWCO polyamide membrane in a reverse osmosis process and was approximately 97 %. The lowest rejection was observed when the nanofiltration – thin film membrane was used, which remained stable around 88 %.

All the membranes exhibited an initial low rejection, but with time this gradually increased and then stabilized for the duration of the experiment. This trend is attributed to the voids not being impregnated with ions or suspended particles during the beginning of the simulation process. It could also be imputed to the pressure applied, thereby compacting the membrane layers and reducing pore size.

The polyamide, low MWCO membrane rejection increased for the first 60 minutes, and then steadily decreased for the next 180 minutes. This was probably due to the constant mass transfer of ions through the membrane with decreasing flux, thereby increasing the concentration of salt in the permeate. Table 5-2 shows the mean rejections for the duration of the experiment for each membrane.

TABLE 5-2. Mean rejection percentages for each membrane

Rejection for each Membrane	
Membrane	**Rejection (%)**
Nanofiltration - TF	88
Reverse Osmosis - PA (low MWCO)	97
Nanofiltration - CA	96
Reverse Osmosis - PA (high MWCO)	95
Reverse Osmosis - CA	99.6

5.1.3 K_w / Salt Mass Transfer

The following figure shows the experimental results for the water mass transfer coefficient divided by the salt mass transfer for each membrane. This ratio normalizes all performance parameters and can aid in making conclusions on the best overall membrane.

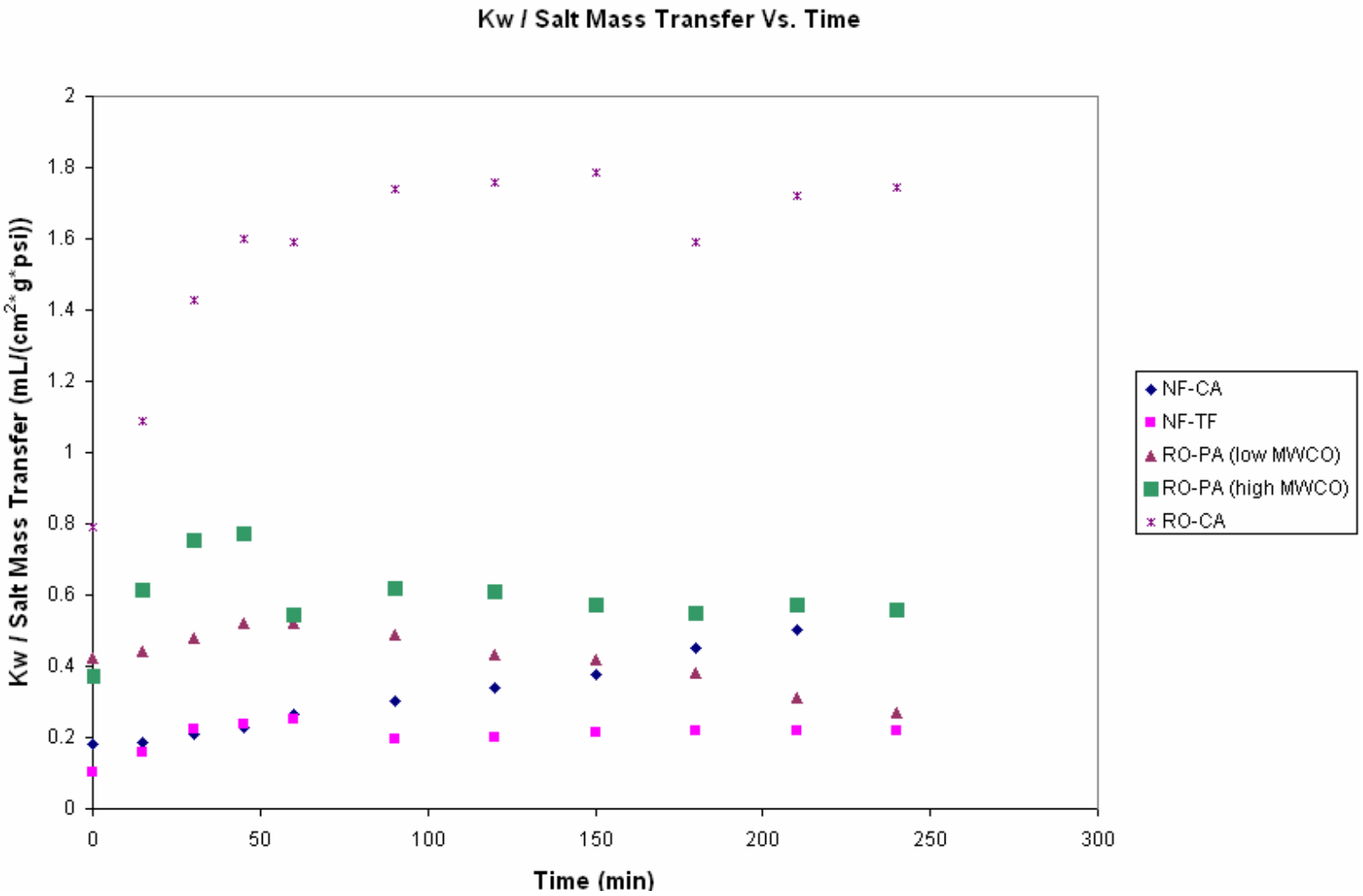

FIG. 5-3. K_w / Salt Mass Transfer Vs. Time

Figure 5-3 shows the experimental data for the transport coefficient ratio (water mass transfer/salt mass transfer) with time. Maximizing this ratio strives to achieve the ideal membrane performance, i.e. the highest flux with smallest amount of salt transferred through the membrane. This quotient takes into account all important variables and can therefore be used to normalize and pin point the best *overall* membrane material

The cellulose acetate membrane when used in reverse osmosis conditions clearly surpasses the other membranes with a quotient steadily stabilizing at approximately 1.7 mL/(cm^2*psi*g). The next highest appears to be the high MWCO polyamide membrane, stabilizing at approximately 0.55 mL/(cm^2*psi*g). This finding concurs with Harries et al. (1985). Table 5-3 shows the mean ratio for all membranes for the duration of the experiment.

The cellulose acetate and thin film membranes used in the nanofiltration process appear to be promising, but with low mean values, while the low MWCO polyamide membrane quotient decreases with time indicating either increasing solute flux or decreasing water flux with time.

TABLE 5-3. Mean water mass transfer coefficient divided by the salt mass transfer for each membrane

Kw / Salt Mass Transfer for each Membrane	
Membrane	**Kw / Salt Mass Transfer mL/(cm^2*psi*g)**
Nanofiltration - TF	0.2
Reverse Osmosis - PA (low MWCO)	0.4
Nanofiltration - CA	0.3
Reverse Osmosis - PA (high MWCO)	0.55
Reverse Osmosis - CA	1.7

5.1.4 Membrane Autopsies

Figures 5-4 and 5-5 show a microscopic view of the membranes after the experiments.

Optical microscopy and scanning electron microscopy reveals the cellulose acetate membranes exhibit the highest amount of abrasive wear for both nanofiltration and reverse osmosis processes, but is more pronounced for the reverse osmosis process. The polyamide membranes both show calcium sulfate scaling with minimal abrasive wear, while the thin film membrane used in the nanofiltration process show little to no scaling or abrasive wear under the OM, but shows abrasive wear under the SEM. The wear observed for the thin film membrane under the SEM is not as pronounced for that of the cellulose acetate membrane when operated under reverse osmosis conditions.

Reverse Osmosis –CA

Reverse Osmosis – low MWCO PA

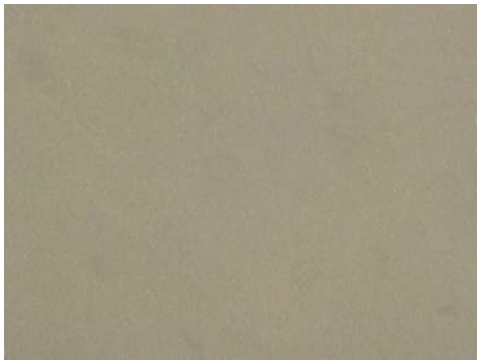

Reverse Osmosis – high MWCO PA

Nanofiltration – TF

Nanofiltration - CA

FIG. 5-4. Optical microscopy view of the membranes after simulations

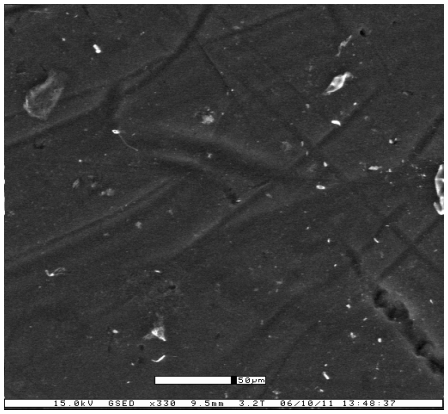

Reverse Osmosis –CA

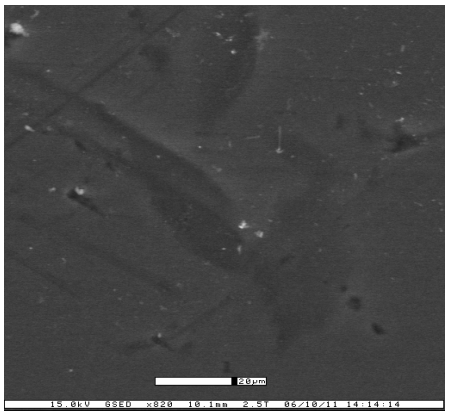

Reverse Osmosis – low MWCO PA

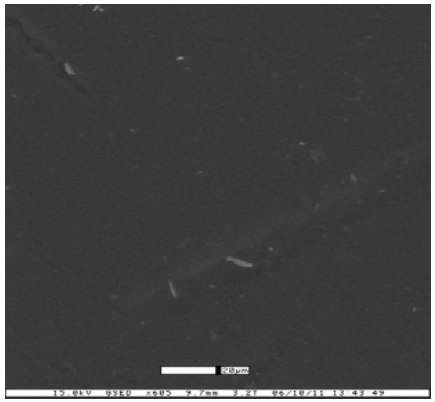

Reverse Osmosis – high MWCO PA

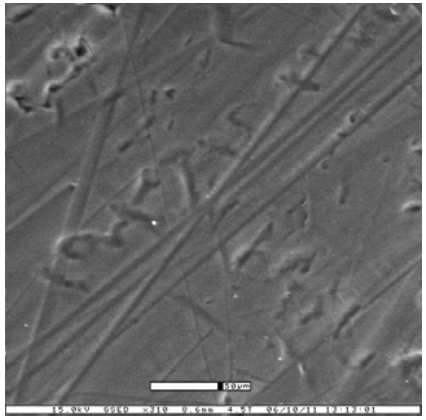

Nanofiltration – TF

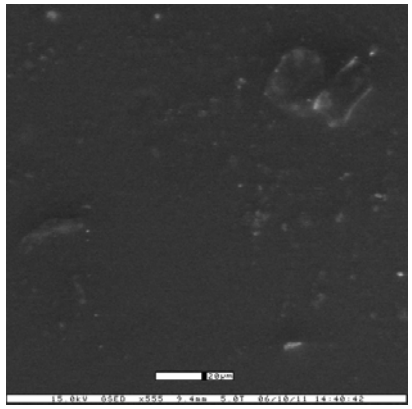

Nanofiltration - CA

FIG. 5-5. Scanning electron microscopy view of the membranes after simulation

5.1.5 Lifetime Test

The cellulose acetate and thin film membranes were chosen to undergo a lifetime test experiment due to their performance surpassing that of the polyamide membranes performance. After a SRO simulation of 8 hours with the maximum pressure (specified by GE Osmonics) applied, there was no decrease in rejection indicating that the membranes did not tear or become less effective in any way. Therefore, a comparison cannot be made between the two membranes. There was an extensive amount of fouling observed for both membranes which is attributed to the extensive pressure compaction of the membrane fibers.

5.2 Summary – Relation to Full Scale, Real World Applications

5.2.1 Drinking Water Standards and Membrane Performance

The U.S. Environmental Protection Agency's maximum concentration level (MCL) for sulfate is 250 mg/L. This membrane performance assessment shows that the only membrane not capable of meeting this standard is the thin film membrane when used in nanofiltration processes which exhibited concentrations higher than 250 mg/L for every sample taken as shown in Table 5-4. Therefore, all other membranes can be used to treat waters contaminated with calcium sulfate. If this membrane was capable in meeting the drinking water standard, then it would be the optimum membrane due to it possessing the highest water mass transfer coefficient.

TABLE 5-4. Permeate concentration when using the thin film membrane

Time (min)	$[CaSO4]_{permeate}$ (mg/L)
0	576.4
15	372.9
30	270.6
45	253
60	239.8
90	308
120	297
150	280.5
180	275
210	272.8
240	273.9

As a result, the cellulose acetate membranes for either the nanofiltration process or reverse osmosis process appear to be most suitable for water treatment. The nanofiltration process shows a steady water transport coefficient of approximately 0.0003 mL/(cm^2*psi*min), while the reverse osmosis processes exhibits a coefficient of 0.00019 mL/(cm^2*psi*min) which is about a 37 % decrease. To illustrate the difference using full scale operational units 0.0003 mL/(cm^2*psi*min) becomes 4320 mL/(m^2*psi*day), while 0.00019 mL/(cm^2*psi*min) becomes 2736 mL/(m^2*psi*day), which amounts to approximately 1.6 L/(m^2*psi*day). This can make a severe difference in operating costs if the dealing with a large desalination plant. In conclusion, the nanofiltration cellulose acetate membrane is the ideal membrane for achieving quality water at the lowest cost. One drawback to these membranes that can not be completely characterized using results from these experiments is the abrasive wear. Therefore, further research should investigate its lifetime in a seeded slurry.

5.2.2 Irrigation Water Standards and Membrane Performance

Irrigation waters should not have calcium sulfate concentrations that exceed 2000 mg/L, making all membranes capable of achieving quality water to irrigate. On the other end of the spectrum, some calcium sulfate (450-1000 mg/L, range depending on the crop) provides benefits such as its ability to flocculates clay soil, thereby eliminating surface crusting and improving water penetration. It also neutralizes bicarbonates and converts sodium bicarbonate into sodium sulfate, which is easily leached from the root zone through typical irrigation practices. Furthermore, it provides a form of calcium that is readily available for uptake by the plant roots, providing a critical micronutrient for healthy and durable crops.

As a result the most suitable membrane appears to be the thin film membrane when used under nanofiltration conditions. This membrane not only gives the highest constant water transport coefficient, but also allows a considerable portion of ions to pass through the membrane. The concentration of calcium sulfate in the product is well under the threshold of 2000 mg/L for irrigation, but it is higher than that in drinking water standards, therefore making it the ideal membrane to use if irrigation is the primary purpose. Furthermore, the membrane did not exhibit serious abrasions or scaling from the membrane autopsies.

5.2.3 Overall Membrane Performance

The overall membrane performance can be interpreted from Figure 5-3. In this figure, the higher the ratio of water mass transfer to salt mass transfer, the more ideal the membrane is. The experimental results show that the reverse osmosis cellulose acetate

membrane surpasses all the membranes. Furthermore, this membrane did not exhibit any fouling from the four hour test. However, one shortcoming that should be investigated further is the excessive wear on the membrane as observed in Figure 5-4.

5.3 Conclusion

The ideal membrane is dependent on the desired application of the water that the membrane is being used to produce. If potable drinking water is the intended use, then the nanofiltration cellulose acetate membrane should be used. If irrigation is the desired use, then the nanofiltration thin film membrane should be used. Overall, the reverse osmosis cellulose acetate membrane was observed to outperform all membranes. However, this membrane was observed to be prone to degradation in a seeded slurry and therefore its lifetime should be analyzed further. The polyamide membrane initially had a high water transport coefficient, but fouling led to its rapid decline which was attributed to the membrane's rough and protrusive surface.

6. PROJECT ACCOMPLISHMENTS AND RECOMMENDATIONS FOR FUTURE WORK

The main accomplishments of the membrane performance assessment are the following:

1) Better understanding of which membranes to allocate more time, money, and research on for further investigation and performance analysis in a seeded slurry.

2) Propositions on which membranes to use for irrigation and potable drinking water.

3) Conclusion that nanofiltration is applicable to desalinating waters with high concentrations of calcium sulfate.

4) Characterization of how five different membranes perform when filtering waters with high levels of suspended solids without any pretreatment.

The following propositions are made for further research:

1) One thing that should be noted before we accept the result of this research without criticism is that it is written based on one data set (one simulation per membrane). This means that one might encounter large variation from the result that is presented in this research. In other words, it is not certain that the repetition of the test would yield the similar test result value. A statistically meaningful result can be obtained by applying various statistical analyses such as "Analysis of variance – ANOVA," but it requires at least 20 repetition of the same test (Montgomery and Runger 2003). Considering the budget and time limitation of the research, it was not feasible to obtain such statistical confidence.

2) Furthermore, the same research should be conducted on a pilot scale using the tubular membrane configuration – the configuration that is used for full scale operation. The tubular membrane configuration is the most suitable configuration for treating seeded calcium sulfate slurries because it aids in preventing scale on the membrane surface. The point in adding a seed crystal is to prevent scaling from occurring on the membrane surface. However, when using the SEPA Cell plate membrane module scaling was observed on the membrane surface and therefore may have been the culprit for extensive fouling on some of the membranes. If a tubular configuration was used, scaling could be completely eliminated from being a culprit of fouling. It therefore would relate more to a full scale operation process and regression models could be devised to predict the performance of full scale operation.

3) Furthermore, in order to predict membrane life, the experiment should be conducted for a longer period of time.

4) Also, source feedwater should be used to make more reliable comparisons among the membranes for that particular feedwater desalination.

5) The optimum cross flow velocity should be investigated on those membranes that performed well. A crossflow that corresponds to minimal abrasions and fouling with high fluxes would be optimum.

6) An operational comparison should be conducted: is constant pressure, declining flux more efficient then constant flow, increasing pressure?

7) An investigation on the effect of anti-scalants/dispersants such as Flocon 260 on the SRO process should be conducted.

8) Further investigation on the cellulose acetate and thin film membranes lifetime in a seeded slurry using the source feedwater.

REFERENCES

Al-Roumi, Y., Hisham, M., Hisham, T., (1999). "Multi-stage flash desalination: present and future outlook", *Chemical Engineering Journal*, 73 (2), 173-190.

AMTA, "How Good is Desalted Water?", *Desalting Facts*, July 18, 2001, American Membrane Technology Association. Website: http://www.membranes-amta.org/media/pdf/reliable.pdf

Bahar, R., Hawlader, M., Woei, L.S., (2004). "Performance evaluation of a mechanical vapor compression desalination system", *Desalination*, 166, 123-127.

Benjamin, M. (2002). *Water Chemistry*, McGraw Hill Series. New York, NY

Chen, S., Mulford, L., Norris, C., Taylor, J., (2000). "Development and Verification of ICR Membrane Protocol for Bench and Pilot Studies", *AWWA Research Foundation and the American Water Works Association*. Denver, CO

Cheryan, M. (1998). *Ultra-filtration and Microfiltration Handbook*, Technomic Publ. Lancaster, PA

Cipollina, A., Sommariva, C., Micale, G., (2005). "Efficiency increase in thermal desalination plants by matching thermal and solar distillation: A theoretical analysis", *Desalination*, 183, 127-136.

Devmurari, C.V., Ghosh, P.K., Joshi, S.V., Rao, P., Singh, P., Trivedi, J.J. (2006). "Probing the structural variations of thin film composite RO membranes obtained by coating polyamide over polysulfone membranes of different pore dimensions", *Journal of Membrane Science*, 278, 19-25.

Gutman, R.G. (1987). *Membrane Filtration: The Technology of Pressure-Driven Crossflow Processes*, Adam Hilger, Bristol, England

Harries, R. C. (1985). "A field trial of seeded reverse osmosis for the desalination of scaling-type mine water", *Desalination*, 56, 227-236.

Hess, M.C., Jone, G., Micheletti, W., Tomlinson, J., (1988). "Wastewater concentration by seeded reverse osmosis: A field demonstation in the electric power industry", *Environmental Progress*, 7(1), 7-12.

Jacangelo, J.G., Laîné, J., Carns, K.E., Cummings, E.W., Adham, S.S. (1995). "UF with pretreatment for removing DBP precursors", *Journal AWWA*, 87(3), 100.

Juby, G.J.G., Schutte, C.F., (2000). "Membrane life in a seeded-slurry reverse osmosis system", *Water SA*, 26(2), 239-248.

Jucker, C., Clark, M.M. (1994). "Adsorption of aquatic humic substances on hydrophobic ultrafiltration membranes", *Journal of Membrane Science*, 97, 37.

Karama, A., Wurbs, R., (1995). "Salinity and water-supply reliability", *Journal of Water Resources Planning and Management*, 121(5), 352-358.

Kim, M., Zydney, A. (2006). "Theoretical analysis of particle trajectories and sieving in a two-dimensional cross-flow filtration system", *Journal of Membrane Science*, 281, 666-675.

Kurihara, Masaru, "The progression of water treatment technology with the combination of the RO membrane and the advanced disinfection method", *IDA News*, January/February 2003, Volume 12, Issue 1-2, The International Desalination Association. Website: http://www.idadesal.org/03%%20JanFeb.pdf

Lahoussine-TurCaud, V., Weisner, M.R., Bottero, J., Mallevialle, J. (1990). "Coagulation pretreatment for ultra-filtration of surface water", *Journal AWWA*, 82(12), 76.

Laîné, J., Hagstrom, J.P., Clark, M.M., Mallevialle, J. (1989). "Effects of ultra-filtration membrane composition", *Journal AWWA*, 81(11), 61.

Maartens, A., Swart, P., Jacobs, E.P. (1998). "Humic membrane foulants in natural brown water: characterization and removal", *Desalination*, 115(3), 215.

Maartens, A., Swart, P., Jacobs, E.P. (2000). "Membrane pretreatment: A method for reducing fouling by natural organic matter", *Journal of Colloid and Interface Science*, 221(2), 137.

Montgomery, D., Runger, G. (2003). *Applied Statistics and Probability for Engineers*, John Wiley and Sons, Inc. New York, NY

Mulder, M. (1996). *Basic Principles of Membrane Technology*, Kluwer Academic, Boston, MA

Pankratz, T., Tonner, J. (2003). *Desalination.com and Environmental Primer*, Loan Oak Publishing, Houston, TX

Pulles, W. (1992). Development of the slurry precipitation and recycle reverse osmosis (SPARRO) technology for desalinating scaling mine waters", *Water Science and Technology*, 25(10),177-192.

RosTek Associates, Inc., Tampa, Florida, DSS Consulting, Inc., Blue Ridge, Georgia, Aqua Resources International, Inc., Evergreen Colorado, United States Department of the Interior, Bureau of Reclamation, *Desalting Handbook For Planners, Third Edition*, Desalination and Water Purification Research and Development Program Report No. 72. Website: http://www.usbr.gov/pmts/water/media/pdfs/report072.pdf.

Wiesner, M.R., Chellam, S. (1992b). "Mass transport considerations for pressure-driven membrane processes." *Journal AWWA*, 84(1), 88.

APPENDIX A

OPTICAL MICROSCOPY OF MEMBRANES AFTER PILOT TESTING

A-1: RO-CA, membrane abrasions

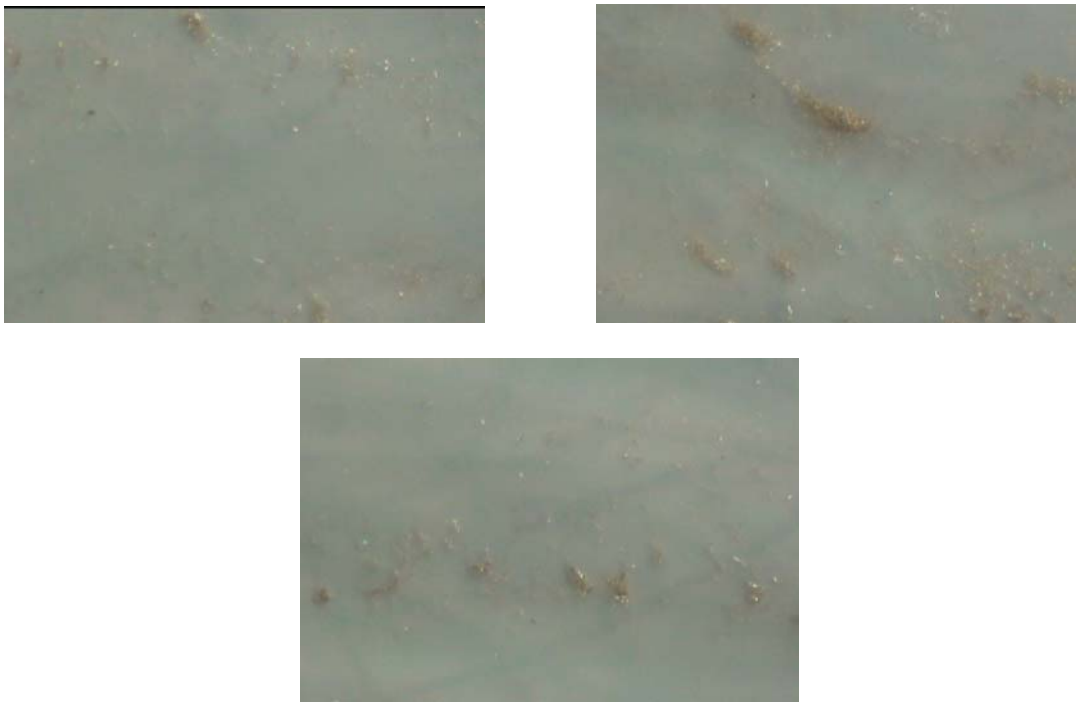

FIG. A-1. Reverse osmosis – cellulose acetate membrane

A-2: RO-PA (low MWCO), membrane abrasions

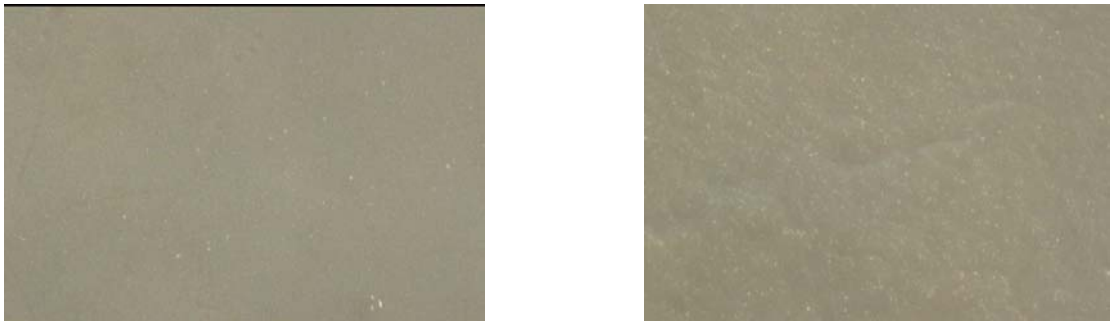

FIG. A-2. Reverse osmosis – polyamide membrane (low MWCO)

A-3: RO-PA (high MWCO), membrane abrasions

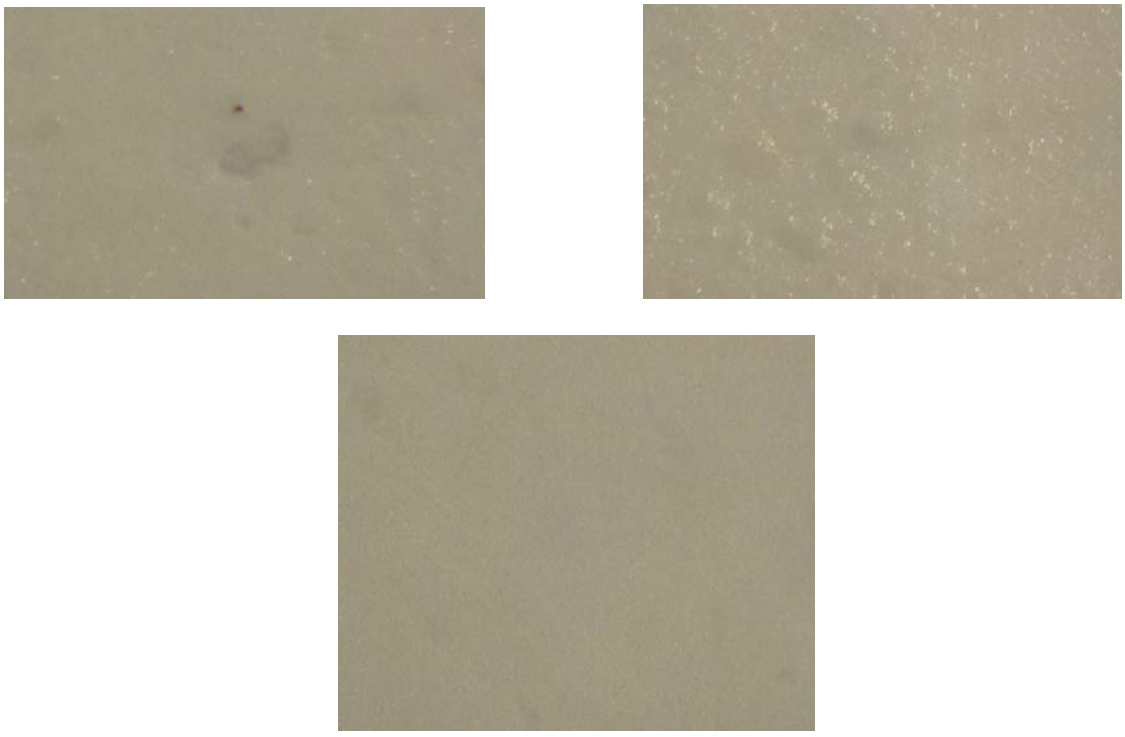

FIG. A-3. Reverse osmosis – polyamide membrane (high MWCO)

A-4: NF-CA, membrane abrasions

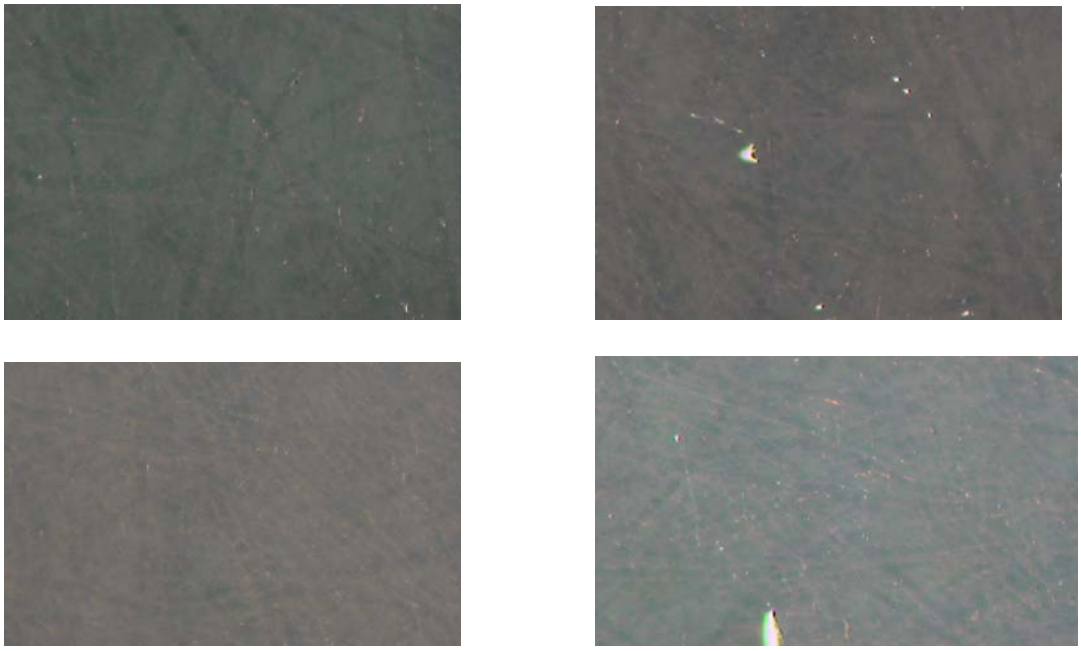

FIG. A-4. Nanofiltration – cellulose acetate membrane

A-5: NF-TF, membrane abrasions

FIG. A-5. Nanofiltration – thin film membrane

APPENDIX B

PILOT TESTING

B-1: Testing solution

FIG. B-1. Seeded calcium sulfate solution

B-2: GE osmonics experiment apparatus

FIG. B-2. Sampling with the GE Osmonics experiment apparatus

B-3: Calcium sulfate scaling

FIG. B-3. Severe calcium sulfate scaling of a membrane

B-4: Transmembrane pressure differential

FIG. B-4. Transmembrane pressure differential within the SEPA Cell

B-5: Inside of the SEPA Cell

FIG. B-5. Inside of the SEPA Cell

B-6: Feed spacer

FIG. B-6. Feed spacer used to promote turbulence to reduce fouling

B-7: Temperature control

FIG. B-7. Ice used to maintain constant temperature

B-8: Permeate carrier

FIG. B-8. Permeate carrier used to reduce resistance of permeate flow

APPENDIX C

DATA COLLECTION

C-1: Reverse osmosis – cellulose acetate data

Time (min)	Pressure In (psig)	Pressure Out (psig)	Inflow Q (gpm)	Inflow Q (mL/s)	Permeate Q (mL/s)	$Conductivity_{influent}$ (µS/cm)	$Conductivity_{permeate}$ (µS/cm)
0	450	440	1	63.09	0.168539326	2400	19.7
15	450	440	1	63.09	0.170454545	2400	14.27
30	450	440	1	63.09	0.182926829	2400	10.89
45	450	440	1	63.09	0.1875	2400	9.72
60	450	440	1	63.09	0.192307692	2400	9.77
90	450	440	1	63.09	0.204081633	2400	8.94
120	450	440	1	63.09	0.2	2400	8.85
150	450	440	1	63.09	0.196078431	2400	8.71
180	450	440	1	63.09	0.186567164	2400	9.78
210	450	440	1	63.09	0.208333333	2400	9.02
240	450	440	1	63.09	0.211267606	2400	8.91

$[CaSO_4]_{permeate}$ (g/L)	$[CaSO_4]_{permeate}$ (M)	Osmotic $Pressure_{permeate}$ (psig)	$[CaSO_4]_{inflow}$ (g/L)	$[CaSO_4]_{inflow}$ (M)	Osmotic $Pressure_{influent}$ (psig)
0.02167	0.00015917	0.10330814	2.64	0.019391233	12.58576331
0.015697	0.000115297	0.074832851	2.64	0.019391233	12.58576331
0.011979	8.79877E-05	0.057107901	2.64	0.019391233	12.58576331
0.010692	7.85345E-05	0.050972341	2.64	0.019391233	12.58576331
0.010747	7.89385E-05	0.051234545	2.64	0.019391233	12.58576331
0.009834	7.22323E-05	0.046881968	2.64	0.019391233	12.58576331
0.009735	7.15052E-05	0.046410002	2.64	0.019391233	12.58576331
0.009581	7.0374E-05	0.045675833	2.64	0.019391233	12.58576331
0.010758	7.90193E-05	0.051286985	2.64	0.019391233	12.58576331
0.009922	7.28787E-05	0.047301494	2.64	0.019391233	12.58576331
0.009801	7.199E-05	0.046724646	2.64	0.019391233	12.58576331

Δ Osmotic Pressure (psig)	Flux (mL/(cm2*min))	Recovery %	Net Driving Force (psig)	Water Mass Transfer, K_w (mL/(cm2*min*psi))
12.48245517	0.07223114	0.267141109	417.8175448	0.000172877
12.51093046	0.073051948	0.270176804	417.7890695	0.000174854
12.52865541	0.078397213	0.289945838	417.7713446	0.000187656
12.53479097	0.080357143	0.297194484	417.765209	0.00019235
12.53452876	0.082417582	0.304814855	417.7654712	0.000197282
12.53888134	0.087463557	0.323476989	417.7611187	0.000209363
12.53935331	0.085714286	0.31700745	417.7606467	0.000205176
12.54008748	0.084033613	0.310791617	417.7599125	0.000201153
12.53447632	0.079957356	0.295715905	417.7655237	0.000191393
12.53846182	0.089285714	0.330216093	417.7615382	0.000213724
12.53903866	0.09054326	0.334867024	417.7609613	0.000216735

Solute Transfer Coefficient, K_s (L/s)	Solute Rejection (%)	Solute Mass Transfer (g/min)	Water Mass Transfer Coefficient / Solute Mass Transfer ((mL/(cm2*g*psi))
1.39488E-06	99.17916667	0.000219135	0.788908037
1.01956E-06	99.40541667	0.000160538	1.089176425
8.33814E-07	99.54625	0.000131477	1.427291737
7.62463E-07	99.595	0.000120285	1.599118857
7.86052E-07	99.59291667	0.000124004	1.590934036
7.63046E-07	99.6275	0.000120416	1.738656318
7.4023E-07	99.63125	0.00011682	1.756339553
7.14193E-07	99.63708333	0.000112718	1.784573175
7.63372E-07	99.5925	0.000120425	1.589307115
7.8594E-07	99.62416667	0.000124025	1.723234132
7.87254E-07	99.62875	0.000124238	1.744511036

FIG. C-1. Reverse osmosis – cellulose acetate data

C-2: Reverse osmosis – high MWCO polyamide data

Time (min)	Pressure In (psig)	Pressure Out (psig)	Inflow Q (gpm)	Inflow Q (mL/s)	Permeate Q (mL/s)	$Conductivity_{influent}$ (µS/cm)	$Conductivity_{permeate}$ (µS/cm)
0	150	140	1	63.09	0.208333333	2400	148
15	150	140	1	63.09	0.202702703	2400	89.2
30	150	140	1	63.09	0.194805195	2400	73
45	150	140	1	63.09	0.185185185	2400	71.1
60	150	140	1	63.09	0.182926829	2400	100.5
90	150	140	1	63.09	0.141509434	2400	89
120	150	140	1	63.09	0.120967742	2400	90
150	150	140	1	63.09	0.081081081	2400	96
180	150	140	1	63.09	0.071428571	2400	100.3
210	150	140	1	63.09	0.069767442	2400	96
240	150	140	1	63.09	0.066964286	2400	98

$[CaSO_4]_{permeate}$ (g/L)	$[CaSO_4]_{permeate}$ (M)	$Osmotic\ Pressure_{permeate}$ (psig)	$[CaSO_4]_{inflow}$ (g/L)	$[CaSO_4]_{inflow}$ (M)	$Osmotic\ Pressure_{influent}$ (psig)
0.1628	0.001195793	0.776122071	2.64	0.019391233	12.58576331
0.09812	0.000720707	0.46777087	2.64	0.019391233	12.58576331
0.0803	0.000589817	0.382816967	2.64	0.019391233	12.58576331
0.07821	0.000574465	0.372853238	2.64	0.019391233	12.58576331
0.11055	0.000812008	0.527028839	2.64	0.019391233	12.58576331
0.0979	0.000719092	0.466722056	2.64	0.019391233	12.58576331
0.099	0.000727171	0.471966124	2.64	0.019391233	12.58576331
0.1056	0.000775649	0.503430532	2.64	0.019391233	12.58576331
0.11033	0.000810392	0.525980025	2.64	0.019391233	12.58576331
0.1056	0.000775649	0.503430532	2.64	0.019391233	12.58576331
0.1078	0.000791809	0.513918668	2.64	0.019391233	12.58576331

Δ Osmotic Pressure (psig)	Flux (mL/(cm2*min))	Recovery %	Net Driving Force (psig)	Water Mass Transfer, K_w (mL/(cm2*min*psi))
11.80964124	0.089285714	0.3302161	118.4903588	0.000753527
12.11799244	0.086872587	0.3212913	118.1820076	0.000735075
12.20294634	0.083487941	0.3087735	118.0970537	0.000706943
12.21291007	0.079365079	0.2935254	118.0870899	0.000672089
12.05873447	0.078397213	0.2899458	118.2412655	0.000663028
12.11904125	0.0606469	0.2242977	118.1809587	0.00051317
12.11379719	0.051843318	0.1917384	118.1862028	0.000438658
12.08233278	0.034749035	0.1285165	118.2176672	0.000293941
12.05978328	0.030612245	0.1132169	118.2402167	0.000258899
12.08233278	0.029900332	0.110584	118.2176672	0.000252926
12.07184464	0.02869898	0.1061409	118.2281554	0.000242742

Solute Transfer Coefficient, K_s (L/s)	Solute Rejection (%)	Solute Mass Transfer (g/min)	Water Mass Transfer Coefficient / Solute Mass Transfer ((mL/(cm2*g*psi))
1.36915E-05	93.83333333	0.002035	0.370283661
7.8246E-06	96.28333333	0.001193351	0.615974965
6.11121E-06	96.95833333	0.000938571	0.753212218
5.6536E-06	97.0375	0.000869	0.773405504
7.99485E-06	95.8125	0.001213354	0.546442096
5.44974E-06	96.29166667	0.000831226	0.617364657
4.71303E-06	96.25	0.000718548	0.610477961
3.37838E-06	96	0.00051373	0.572170761
3.11531E-06	95.82083333	0.000472843	0.547536568
2.90698E-06	96	0.000442047	0.572170761
2.85078E-06	95.91666667	0.000433125	0.560444085

FIG. C-2. Reverse osmosis – high MWCO polyamide data

C-3: Reverse osmosis – low MWCO polyamide data

Time (min)	Pressure In (psig)	Pressure Out (psig)	Inflow Q (gpm)	Inflow Q (mL/s)	Permeate Q (mL/s)	$Conductivity_{influent}$ (µS/cm)	$Conductivity_{permeate}$ (µS/cm)
0	300	290	1	63.09	0.205479452	2400	57
15	300	290	1	63.09	0.208333333	2400	55.1
30	300	290	1	63.09	0.214285714	2400	50.7
45	300	290	1	63.09	0.185185185	2400	46.7
60	300	290	1	63.09	0.185185185	2400	46.4
90	300	290	1	63.09	0.154639175	2400	49.4
120	300	290	1	63.09	0.115384615	2400	55.9
150	300	290	1	63.09	0.1	2400	58
180	300	290	1	63.09	0.089285714	2400	63.4
210	300	290	1	63.09	0.064935065	2400	78.2
240	300	290	1	63.09	0.053571429	2400	89.3

$[CaSO_4]_{permeate}$ (g/L)	$[CaSO_4]_{permeate}$ (M)	Osmotic $Pressure_{permeate}$ (psig)	$[CaSO_4]_{inflow}$ (g/L)	$[CaSO_4]_{inflow}$ (M)	Osmotic $Pressure_{influent}$ (psig)
0.0627	0.000460542	0.298911879	2.64	0.019391233	12.58576331
0.06061	0.00044519	0.288948149	2.64	0.019391233	12.58576331
0.05577	0.00040964	0.26587425	2.64	0.019391233	12.58576331
0.05137	0.000377321	0.244897978	2.64	0.019391233	12.58576331
0.05104	0.000374897	0.243324757	2.64	0.019391233	12.58576331
0.05434	0.000399136	0.259056961	2.64	0.019391233	12.58576331
0.06149	0.000451654	0.293143404	2.64	0.019391233	12.58576331
0.0638	0.000468621	0.304155947	2.64	0.019391233	12.58576331
0.06974	0.000512252	0.332473914	2.64	0.019391233	12.58576331
0.08602	0.000631831	0.410086121	2.64	0.019391233	12.58576331
0.09823	0.000721515	0.468295276	2.64	0.019391233	12.58576331

Δ Osmotic Pressure (psig)	Flux (mL/(cm2*min))	Recovery %	Net Driving Force (psig)	Water Mass Transfer, K_w (mL/(cm2*min*psi))
12.28685143	0.088062622	0.3256926	268.0131486	0.000328576
12.29681516	0.089285714	0.3302161	268.0031848	0.000333152
12.31988906	0.091836735	0.3396508	267.9801109	0.0003427
12.34086533	0.079365079	0.2935254	267.9591347	0.000296184
12.34243855	0.079365079	0.2935254	267.9575614	0.000296185
12.32670635	0.066273932	0.2451089	267.9732937	0.000247315
12.29261991	0.049450549	0.1828889	268.0073801	0.000184512
12.28160736	0.042857143	0.1585037	268.0183926	0.000159904
12.2532894	0.038265306	0.1415212	268.0467106	0.000142756
12.17567719	0.027829314	0.1029245	268.1243228	0.000103793
12.11746803	0.022959184	0.0849127	268.182532	8.56103E-05

Solute Transfer Coefficient, K_s (L/s)	Solute Rejection (%)	Solute Mass Transfer (g/min)	Water Mass Transfer Coefficient / Solute Mass Transfer ((mL/(cm2*g*psi))
4.99886E-06	97.625	0.000773014	0.425058126
4.89538E-06	97.70416667	0.000757625	0.43973165
4.62448E-06	97.8875	0.000717043	0.477934914
3.6749E-06	98.05416667	0.000570778	0.518912141
3.65083E-06	98.06666667	0.000567111	0.522270243
3.24988E-06	97.94166667	0.000504186	0.490524627
2.75159E-06	97.67083333	0.0004257	0.433431747
2.47652E-06	97.58333333	0.0003828	0.417721364
2.42263E-06	97.35833333	0.000373607	0.382102201
2.18706E-06	96.74166667	0.000335143	0.309696512
2.07034E-06	96.27916667	0.000315739	0.271142336

FIG. C-3. Reverse osmosis – low MWCO polyamide data

C-4: Nanofiltration – thin film data

Time (min)	Pressure In (psig)	Pressure Out (psig)	Inflow Q (gpm)	Inflow Q (mL/s)	Permeate Q (mL/s)	$Conductivity_{influent}$ (µS/cm)	$Conductivity_{permeate}$ (µS/cm)
0	150	140	1	63.09	0.159574468	2400	524
15	150	140	1	63.09	0.154639175	2400	339
30	150	140	1	63.09	0.166666667	2400	246
45	150	140	1	63.09	0.161290323	2400	230
60	150	140	1	63.09	0.15625	2400	218
90	150	140	1	63.09	0.178571429	2400	280
120	150	140	1	63.09	0.176470588	2400	270
150	150	140	1	63.09	0.185185185	2400	255
180	150	140	1	63.09	0.180722892	2400	250
210	150	140	1	63.09	0.176470588	2400	248
240	150	140	1	63.09	0.166666667	2400	249

$[CaSO_4]_{permeate}$ (g/L)	$[CaSO_4]_{permeate}$ (M)	Osmotic $Pressure_{permeate}$ (psig)	$[CaSO_4]_{inflow}$ (g/L)	$[CaSO_4]_{inflow}$ (M)	Osmotic $Pressure_{influent}$ (psig)
0.5764	0.004233752	2.747891656	2.64	0.019391233	12.58576331
0.3729	0.002739012	1.777739067	2.64	0.019391233	12.58576331
0.2706	0.001987601	1.290040739	2.64	0.019391233	12.58576331
0.253	0.001858326	1.20613565	2.64	0.019391233	12.58576331
0.2398	0.00176137	1.143206834	2.64	0.019391233	12.58576331
0.308	0.00226231	1.468339053	2.64	0.019391233	12.58576331
0.297	0.002181514	1.415898372	2.64	0.019391233	12.58576331
0.2805	0.002060318	1.337237352	2.64	0.019391233	12.58576331
0.275	0.00201992	1.311017011	2.64	0.019391233	12.58576331
0.2728	0.002003761	1.300528875	2.64	0.019391233	12.58576331
0.2739	0.00201184	1.305772943	2.64	0.019391233	12.58576331

Δ Osmotic Pressure (psig)	Flux (mL/(cm2*min))	Recovery %	Net Driving Force (psig)	Water Mass Transfer, K_w (mL/(cm2*min*psi))
9.837871654	0.068389058	0.2529315	120.4621283	0.000567722
10.80802424	0.066273932	0.2451089	119.4919758	0.000554631
11.29572257	0.071428571	0.2641729	119.0042774	0.000600219
11.37962766	0.069124424	0.2556512	118.9203723	0.000581266
11.44255648	0.066964286	0.2476621	118.8574435	0.0005634
11.11742426	0.076530612	0.2830424	119.1825757	0.000642129
11.16986494	0.075630252	0.2797125	119.1301351	0.000634854
11.24852596	0.079365079	0.2935254	119.051474	0.000666645
11.2747463	0.077452668	0.2864525	119.0252537	0.000650725
11.28523443	0.075630252	0.2797125	119.0147656	0.000635469
11.27999037	0.071428571	0.2641729	119.0200096	0.000600139

Solute Transfer Coefficient, K_s (L/s)	Solute Rejection (%)	Solute Mass Transfer (g/min)	Water Mass Transfer Coefficient / Solute Mass Transfer ((mL/(cm2*g*psi))
4.4572E-05	78.16666667	0.005518723	0.102872066
2.54356E-05	85.875	0.003459897	0.160302701
1.90344E-05	89.75	0.002706	0.221810244
1.70953E-05	90.41666667	0.002448387	0.237407909
1.56107E-05	90.91666667	0.002248125	0.250608848
2.35849E-05	88.33333333	0.0033	0.194584607
2.23695E-05	88.75	0.003144706	0.201880272
2.2015E-05	89.375	0.003116667	0.213896817
2.10143E-05	89.58333333	0.002981928	0.218222815
2.03368E-05	89.66666667	0.002888471	0.220002063
1.92934E-05	89.625	0.002739	0.219108866

FIG. C-4. Nanofiltration – thin film data

C-5: Nanofiltration – cellulose acetate data

Time (min)	Pressure In (psig)	Pressure Out (psig)	Inflow Q (gpm)	Inflow Q (mL/s)	Permeate Q (mL/s)	$Conductivity_{influent}$ (µS/cm)	$Conductivity_{permeate}$ (µS/cm)
0	255	245	1	63.09	0.189873418	2400	160
15	255	245	1	63.09	0.194805195	2400	157
30	255	245	1	63.09	0.194805195	2400	140
45	255	245	1	63.09	0.197368421	2400	126.6
60	255	245	1	63.09	0.197368421	2400	110.5
90	255	245	1	63.09	0.205479452	2400	96.7
120	255	245	1	63.09	0.194805195	2400	85.4
150	255	245	1	63.09	0.163043478	2400	77
180	255	245	1	63.09	0.161290323	2400	64.4
210	255	245	1	63.09	0.154639175	2400	57.9
240	255	245	1	63.09	0.15	2400	52.8

$[CaSO_4]_{permeate}$ (g/L)	$[CaSO_4]_{permeate}$ (M)	$Osmotic\ Pressure_{permeate}$ (psig)	$[CaSO_4]_{inflow}$ (g/L)	$[CaSO_4]_{inflow}$ (M)	$Osmotic\ Pressure_{influent}$ (psig)
0.176	0.001292749	0.839050887	2.64	0.019391233	12.58576331
0.1727	0.00126851	0.823318683	2.64	0.019391233	12.58576331
0.154	0.001131155	0.734169526	2.64	0.019391233	12.58576331
0.13926	0.001022888	0.663899015	2.64	0.019391233	12.58576331
0.12155	0.000892805	0.579469519	2.64	0.019391233	12.58576331
0.10637	0.000781305	0.50710138	2.64	0.019391233	12.58576331
0.09394	0.000690005	0.447843411	2.64	0.019391233	12.58576331
0.0847	0.000622135	0.40379324	2.64	0.019391233	12.58576331
0.07084	0.000520331	0.337717982	2.64	0.019391233	12.58576331
0.06369	0.000467813	0.30363154	2.64	0.019391233	12.58576331
0.05808	0.000426607	0.276886793	2.64	0.019391233	12.58576331

Δ Osmotic Pressure (psig)	Flux (mL/(cm2*min))	Recovery %	Net Driving Force (psig)	Water Mass Transfer, K_w (mL/(cm2*min*psi))
11.74671242	0.081374322	0.3009564	223.5532876	0.000364004
11.76244463	0.083487941	0.3087735	223.5375554	0.000373485
11.85159378	0.083487941	0.3087735	223.4484062	0.000373634
11.92186429	0.084586466	0.3128363	223.3781357	0.000378669
12.00629379	0.084586466	0.3128363	223.2937062	0.000378813
12.07866193	0.088062622	0.3256926	223.2213381	0.000394508
12.1379199	0.083487941	0.3087735	223.1620801	0.000374113
12.18197007	0.069875776	0.25843	223.1180299	0.000313179
12.24804533	0.069124424	0.2556512	223.0519547	0.000309903
12.28213177	0.066273932	0.2451089	223.0178682	0.000297169
12.30887652	0.064285714	0.2377556	222.9911235	0.000288288

Solute Transfer Coefficient, K_s (L/s)	Solute Rejection (%)	Solute Mass Transfer (g/min)	Water Mass Transfer Coefficient / Solute Mass Transfer ((mL/(cm2*g*psi))
1.35624E-05	93.33333333	0.002005063	0.181542468
1.36355E-05	93.45833333	0.002018571	0.185024453
1.20676E-05	94.16666667	0.0018	0.207574491
1.0991E-05	94.725	0.001649132	0.229617462
9.52575E-06	95.39583333	0.001439408	0.263172508
8.62669E-06	95.97083333	0.001311411	0.300827198
7.18758E-06	96.44166667	0.001098	0.340722652
5.40437E-06	96.79166667	0.000828587	0.377967003
4.44729E-06	97.31666667	0.000685548	0.452050942
3.8229E-06	97.5875	0.000590938	0.502876169
3.37423E-06	97.8	0.00052272	0.551515574

FIG. C-5. Nanofiltration – cellulose acetate data

VITA

Trenton Whiting Hughes

PERMANENT ADDRESS

Hughetr@tamu.edu 7224 Panorama Drive, Rockville, MD, 20855

EDUCATION

M.S. in Civil Engineering Dec.2006
Texas A&M University, College Station, Texas
B.S. in Biological Systems Engineering May 2004
Auburn University, Auburn, Alabama

WORK EXPERIENCE

Engineering Intern, Apex Engineering, Rockville, Maryland *(June 2006 –Sept. 2006)*

- Facilitated with design plans regarding all parts of land development, including: sediment control, water & sewer, storm drain & paving, stormwater management, and grading. Also conducted frequent site inspections
- Applied for construction permits for all of the land development facets (listed above)

Engineering Intern, Black and Veatch, College Station, Texas *(Jan. 2006 –June 2006)*

- Developed wiring diagrams for electrical engineers using AutoCAD and MicroStation

Teaching Assistant (for two classes), Texas A&M University, College Station, Texas *(Sept. 2004 –)*

- Facilitated undergraduate students with typical environmental engineering/geotechnical engineering problems and instructed labs.

Engineering Intern, Stearns & Wheler, LLC, Bowie, Maryland *(June 2005 – Aug 2005)*

- Co-designed a ENR upgrade for the WWTP in Havre de Grace, MD with a project engineer from start to finish
- Analyzed a previous design deficiency for a aerated grit chamber located in Cox Creek, MD
- Conducted frequent site inspections of the contractors work at Havre de Grace, MD

Research Assistant, National Science Foundation, Virginia Tech, Blacksburg, Virginia *(May 2003 – Aug. 2003)*

- Selected on a nationwide basis by the National Science Foundation to conduct research for the biological systems engineering department
- Led a research project on nutrient transport through soil and presented a dissertation to the faculty on my results.
- Used SAS to analyze data given from water quality test